ARL 64-109

AN EXPERIMENTAL STUDY OF INFRA-RED SCATTERING BY CLOUDS OF PARTICLES

T. J. LOVE
R. A. WHEASLER

SCHOOL OF AEROSPACE AND MECHANICAL ENGINEERING
UNIVERSITY OF OKLAHOMA
NORMAN, OKLAHOMA

JUNE 1964

Contract AF 33(657)-8859
Project 7063
Task 7063-03

AEROSPACE RESEARCH LABORATORIES
OFFICE OF AEROSPACE RESEARCH
UNITED STATES AIR FORCE
WRIGHT-PATTERSON AIR FORCE BASE, OHIO

NOTICES

When Government drawings, specifications, or other data are used for any purpose other than in connection with a definitely related Government procurement operation, the United States Government thereby incurs no responsibility nor any obligation whatsoever; and the fact that the Government may have formulated, furnished, or in any way supplied the said drawings, specifications, or other data, is not to be regarded by implication or otherwise as in any manner licensing the holder or any other person or corporation, or conveying any rights or permission to manufacture, use, or sell any patented invention that may in any way be related thereto.

- - - - - - - - - -

Qualified requesters may obtain copies of this report from the Defense Documentation Center, (DDC), Cameron Station, Alexandria, Virginia.

- - - - - - - - - -

This report has been released to the Office of Technical Services, U. S. Department of Commerce, Washington 25, D. C. for sale to the general public.

Stock available at OTS $ 3.00 .....

- - - - - - - - - -

Copies of ARL Technical Documentary Reports should not be returned to Aerospace Research Laboratories unless return is required by security considerations, contractual obligations or notices on a specific document.

500 - July 1964 - 162-47-955

FOREWORD

The work reported herein was performed by the University of Oklahoma, School of Aerospace and Mechanical Engineering and the University of Oklahoma Research Institute, Norman, Oklahoma under Air Force Contract AF 33(657)-8859, Project 7063, Task 7063-03, sponsored by the Thermo-Mechanics Branch, Aerospace Research Laboratories, Office of Aerospace Research, United States Air Force.

In addition to the authors listed a special note should be made of the efforts of Mr. J. H. Ingram and Mr. Han-Min Hsia. Mr. Ingram was responsible for the early work on the development of the particle generator and Mr. Hsia assisted in the experimental phases and the reduction of the data.

Mr. Paul Schreiber, Aeronautical Research Laboratories served as the monitoring scientist. His interest, critical reviews and helpful suggestions are greatly appreciated.

This is an interim technical report for work performed beginning January 1963 and ending January 1964. ARL 63-3 was a previous interim report on this project covering work accomplished prior to January 1963.

The experimental equipment utilized for this study was purchased under the National Science Foundation Grant No. GP360.

ABSTRACT

This report describes a study of the extinction and scattering of infra-red radiation from an aerosol of fine particles. A description is given of the method developed for generation of a uniform optically thin cloud of particles. Reynolds aluminum 40XD powder was used for this test. The optical equipment including glo-bar source, focusing optics, traversing mechanism and Perkin Elmer model 98 monochromator is described. The extinction coefficient and normalized scattering function is reported for 21 wave lengths of incident radiation.

TABLE OF CONTENTS

LIST OF ILLUSTRATIONS

LIST OF ILLUSTRATIONS--Continued

LIST OF TABLES

SECTION I

INTRODUCTION

The study of radiation heat transfer in absorbing, emitting and scattering media was initiated by an analytical study of systems of particles bounded by infinite plane diffuse walls. The results of this study are reported in Aeronautical Research Laboratories report number ARL63-3. The analysis assumed plane parallel systems of uniform spherical particles. The refractive index of the particles was assumed known and constant for all wave lengths. Cases of isothermal clouds of particles and radiative equilibrium were considered.

In many situations of engineering interest, the particles will be neither spherical, uniform nor isothermal. In addition, information on the complex refractive index of most materials is rather scarce. The purpose of the present investigation is to develop a method of determining the necessary scattering functions and extinction coefficients of clouds of particles. Such determinations would thus allow the previous analysis to be applied to systems composed of these particles.

Analytical prediction of the scattering parameters of typical dusts would be impractical. Not only would the mathematical extension of Mie theory to irregular particles of mixed sizes be difficult, but, it is often impossible to accurately describe the particle size and shape as well as the refractive index for all wave lengths of radiation. The study described in this report is therefore concerned primarily with the development of a method of experimental determination of these parameters.

There is no unique design for a light scattering device, and no such devices are offered on the market. It is the responsibility of each investigator to use his ingenuity and experience to custom-build or fashion a device that will perform to meet the criteria which have been established. The intended use of the data will dictate, for the most part, the design of the instrument. It is for this reason that a literature survey, per se, is not presented. Instead, only a few comments from some of the literature that has been surveyed will be presented, while additional notes will be attached as an appendage for those interested in the vast number of applications for light scattering experiments or the uses of light scattering for experimental work.

Although a search of the literature did not produce a design of light scattering equipment which could be used in this investigation to determine the scattering function for an aerosol of irregular shaped particles, much information can be gained from previous work in light scattering measurements.

Manuscript released January 31, 1964 by the authors for publication as an ARL Technical Documentary Report.

Through the efforts of Gustav Mie the electromagnetic wave theories had been fairly well developed by 1908; however, very little experimental work in light scattering was done prior to World War II. Interest in colloids, with a great need to develop techniques which would accurately determine particle size and particle concentrations, provided the stimulus needed to recognize the versatile tool available in light scattering measurements. Work on aerosols for the Office of Scientific Research and Development by LaMer and Sinclair in the years 1940-42 undoubtedly helped to provide this stimulus. Their work was published as an OSRD report which appeared in part in various scientific journals during the postwar years.

LaMer and Barnes (89) were among the first, if not the first, to confirm experimentally the general theories of Rayleigh and Mie, particularly Mie. For this reason some detail of their work will be presented here, whereas other contributions will not be noted at this time. This should not be construed to mean that this was the most significant contribution to the field, however. The first problem they encountered, prior to their experiments to confirm the electromagnetic wave theory of the scattering of light of transparent spheres, was the development of a method for comparison of sols with a high degree of uniformity of particle size as a base for fundamental measurements for checking theory and calibrating methods. They were successful in preparing a mono-dispersed sol of different particle sizes. Prior to their success it was difficult to obtain colloidal and macromolecular systems of a well-defined and fairly uniform particle size. It is believed by some (150) that this was the reason for the lag in experimental work, together with the fact that dimensions on colloidal systems and their molecular weights was not considered important until the early 1940's. Along with this contribution they developed a device (2) which enabled them to make light scattering measurements on hydrophobic colloidal dispersions of a sulfur sol using light in the visible range; i.e., wave lengths 0.37 to 0.85 microns. A Coleman double monochromator Model 10-S was used for monochromatic light transmittance measurements. Their measurements were alternated between distilled water and a dispersion tube containing the sulfur sol. Their data were corrected for variations in readings (explained as being due to settling and redissolving of particles), by taking readings in rapid succession at specified points and using these specified points to adjust the curves. The curves which they plotted were total scattering versus wave length (in water). Reproducibility was reported to be good. The sols contained spheres or at least seemed to under the ultra-microscope. It was in this early work that the experimenters noticed scattering minimum which shifted to longer wave lengths with larger particle sizes. This is one of the earliest reports where researchers, or experimenters, reported the influence of superposition. Considerable variation or irregularity of curves was noted, including secondary maxima not before reported, which became increasingly apparent and more pronounced with more homogeneous particle sizes, although practically absent in heterogeneous sols. Smooth total scattering curves resulted when heterogeneous sols were used. These sols were prepared by adding a solution of sulfur in acetone to water and were observed

by ultra-microscopic examination. The presence of a few secondary maxima in total scattering had been considered previously, at least theoretically, by Lowen. Their method of determining particle radius and refractive index as a result of plotting their data was rather unique.

It is interesting to note that early experimenters (90) using light scattering measurements as a tool recognized the need for a standardization of symbolism, yet some twenty years later no progress seems to have been made toward this end.

DeVore and Pfund (29) made use of the Mie minimum observed in total scattering measurements for their work on dielectric powders of zinc sulfide and titanium dioxide. Using the changing of position of the Mie minimum with variation of refractive index, they were able to develop methods for measuring the refractive indices of some powders of uniform particle size. Henry (66) found in his investigation that the transmission of powder films in the infra-red region had spectral transmission curves considerably different from those of the same material in bulk form.

The majority of investigations seeking to confirm the Mie and Rayleigh theories have been successful; however, great care must be exercised in developing equipment necessary to make such measurements. The theories, in general, have been accepted as fact and confirmed experimentally. Little work, however, has been done to confirm the Mie theory for regions of large size parameters (alpha) (22), probably due to the difficulty involved in producing suitable distributions of uniform scattering particles of large sizes. LaMer was very successful in confirming the region for alpha from 2 to 13. Cleveland and Raymond (22) were evidently the first to make measurements of integrated scattering by metallic spheres; however, their results were obtained from layers of particles rather than from an aerosol. A Perkin-Elmer Model 12A Spectrometer was used for their measurements and the slit width was varied to maintain full deflection on the chart; consequently, the angle of reception also varied for measurements of different wave lengths, which is contrary to the constant angle of reception used in the present investigation. Using a sodium chloride prism, their investigation covered a wave length range of 0.45 to 15 microns, which would extend the low side of the useful range of the sodium chloride prism to such an extent that one should be skeptical of the results. Curves of scattering area coefficient as a function of size parameter (alpha) were presented. Since a hetero-disperse system was being investigated, the particle size parameter was necessarily based on an average particle size. Consequently, Cleveland and Raymond were faced with the same dilemma as the authors of this investigation in that any comparison of experimental work on poly-disperse systems with the theoretical work of Mie requires that an average or pseudo particle size be used.

Much of the work published on light scattering measurements has attempted to verify the theories of Mie and Rayleigh or, accepting these theories as fact, to determine particle size distributions of

colloids, particle concentrations, and/or refractive indices of substances. Since the particle size parameter can be varied by varying the size of the particle, it is no wonder that most investigations have been made using white light and that very little work has been done in the infra-red region.

Considerable effort is required on the part of the investigator to obtain exact numerical solutions to the Mie equations, and for this reason results of electronic computer calculations have been published in tables to minimize the work required to obtain answers. The tables of Chu, Clark, and Churchill (17)(21), and Gumprecht and Sliepcevich (47) are particularly noteworthy and were used to obtain solutions to the Mie equations for a few cases reported in this investigation.

In order to establish a well-founded background and understanding of the electromagnetic wave theory, most experiments and analyses reported in the literature have necessarily been for mono-disperse systems; consequently, little is reported on poly-disperse systems. Numerous works by Heller and his co-workers have appeared in the literature over the past fifteen years. Their theoretical analyses and experimental confirmations of the Mie theory are probably the most extensive and complete of any work published to date. Obviously, few systems found in nature are mono-disperse. It is for this reason, as pointed out in the introduction, that the experimental work for poly-disperse systems is being extended as in this investigation. The experimental approach is obvious since, except for certain special cases, no suitable solutions exist for non-spherical particles.

Light scattering measurements on poly-disperse systems have been made by the astrophysicist and meteorologist. The nephelometer and the transmissometer are two devices used for measuring light scattering and transmission of the atmosphere (124) which usually utilize a photo-multiplier detector.

It is of particular interest to this investigation to cite the works published by Pritchard et al (124), and Gibbon et al (41), on their investigations of light scattering and transmissions through atmospheres. These papers further support the conclusions of this investigation that angular distribution of intensity curves for systems containing particles of non-uniform size and distributions will be smooth functions.

This investigation succeeded in obtaining the scattering function for an aluminum oxide powder dispersed in air for 21 values of wave length. In addition, the investigation produced the mass scattering coefficient and the mass extinction coefficient for the same media.

Considerable attention was given to the design of the apparatus for measuring the mass scattering coefficient, the mass extinction coefficient, and the scattering function for the real substance, so that the values obtained would be valid for optically thin media.

Single scattering phenomena was considered since radiant heat transfer in scattering and absorbing media that is optically thin is of primary interest for the present-day heat transfer analysis.

SECTION II

DESCRIPTION OF EQUIPMENT

The physical arrangement of the apparatus used to measure the angular distribution of intensity was a result of several compromises involved in cost, versatility and utility. Several configurations were studied before a proposed final design was considered acceptable.

Prior to the initiation of the design the literature was surveyed to ascertain whether or not there was a configuration that was typical for this purpose. It was soon concluded that there was no standard design available for measurements of this kind and that a device would have to be custom-made to meet the criteria established for this investigation. The problem was approached by first considering the objectives for which the apparatus was being designed; i.e., establishing a criteria for the design. In following this approach the end result may appear to be somewhat unorthodox for this type of apparatus. The objective was to develop a device which would measure the angular distribution of intensity or "scattered" radiation from a "cloud" of particles which had been irradiated by a ray of energy. It was desirable to measure the angular distribution of intensity through a range of 180 degrees, that is from $\theta = 0^{\circ}$ (forward scattering) to $\theta = 180^{\circ}$ (backward scattering), with the angle θ being defined as that angle between the direction of the scattered energy and the direction of the incident ray. Continuous angular scanning was considered more desirable than the less acceptable method of obtaining intensity readings at discrete angles. The "cloud" of particles was to be irradiated with monochromatic energy, or a device would be designed to measure the monochromatic intensity of the scattered radiation from the "cloud." The "cloud" of particles was not to be suspended in a cell, tube, or container that would introduce extraneous cell reflections or require the scattered light to traverse media with different refractive indices, since it was desirable to measure the scattered intensity of particles of irregular shape and size dispersed in air. Also, since "single scattering" phenomena was being investigated, it would be necessary to construct a particle generator that would provide a "cloud," or what might be called an aerosol, of finely dispersed particles. It was vitally important that the design provide for the following: Uniform distribution of particles supplied continuously for the period of time required to take measurements, controlled density, and the ability to reproduce conditions consistently. It was also recognized that it would be necessary to collect the particles through the use of some suitable device, if a continuously moving cloud were considered, and either to discard the particles or reclaim them. To extend the versatility of the apparatus to include extinction measurements, it would be necessary to find some method of determining the density of the "cloud."

With the criteria established, a configuration was visualized, and after many compromises the design was formalized. In presenting a description of the apparatus, a general description will be given first, which will be followed by more intricate design details of the component parts.

GENERAL DESCRIPTION OF APPARATUS

Aluminum oxide particles of irregular shape and size were dispersed in an air stream by a suitably-designed generator to form a poly-dispersed system of fluidized particles (See Schematic of Particle Generator Design). These particles were injected vertically, under air pressure, through a highly-polished tube 0.375 inch in diameter, forming a column of fluidized particles bounded by the ambient air (free stream). The relatively low differential pressure between the mainstream and the bounding surfaces, plus the kinetic energy of stream, were sufficient to permit the column of fluidized particles to remain essentially cylindrical for approximately 0.6-inch beyond the exit of the tube before diverging or "fanning out." It was this cylindrical region near the exit of the tube that constituted the specimen area. The stream tube was positioned concentrically through a 1-1/2-inch hole located in the center of a 36-inch rotating platform, on which was located a glo-bar source and source optics. The source optics consisted of a spherical mirror positioned with one of its foci on the glo-bar and the other on the specimen (See Figures 1, 2 and 3). The circular platform served as a pulley in the speed reduction mechanism which allowed the glo-bar source to be rotated at a constant speed in a horizontal plane while maintaining the focus of the incident ray on the specimen area. The scattered intensity was received by the optics located adjacent to the rotating platform and focused on the slits of a double-pass monochromator which permitted selective wave length detection of the scattered radiation. The monochromatic scattered intensity was detected by a thermocouple, amplified, and recorded on a strip chart. The fluidized particles being ejected from the tube were collected by a "bell-mouth" attached to a vacuum hose, and the waste particles were discarded. The bell-mouth device also housed the filters, screens and retainers used to collect the particles for weighing, which was necessary in particle-density determination.

ROTATING PLATFORM

A 36-inch diameter, 3/8-inch thick aluminum disc was mounted on a central hub which rotated freely on a close-tolerance ball-bearing mount. The disc and mount were designed with a 1-1/2-inch hole in the center to permit centering of the fluidized particle tube in the disc and to allow the mounting of the particle generator in a vertical position in a convenient location beneath the test bench. The disc was provided with a 15° off-axis slot, 10-inches long and 3/4-inch wide, which allowed flexibility in focusing the glo-bar source on the specimen for several arrangements of optics. A 1/2-inch V-type belt was attached in an inverted position to the circumference of the disc with machine screws (See Figure 4). The disc served as one wheel of the speed-reduction mechanism which controlled the specimen scanning rate. The driving motor was a Master gear-head motor, Model 104530, 1/8 HP, Type RA, manufactured by the Master Electric Company, Dayton, Ohio. The output shaft RPM was 4.9. The disc was belt-driven through a pulley reduction system, the arrangement and details of which can be seen in Figures 3 and 4. With this reduction system the

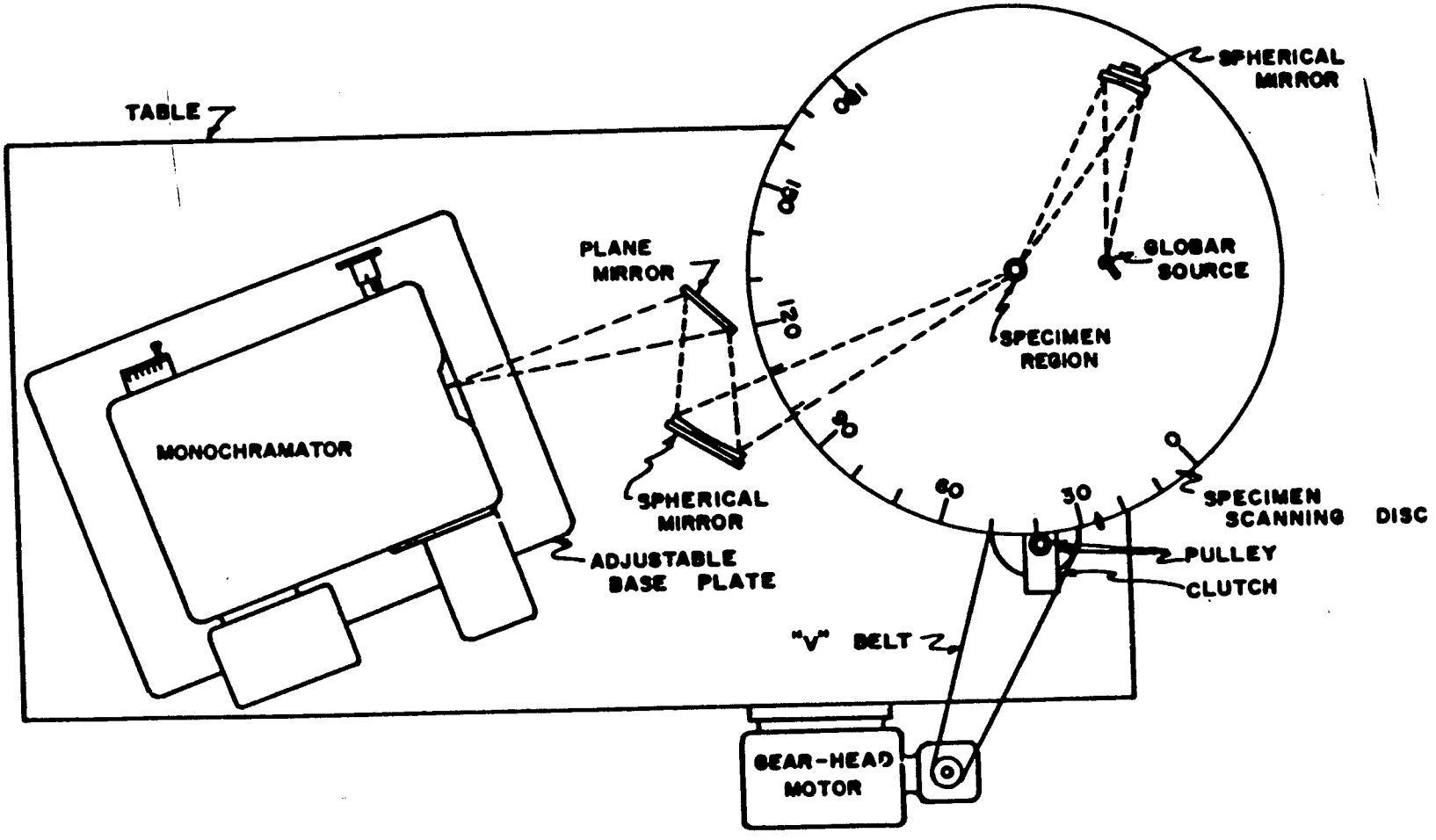

Figure 1. Plan View Schematic of Equipment

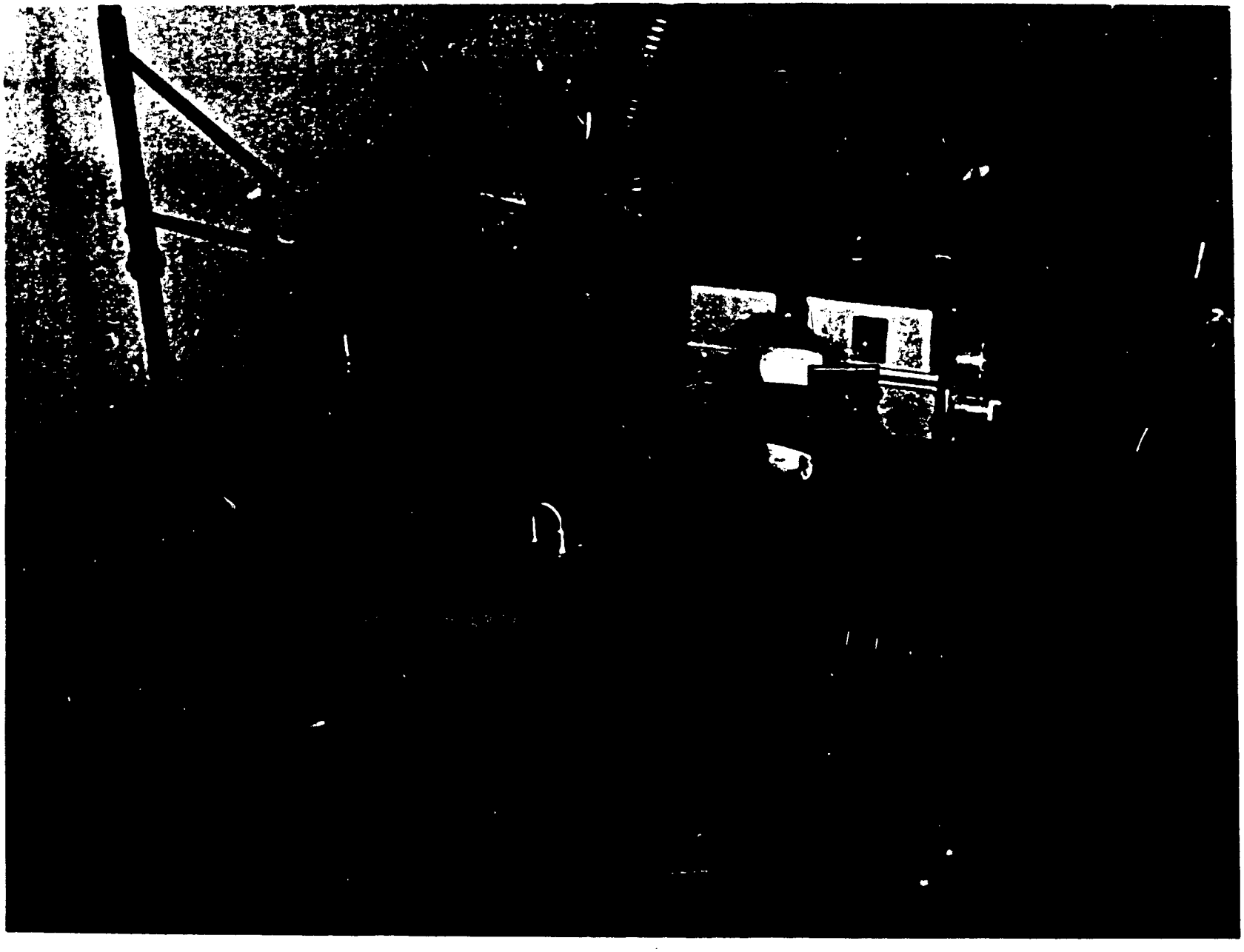

Figure 2. Radiation Scattering Equipment. View 1

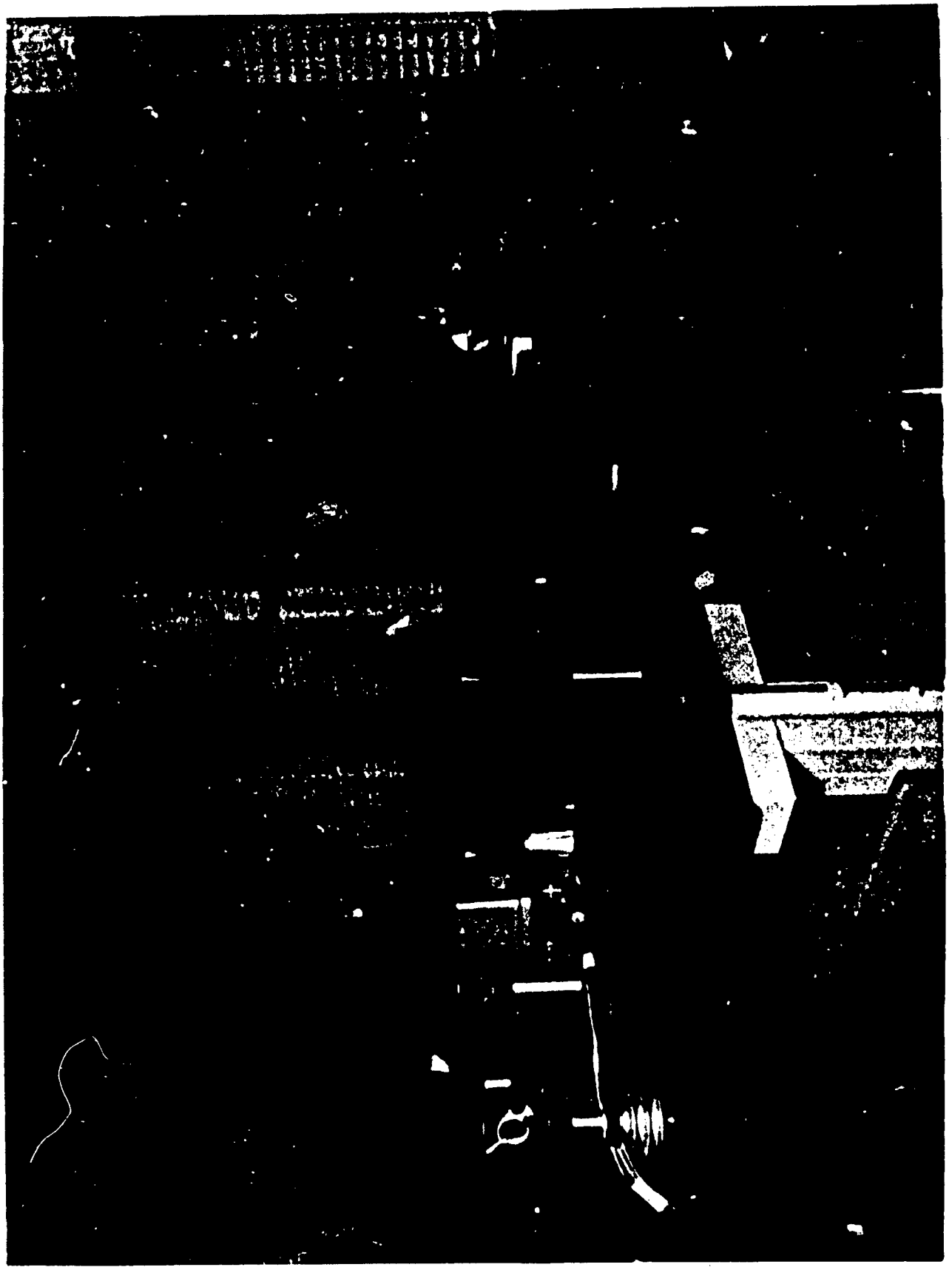

Figure 3. Radiation Scattering Equipment. View 2

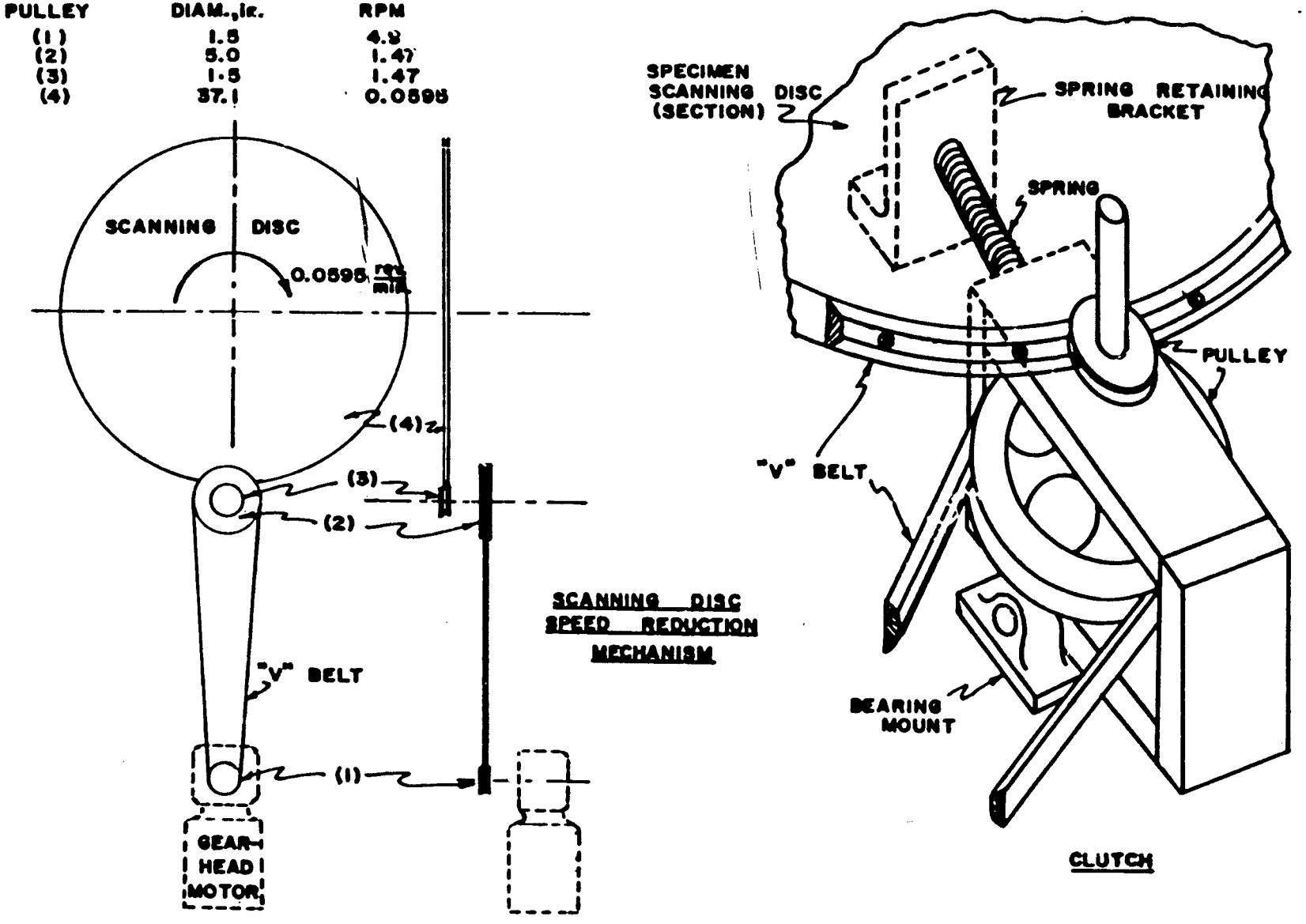

Figure 4. Schematic--Scanning Disc Speed Reduction Mechanism and Clutch

Figure 5. Radiation Scattering Equipment, View 3

disc (source platform) rotated at a constant speed of 0.0595 RPM; consequently, 8.4 minutes were required to scan the specimen through 180 degrees. For this experiment only one scanning speed was used; however, the scanning speed could have been varied without difficulty by changing pulley sizes. Since a reversible gear head motor was not available, the speed reduction mechanism was provided with a clutching arrangement which allowed manual movement of the disc to any desired position. The manual control was realized through a simple spring load clutch (See Figure 4).

OPTICAL SYSTEM

Two optical systems were considered for this investigation. The first system made use of two 267-mm. focal length, 18° off-axis parabolic mirrors. One off-axis mirror was focused on the glo-bar source provided for the irradiation of the fluidized column of particles with a collimated beam of energy. The second off-axis mirror, which was used to collect the intensity scattered from the column of particles, was then focused onto the slits of the monochromator. This optical arrangement did not prove satisfactory since the collimated beam of energy directed onto the specimen area was not of sufficient intensity to detect adequately the intensity scattered by the particles. This difficulty could be alleviated with a source of higher intensity than that provided by the glo-bar; however, this was not feasible in this investigation. Therefore, an alternate system was used which proved to be quite satisfactory.

The physical arrangement of optics for the alternate system can best be understood by referring to Figure 6. In this system a 13.9-cm. focal length, 7.9-cm. diameter spherical mirror was used to focus the glo-bar source onto the specimen area. An image of the glo-bar source 0.977-cm. (0.385 in.) in width and 3.01-cm. (1.875 in.) in height was projected onto the specimen region. Thus, the column of fluidized particles was irradiated by a rather intense beam of energy of width approximately equal to the width (0.952 cm.) of the particle column. The source optics were mounted on the rotating platform as described in the previous section. A second spherical mirror with a 27.94-cm. focal length was positioned with one of its foci located at the center of the specimen region and the other reflected by a plane mirror onto the slits of the monochromator. The section of the column of fluidized particles (specimen region) which was "seen" by the monochromator slits was an area 0.264-cm. wide and 0.91-cm. high. It can, therefore, be visualized that the region of the specimen as "seen" by the detection device can be considered as being constant for all directions of angular measurement; i.e., for all measurements of the angular distribution of intensity scattered by the particles an equal region of the specimen section was considered.

In order that the monochromator slits would not "see" the specimen region except through the reflections dictated by the arrangement of the mirrors, an opaque non-reflecting surface was placed in the direct line of sight.

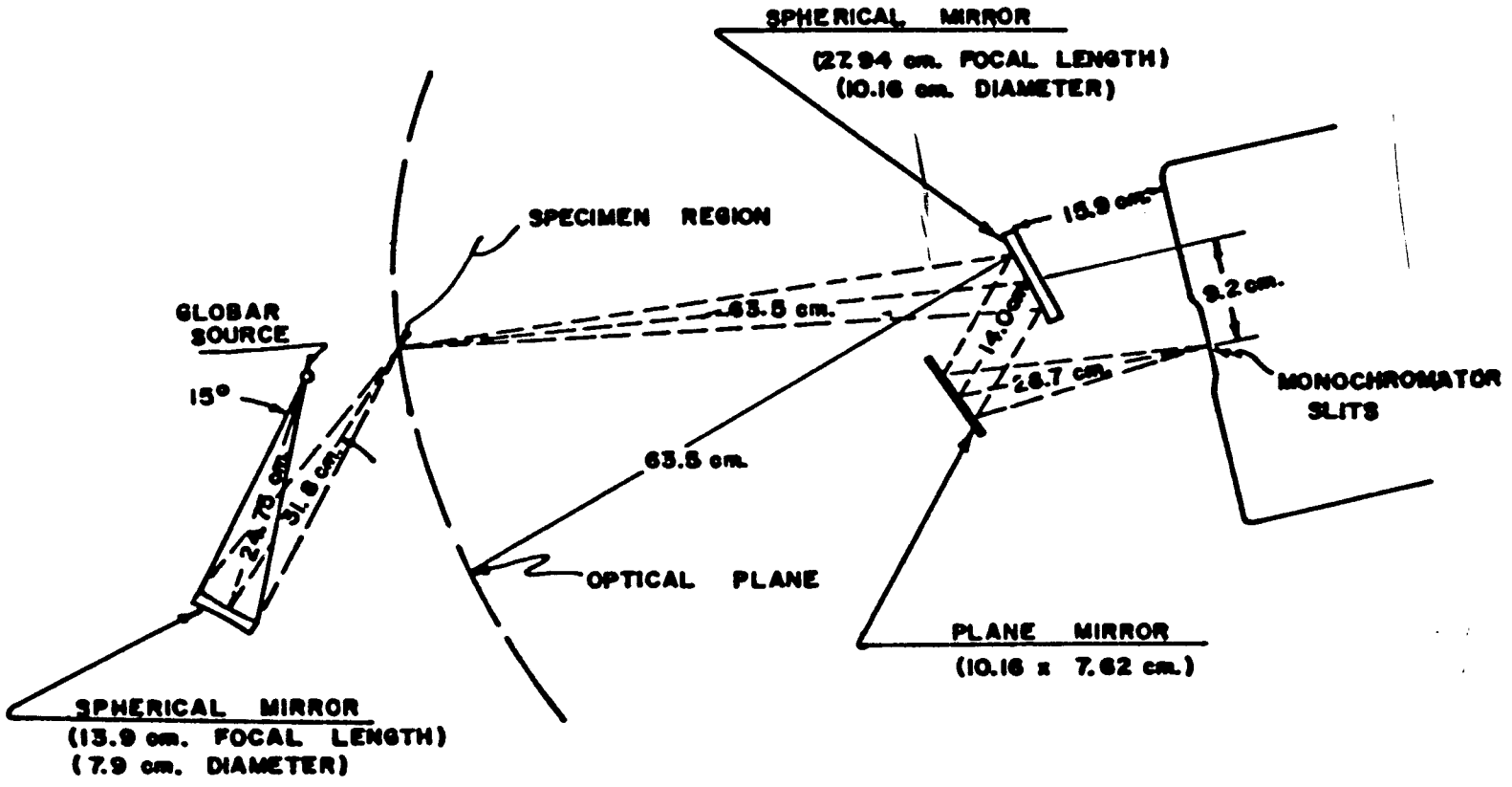

Figure 6. Optical Layout

All mirrors used in the optical system were front surface aluminized, of high quality, to minimize optical imperfections. All mirror mounts were designed to give wide latitude in adjustment.

MONOCHROMATOR

The monochromator used for this experiment was a Perkin-Elmer Model 99, single-beam, double-pass, instrument. The path followed by the radiant energy through the monochromator may be best understood by referring to the optical schematic, Figure 7. The infra-red radiation beam focused on the slit S-1 was collimated by the off-axis paraboloid M-3, and a parallel beam traversed the NaCl prism P for a first refraction, Path 1, after which it was reflected by the Littrow mirror M-4 through the prism for a second refraction and focused by the paraboloid at the corner mirror M-6 through the mirror M-5, Path 2. The radiation, after being chopped, was reflected again by mirror M-5 to the paraboloid along Path 3 and again traversed the prism and was reflected back along Path 4 for reflection by M-7 and brought to a focus in a spectrum falling across the exit slit S-2. The exit slit passed only chopped radiation of a narrow wave length range whose band width depended on the slit width S-2 and whose mid-band wave length depended on the Littrow angle setting. The band width which passed through slit S-2 was focused by plane mirror M-8 onto spherical mirror M-9 and then onto the thermocouple T-C. Since the energy focused by the ellipsoid mirror M-9 onto the thermocouple was chopped, a pulsating signal was produced. The purpose in chopping the energy was to produce an AC voltage at the thermocouple which was proportional to the radiant power, or intensity, of the beam. It was this signal that was amplified and recorded by the electronic potentiometer. Since the wave length band falling across slit S-2 depended on the Littrow angle setting, the wave length reaching the detector could be controlled by rotation of the Littrow mirror. Consequently, a wave length control could be manually operated which could detect monochromatic radiant energy of a known wave length. One of the advantages of the double-pass monochromator was that the scattered light which is normally present after a single pass (due to dust and optical imperfections) was dispersed out of the path by the second pass in the same manner as it would be with a double monochromator. The NaCl prism instrument was used in this instance because of its greater range and simplicity, even though the dispersion could have been obtained by a diffraction grating, which in general would give higher dispersions than a prism instrument but which had the disadvantage of being usable only over a short spectral range. The usable range for a sodium chloride prism was between 0.2 to 17 microns; however, the manufacturer recommended a range between 2 and 15 microns. The long wave length limit was set by prism absorption, whereas the shorter wave length was limited by experimental circumstances such as light scattering or limited dispersion. One of the chief disadvantages of the sodium chloride prism was its poor resistance to water vapor, which required that particular attention be given to the instrument to protect it from a humid atmosphere.

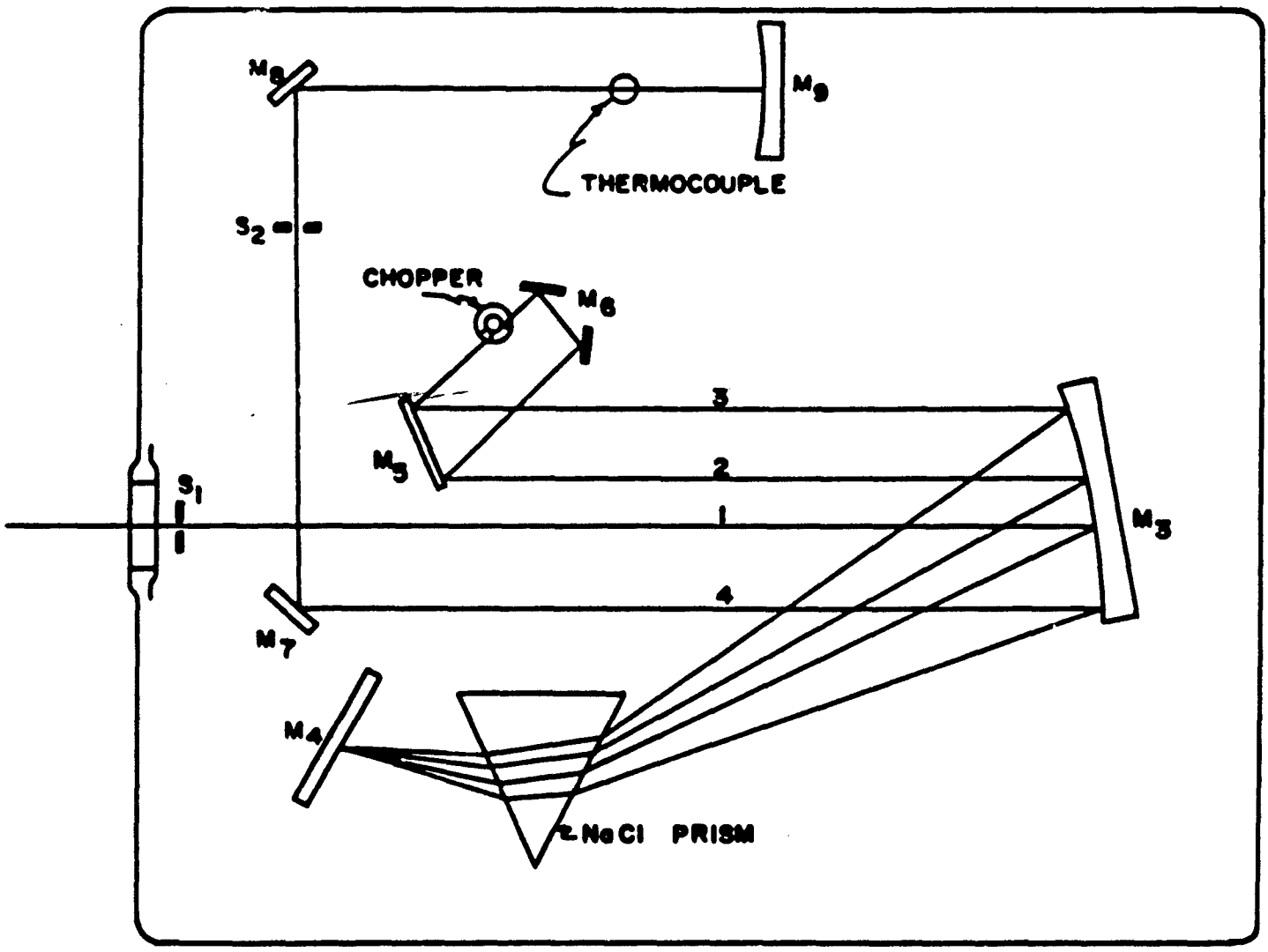

Figure 7

Monochromator Optical Layout

Consequently, a heater was provided to aid in drying the atmosphere surrounding the prism at all times. In addition silica gel crystals (a mild dessicant) were kept in a container within the monochromator as a further aid in protecting the sodium chloride prism.

To supplement the wave length calibration curve supplied by the manufacturer, a calibration curve (Figure 6) was made for the instrument used in this experiment. The calibration was made using a sample of polystyrene in the atmosphere, with additional points of calibration being obtained by "running the spectra" for an atmosphere that included the 15-micron water vapor region, the 6-micron water vapor region, and the CO_2 absorption band. A total of 8 polystyrene points, 5 CO_2 wave lengths including the CO_2 doublet, and 8 wave lengths in the 6-micron region were located, giving a total of 21 wave lengths which were definitely identified and from which a calibration curve could be drawn. The calibration curve for the monochromator used in this experiment is included in the appendix, together with a tabulation of the specific wave length identified in the calibration. This calibration was repeated on three different occasions on three different days, and the three calibration curves were identical. Therefore, the calibration curve obtained was considered acceptable. The spectra obtained for this calibration are not included in this report but are on file at the Engineering College, University of Oklahoma, Norman, Oklahoma.

THE INFRA-RED SOURCE

The ideal infra-red source is a black body radiator. The nearest approximation to the ideal source is a heated cavity. However, these are very difficult to build, and the energy requirements are usually quite high. The most common source is the so-called glo-bar, which is a silicon carbide rod. Sometimes a Nernst Glower, which is a bonded mixture of rare earth oxides in a rod form, is used. The rods are usually electrically heated to temperatures in the range 1200 to 2000 degrees Kelvin. These are practical approximations to the black body. The glo-bar was the source used for this experiment. The glo-bar rod was silver-coated on the tips for better contact, and the temperature of the glo-bar was approximately 1100 degrees Centigrade, when 200 watts of energy were supplied. The energy distribution was similar to the black body radiation for the temperature corresponding to the temperature of the glo-bar. Therefore, the peak energy occurred at about 2.5 microns. The glo-bar was surrounded by a water-cooled jacket.

INFRA-RED DETECTORS

Several types of infra-red detectors have been devised; however, the most commonly used are of the servo or the thermo type, such as the thermocouple, the bolometer, or the pneumatic cell. With the thermo detector it is necessary to distinguish signal changes caused by ambient temperature from those caused by radiation. In the instrument used for this experiment the detection of the different signals was accomplished by chopping the radiation beam at a frequency of

BLANK PAGE

13 cycles per second and measuring the AC signal at this frequency; however, this method required that the detector have a very short response. The thermocouple type of detector was used in this experiment. It was a high-speed type thermocouple, which consisted of a blackened, gold-leafed target welded to pillars made of one of the active elements, while the other active element, of fine wire, connected the target to one of the silver leaves, with the other leaf soldered to the pillars at one end. Both leaves were run through a ceramic rod and were soldered to an output plug at the base of the housing. The average thermocouple characteristics are: sensitivity, 4 micro-volts per micro-watt; response time, 75 percent of D-C response at 13-cycle modulation; target size, 0.2 x 2 mm.; resistance, 12 ohms. The signal from the thermocouple was fed through a low impedance preamplifier before entering a 13-cycle amplifier where it was rectified. The rectified signal passed through a network of filters before entering a Leeds and Northrup Speedox Strip Chart Recorder.

PARTICLE GENERATOR AIR SUPPLY SYSTEM

The particle generator was supplied with filtered dry air. Upon leaving the compressor the air entered a storage tank (approximately 21 ft.^{3} capacity) which dampened any pulsations induced by the reciprocating action of the compressor; consequently, a steady flow of air was provided. Air passed from the reservoir at 100 psig through a condenser fabricated from 15 feet of 3/8-inch copper tubing formed into 5-inch diameter coils. A water trap was located at the bottom of the condenser, which was immersed in a 55-gallon drum filled with cold water (and/or ice as required). This served to condense part of the water from the air. The air supply was then diverted through a Norgren 12-002 centrifugal-type oil-and-water filter before passing through two chambers containing a dessicant (approximately 100 cubic inches of silica gel) at room temperature. By means of a manually controlled pressure regulator, the air was regulated to approximately 30 psia before it was passed through an 8-foot heater capable of controlled heating of a 2 cfm air supply to a temperature of over 250° F. The temperature of the resistance-type heater was controlled by a variable auto transformer Powerstat type 236, 2.5 kva, manufactured by the Superior Electric Company, Bristol, Connecticut. The air temperature was sensed by an iron-constantin thermocouple positioned in the air line and it was measured by a Leeds and Northrup potentiometer, Model 8657C. The temperature-controlled air was passed through a 0-100 psig pressure gauge before entering the precision-bore, variable-area flowrater. A Stabil-Vis Flowrater, 0-2.55 cfm, manufactured by Fischer and Porter, Hatboro, Pennsylvania, was used to measure the air-flow rate. From the diagram (Schematic of Air Supply System), it can be seen that the air passed from the flow regulator through a Norgren Type 11-018 pressure regulator and through a 0-30 psig pressure gauge, manufactured by the Ashcroft Instrument Company, before it entered the particle generator. This arrangement supplied well-regulated, steady-flow, dry air to the particle generator at a continuous rate (up to 1.5 cfm) for an indefinite time period. For the measurements made and reported herein

the air was not pre-heated since the experiment did not require it; however, the heating device was included to enhance the versatility of the equipment.

AEROSOL COLLECTOR AND VACUUM SYSTEM

Studies were made on the feasibility of reclaiming the particles for re-use in the experiment; however, the nature of the aluminum oxide particles used for this particular investigation precluded their reclamation and re-use.

In the actual investigation two vacuum systems were necessary: One system to collect all waste particles when particle density measurements were not being taken; the other system for particle density measurements, exclusively. The purpose of the latter system will be related more fully under the section describing particle density measurements; however, the two systems were essentially the same and the details of both will be given here.

In both cases the steady stream of fluidized particles (aerosol) flowing from the specimen region was collected by a 2-inch flexible hose to which was attached an industrial-type vacuum cleaner (see Figure 5). Some of the particles were trapped by the commercial filter provided with the vacuum cleaner; however, the commercial filter was not suitable for complete filtering. Consequently, some particles contaminated the driving motor, necessitating frequent cleaning and periodic maintenance of the vacuum system. Attached to the flexible hose was a bell-mouth entrance which was followed by a section in the line for housing screens, filters, and their respective retainers.

The two bell-mouth entrances for the separate systems were located adjacent to one another and were fastened securely to a movable cantilever arm. Either of the two systems could be put into operation by rotating (or swinging) the proper bell-mouth inlet into position.

The two types of vacuum cleaners used for this experiment were an industrial vacuum cleaner (Black and Decker, Type A) and an ordinary household-type vacuum cleaner. Vacuum cleaners of different types were used because of availability, not performance.

It should be pointed out that a vacuum cleaner selected for this purpose should be "oversized" to assure sufficient vacuum for complete collection of the particles, for the following reason: The aluminum oxide particles used in this investigation were of a flaky nature and were in the 1-40 micron range. The handling problems associated with an aerosol of such material can cause a great deal of difficulty, even at low concentrations. If great care is not taken to collect and discard all waste particles, the equipment and surrounding working area will quickly accumulate a "dust" coverage of aluminum oxide particles. Usually a paint thinner, or an equivalent solvent, is necessary for removal of the aluminum dust. The finely

atomized aerosol, after becoming suspended in the atmosphere, has a settling rate approximately equal to that of ordinary house dust and can easily be inhaled into the respiratory system, causing a health hazard. The possibility of this hazard is only presumed by the writer and is not founded on medical evidence. Experience has shown that the vacuum system used in this experiment was barely adequate and left much to be desired.

PARTICLE GENERATOR

The particle generator design was based on an investigation of aerosol generators conducted at the University of Oklahoma, to be reported in a master's thesis. Basically, the idea was to feed the powder mechanically into a region in which air jets could be used to disperse the particle into an aerosol. The particle generator design developed for this study was perfected after several modifications of the original conception of the idea. Early experiments indicated a need for a device that would eject and continue to disperse the particles from the region in which the powder in compact form was separated into small aggregates. The early experiments also pointed up the importance of air-jet velocity and feed-rate regulation. All future developments bore out this observation--the particle feed rate and the air flow rate were critical adjustments for a well dispersed uniform flow of fluidized particles.

A general description and principle of operation of the generator follows.

The aluminum powder in packed form was fed from the 6-inch particle cartridge, by a 3/8-inch diameter piston, into the dispersion and ejector tube. Refer to Figures 10 and 11. The dispersion and ejector tube consisted of a tube with a 3/8-inch bore with small holes drilled through its walls through which air, under pressure, formed jets which broke up the packed powder into small aggregates and dispersed and ejected them as a fluidized stream of particles. The first set of jets was four equi-spaced holes drilled with a #70 drill tangentially to the bore.

The purpose of the first set of tangentially drilled holes was to provide a vortex or "swirling" motion which would disperse the powder from its compact form more readily. Downstream 3/16-inch from the first set of holes was another set of four equally-spaced holes, drilled with a #70 drill, with their centerlines directed at a 45-degree angle upstream and 3/32-inch off-center, i.e., spaced 3/32 of an inch off of, but parallel to, the diametric axis of the bore. The purpose of this second set of holes was to propel the particles in aggregate form in a spiralling motion along the stream tube and to continue the dispersion of the aggregates into individual particles.

The third set of holes was located approximately 2-5/16-inches downstream from the second set, and the holes were drilled at a 45-degree angle in a downstream direction, their centerlines forming a

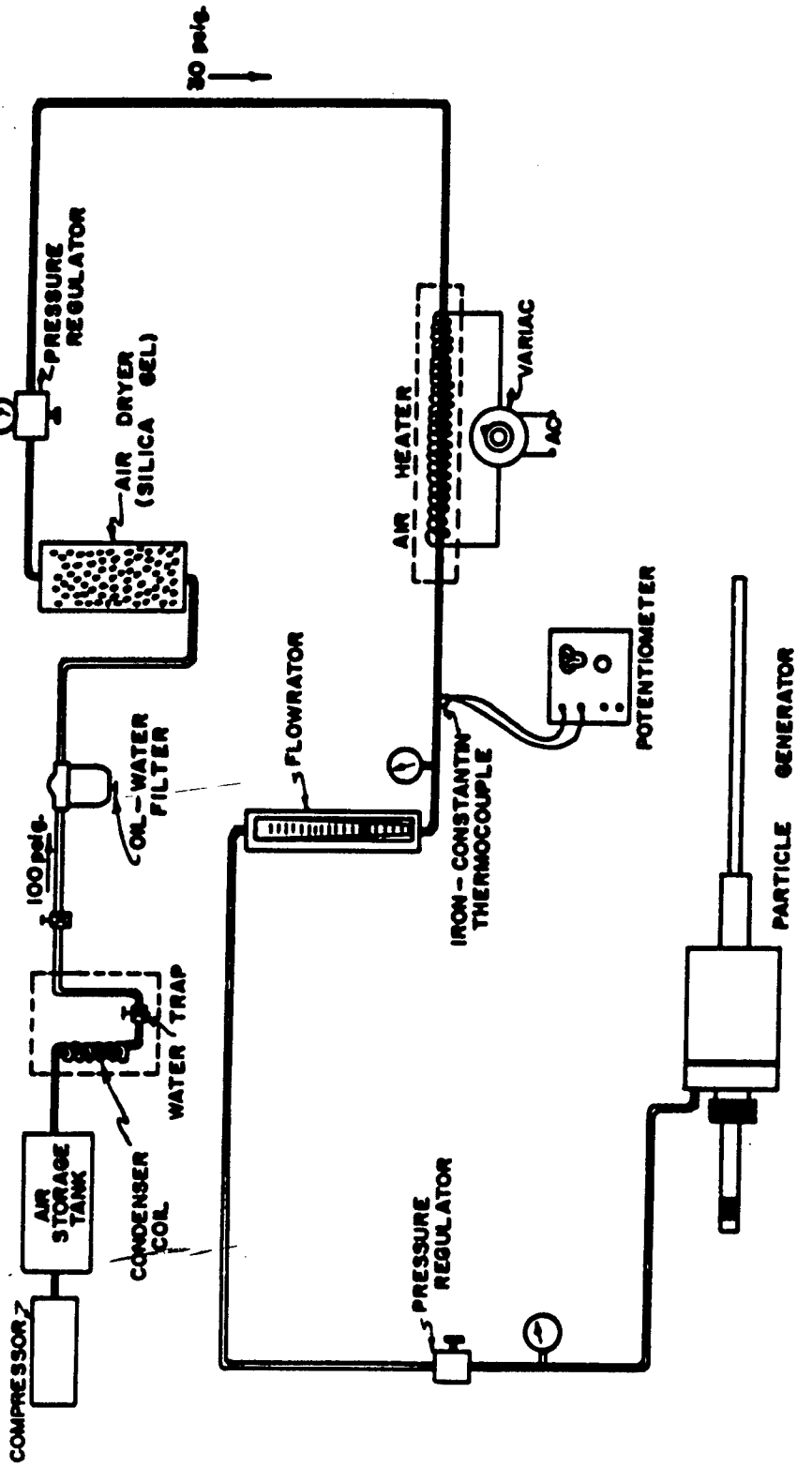

Figure 9

Schematic of Air System

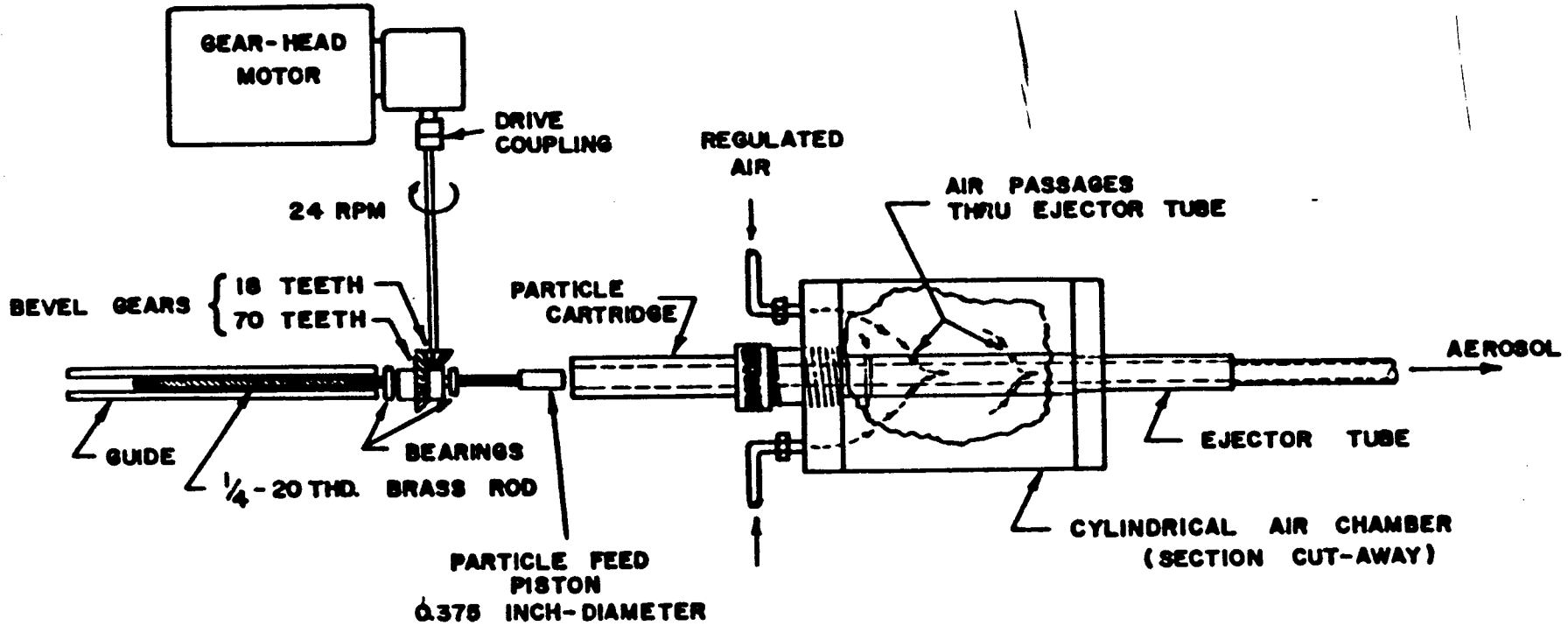

Figure 10

Schematic--Particle Generator and Feed-Mechanism

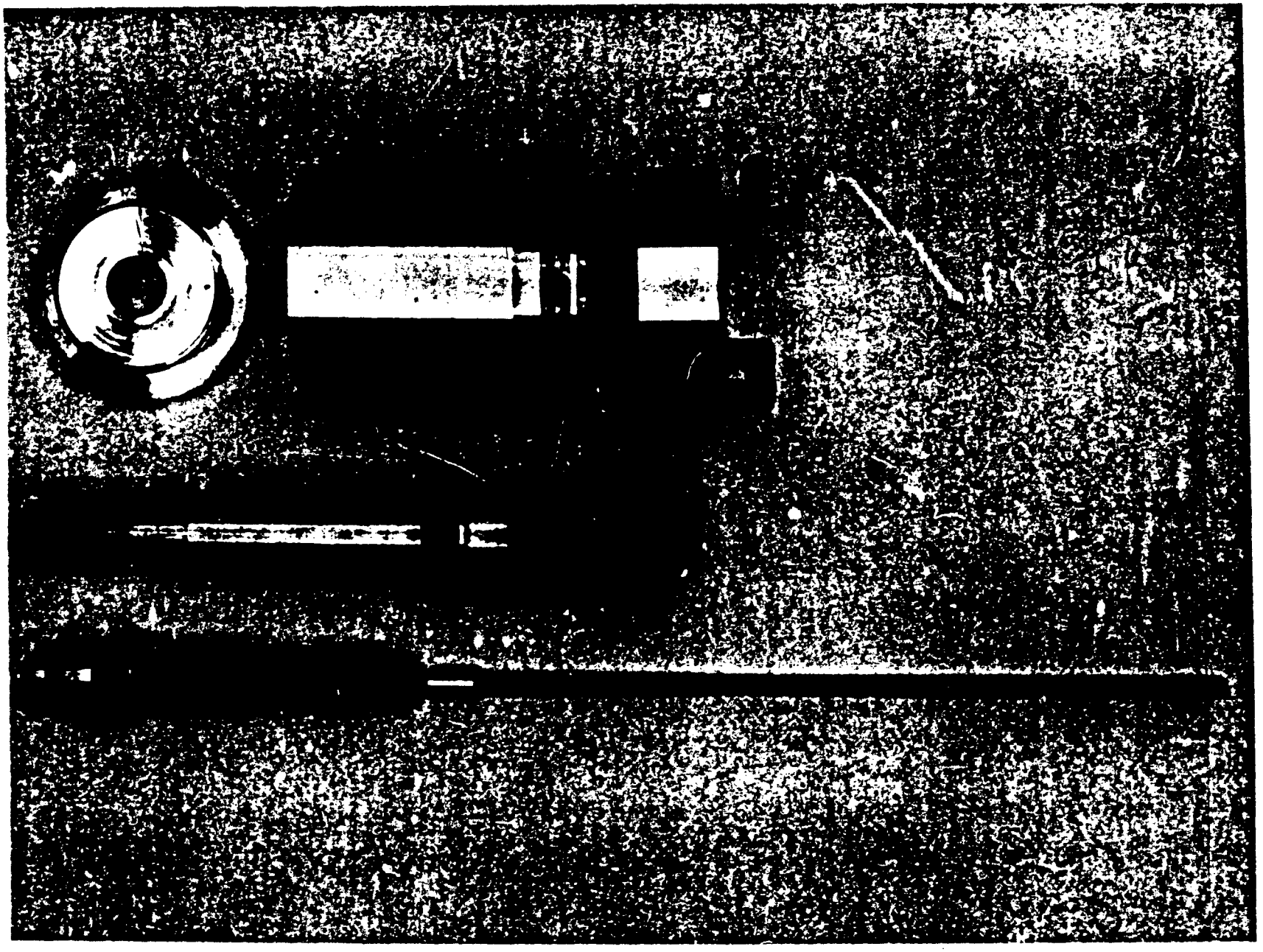

Figure 11. Particle Generator. Exploded View

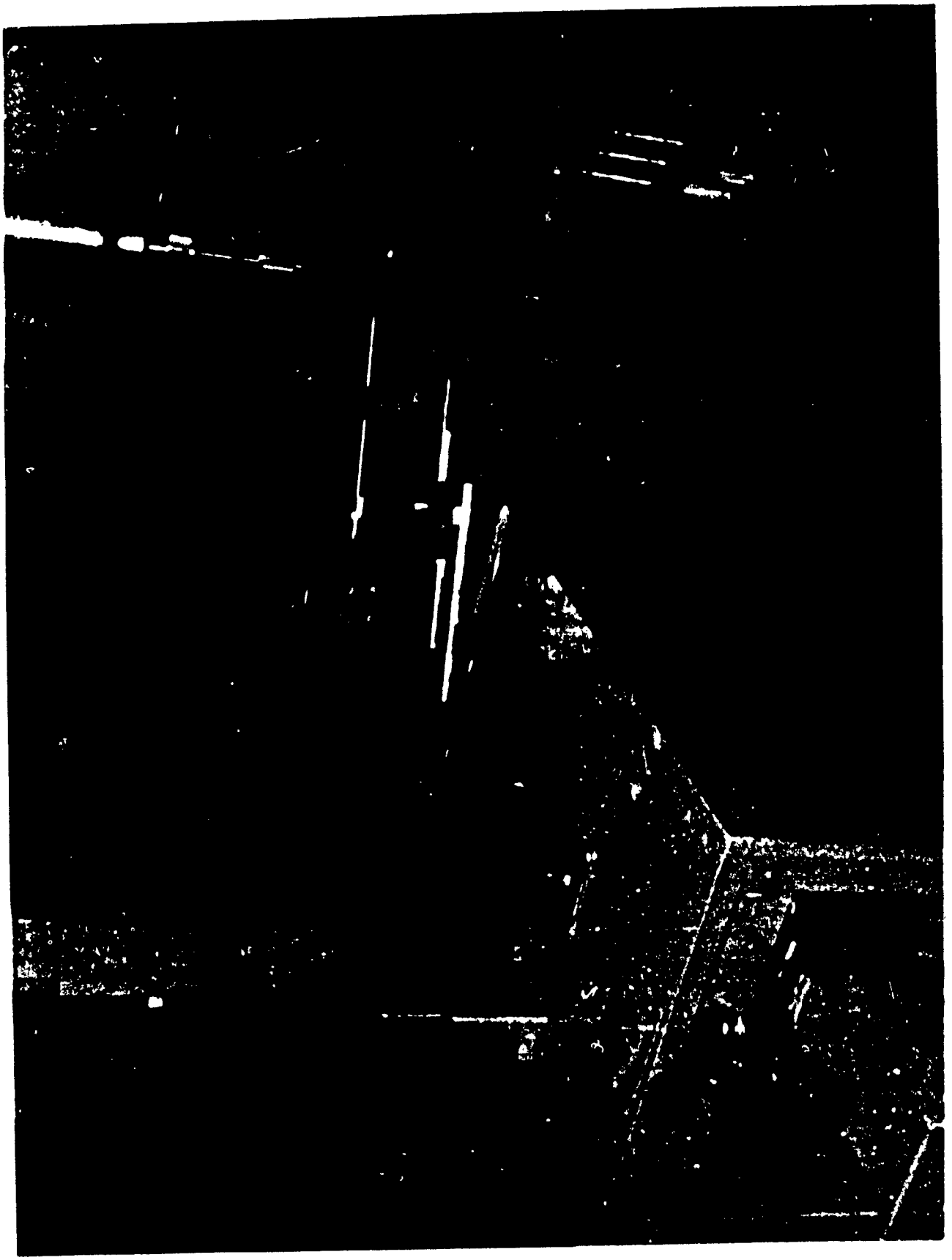

Figure 12. Particle Generator and Feed Mechanism

cone whose apex was located at the center of the bore. The intent of the third set of jets was to further accelerate and disperse any aggregates that remained in the powder, so that a finely-dispersed, uniform stream of fluidized single particles was ejected from the generator. Surrounding the ejector tube is an air-tight cylindrical chamber which provides a plenum chamber of high pressure (normally 6-9 psig) air which is exhausted as small air jets through the walls of the ejector tube. The cylindrical chamber is supplied with pressure-controlled air through two 1/4-inch copper tubes coupled to the head of the chamber.

The entire particle generator design was based on the ejection-pump principle, which is essentially the principle by which a primary stream of high-pressure fluid is ejected into a region of low pressure fluid (called secondary fluid). The kinetic energy of the primary stream establishes a pumping action which will pump a secondary fluid into a mixing zone where the primary fluid and the secondary fluid are mixed prior to being ejected downstream.

Summarizing, the first set of jets was used primarily to break up the packed particles into smaller aggregates; the second set of jets continued to break up the particles into a finer dispersion and to create a turbulence and a secondary fluid composed of small aggregates of particles; whereas the third set introduced a primary fluid, located upstream, with which kinetic energy was associated which established a region of low pressure in the neighborhood of the so-called secondary fluid. The action of this third set of jets accelerated the movement of the secondary fluid downstream to be mixed with the air of the so-called primary zone.

The particle feed mechanism can best be understood by referring to the system schematic (Figure 10). The particles were forced from the packed particle cartridge by an 0.374-inch diameter piston, 1 inch in length. A gear-head motor driving a 45-degree bevel gear arrangement translated a 1/4-inch-20 threaded brass rod to which the piston was attached. The piston rate of travel was 0.309 inch per minute with the gear ratios and motor shaft speed indicated in the schematic (Figure 10). For this arrangement 19.45 minutes was required to discharge a fully-packed particle cartridge 6 inches in length. Obviously the particle feed rate could be varied through judicious selection of the bevel gear ratio and/or the number of threads per inch on the feed rod. Another method by which the feed rate might have been varied was through a gear reduction mechanism or gear train placed between the motor output shaft and the bevel gears. To increase the versatility of the equipment a small gear train was designed (not shown in photographs) which permitted the motor output shaft speed to be increased or decreased by a factor of two.

Four brass particle cartridges were fabricated so that a greater length of time for taking data could be provided before it was necessary to repack the cartridges. The design of the cartridges, particularly the design of the coupling between the ejector tube and the particle cartridge, was achieved after attempted use of other designs.

As can be seen from the drawings, the advantage of the design used lay in the fact that bore alignment could be maintained between the ejector tube and several cartridges.

PARTICLE CARTRIDGE PACKING PROCEDURE

It was soon realized that the technique for packing the particle cartridge had an important effect on the dispersion of the particles into an aerosol. The procedure, determined through trial and error, and found to be the best method for conditions of this investigation, is outlined below. Experience had shown that success in obtaining a uniformly-dispersed aerosol depended upon several factors; namely, the type of particle or powder used; the particle feed rate; the air pressure used in the particle generator, i.e., the velocity of the air jets used to disperse the particles; and the compactness of the particles within the cartridge. Of the influencing factors mentioned, the proper technique of packing the particles was the most difficult to acquire.

One of the important things to remember in packing the cartridge was that a procedure must be defined and consistently used. The procedure used in packing aluminum powder of the consistency of the 40XD powder may differ from that used in carbon powders or, for that matter, aluminum powder of different size and different shaped particles. However, a procedure based on experience and needs of the user must be set up. The procedure that follows was one that was felt to be satisfactory for this experiment, and it proved to be quite successful. It was found, also from experience, that a non-uniform distribution of the particles resulted from any deviation from a set procedure which greatly influenced the results.

The first step of the procedure was to fill the cartridge with the aluminum powder. No attempt was made to pack the powder within the cartridge since experience showed that a rather loose pack was desirable for, if the cartridge was packed too tightly, binding of the piston within the cartridge would result, causing a stoppage of the flow.

The second step of the procedure involved shaking the cartridge for a period of two minutes on a sieve shaker. This shaking process was not, in essence, a vibration of the cartridge, but was a tapping of the cartridge to jar the particles into a more compact form. The particle cartridge was allowed to tap against a vibrating piece of wood placed on the shaker platform in a motion with a frequency of approximately the order of 300 cycles per minute. It was this tapping motion that caused the particles to settle within the cartridge.

After the two-minute "jarring" procedure, the cartridge was again filled with aluminum powder in a loose-packed condition. Once again the two-minute "jarring" procedure followed. The second two-minute tapping procedure was followed with six one-minute tapping periods, and between each of these periods the cartridge was refilled with aluminum particles. Consequently, the cartridge was tapped for a

total of ten minutes for each packing of a cartridge. It was found from experience that the length of time used in shaking influenced the compactness of the aluminum powder within the cartridge; i.e., longer periods of vibration resulted in a more tightly-packed cartridge.

It should be emphasized once again that the tapping procedure was found to be a rather important part of the packing procedure, since a steady shaking or vibration of the cartridge did not give results as satisfactory as those obtained with this tapping procedure, and the procedure specified here was found to give particularly consistent results. A procedure different from the one specified could give equally good results; however, it should be obtained by a trial and error process.

PARTICLES UTILIZED FOR THIS STUDY

Since mono-disperse media are not found in nature, the apparatus was designed to measure the angular distribution of intensity (radiation scattering) from a poly-disperse system. The particles were selected, however, with certain criteria in mind. They were to be very irregular in shape, relatively non-conductive, non-uniform in size, but they were to fall within a size range of 1 to 20 microns with 90 percent in the 5 micron range.

Reynolds Aluminum Company donated their 40XD aluminum powder for use in this study, and they supplied the following specifications: average particle size, 6 microns (determined by the Fisher Sub-sieve Sizer); particle range, 0.1-44 microns; thickness, 1.7 microns; density, 2.58 g/cc (the difference between this and massive aluminum is due to the presence of stearic acid.); apparent density, 0.23 g/cc; coverage (water), 3500 sq. in./gram.

The 40XD powder was further analyzed for this investigation to confirm and/or complement the information supplied by the manufacturer. The average particle size was determined by microscopic analyses, using a 400-power Bausch and Lamb microscope and a hemacytometer.

The hemacytometer is an instrument that is used under ordinary circumstances for making red- and white-blood-cell count; however, it has other uses, including the determination of dust counts and counts in spinal salivary or other body fluids. The instrument is essentially a glass plate with ruled lines which form a grid work or counting area. The counting area is a 1-millimeter squared section, which is divided into 25 equal squares, each of which is separated by 3 ruled lines with a spacing of 2.5 microns between each of the lines. Each of the 25 squares is sub-divided into 16 squares, giving $25(10)^{-4}$ square millimeters for each area. In addition, the grid work is engraved 1/10 millimeter below the surface, thus giving a region of known volume. For example, for each of the 16 squares the known volume would be $2.5(10)^{-4}$ cubic millimeters or for a group of 16 squares the known volume would be $4(10)^{-3}$ cubic millimeters. Therefore, it would be possible to ascertain the number of particles

in a given volume, if this information were required. The method used in counting followed the procedures outlined by George E. Cartwright in the book Diagnostic Laboratory Hematology, published by Grune and Stratton, New York and London, 1954.

To prepare a sample for counting, a known quantity of aluminum powder was diluted with ethanol. Usually the quantity of powder was approximately 1/10 gram, whereas the suspending agent used for dilution varied from 25 milliliters to 150 milliliters. The mixture of powder and suspending agent was thoroughly agitated for one or two minutes before a sample was withdrawn by means of a thin glass rod, which had been drawn to a point by heating, and a droplet was inserted on the lined area of the hemacytometer. A thorough agitation of the solution was necessary, of course, in order to get a uniform distribution or an average sample. In order to insure that an average sample was being taken the volume of the suspending agent was varied, and a check was made to see if the number of particles counted was directly proportional to the increase in suspending agent. For each sample, the number of particles contained in 16 squares was counted. A total of 25 squared sections containing 16 squares each was counted. From these 25 counts the average number of particles per group of 16 squares was determined. This procedure was repeated for 25, 75, and 150 milliliter ethanol solutions, containing approximately 1/10 gram powder in each solution. Consequently, the total number of counts covered 100 16-squared sections, or a total of 1600 squares. The particle density calculation for the average of the 100 counts indicated that there were $6.05(10)^{9}$ particles per gram, or a mass of each particle was $1.655(10)^{-10}$ gram. The average particle size determination indicated that the average particle size was 7.9 microns across the largest diameter. The largest diameter was selected for a reference point, since the particles were very irregular in shape. An attempt was made to determine the approximate surface area. Several assumptions were made. If it is assumed that the particles are rectangular in shape, having the dimensions 2 microns in thickness, 7.9 microns in the longest length, and 4 microns in width, the total surface area is $110.8(10)^{-8}$ square centimeters. An equivalent diameter can be determined if it is assumed that the total surface area of the particle is equivalent to the surface area of a sphere from which the equivalent diameter is obtained, i.e., the diameter of a sphere whose surface area is equal to the surface area of the particle. A calculation using the dimensions of the particles described above will be 5.94 microns, or roughly 6 microns. It is interesting to note that the volume of the particle based on the above assumptions is $6.32(10)^{-11}$ centimeters cubed, which gives a density for the particles of 2.62 grams per cc, compared to the manufacturer's figure of 2.58 grams per cc.

The particles, when observed under a microscope (see Figure 13), can be seen to be very irregular in shape, having void spaces and possibly having fissures; consequently, the apparent density should be used. The actual volume of the particles was determined by displacement by the particles in a liquid of known volume, and an apparent density of 0.23 grams per cc was obtained. A check of the

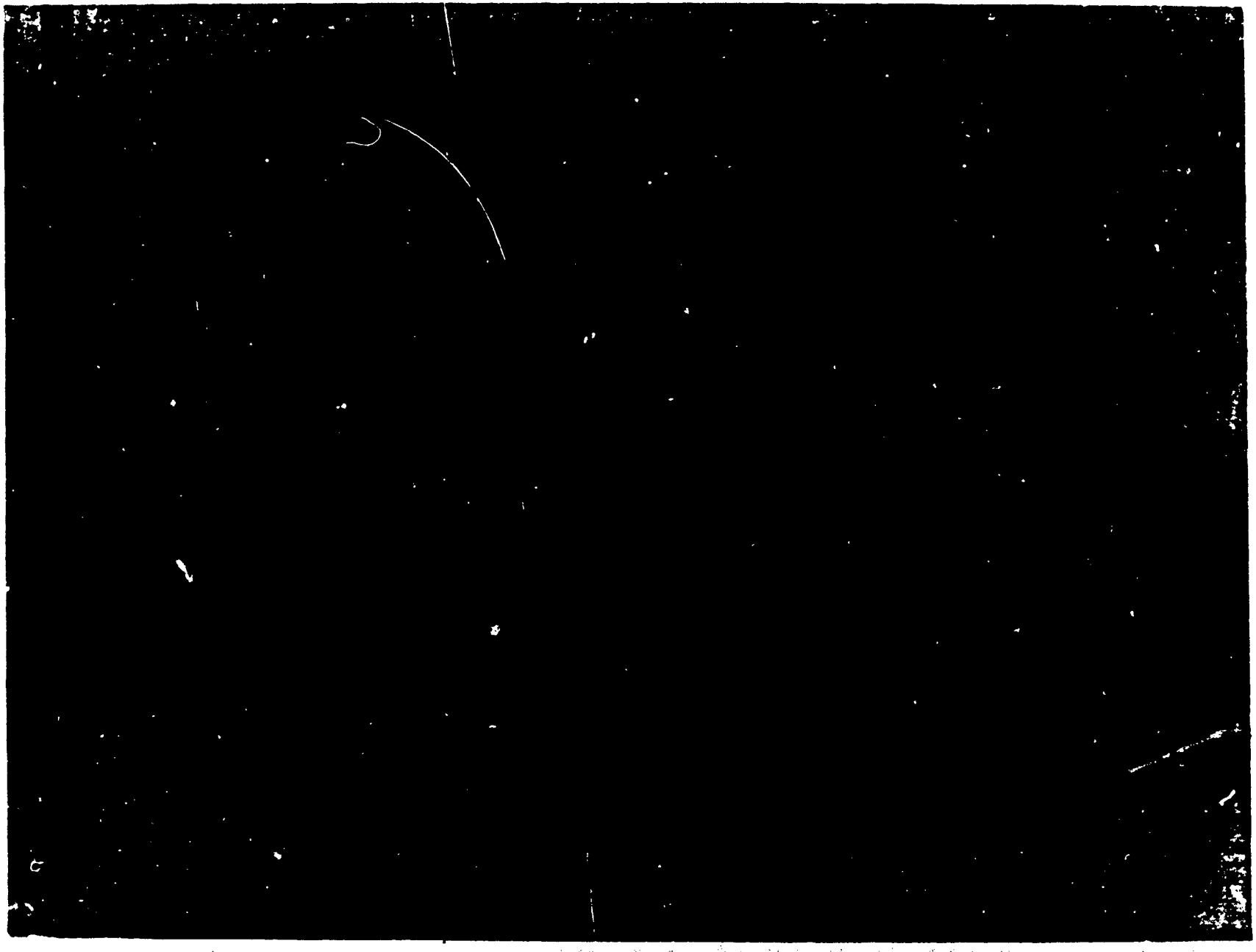

Figure 13. Microscopic View of Particles -- 400X

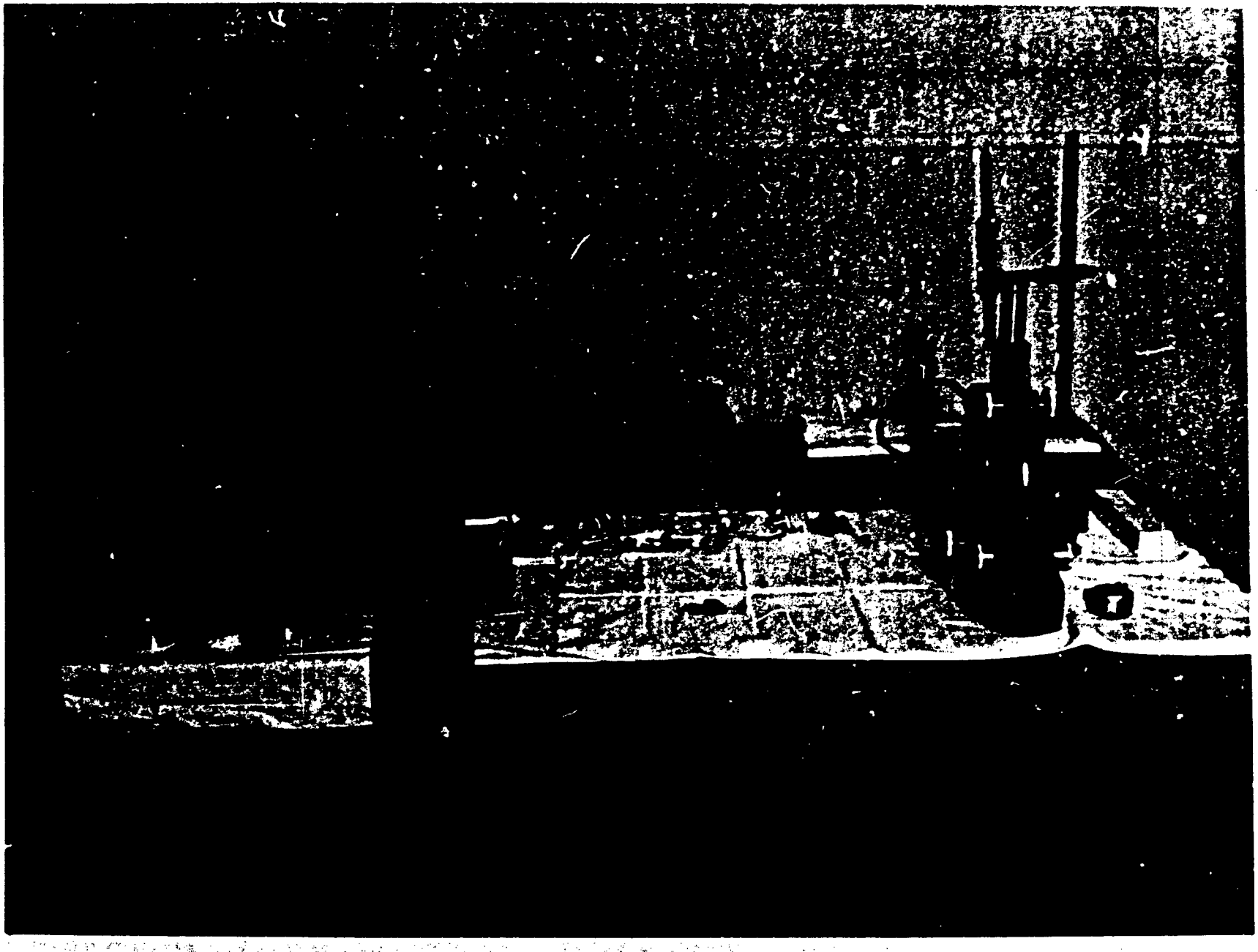

Figure 14. Particle Analysis Equipment

particle size has been made using the extinction equation, i.e., the extinction coefficient. A relationship exists between the mass extinction coefficient (β) and the extinction cross-section K^e as used by some authors. This relationship is,

$$\beta = \frac{3}{4} \frac{K^e}{r \rho_a}$$

where r is equal to the particle radius and ρ_a is equal to the mass density of the particle. From geometrical optics at large values of particle size parameter alpha, a plot of extinction cross-section as a function of alpha will generally be a constant value of 2.

Using a value for K^e of 2 and the calculated value determined by experiment of 11,350 for high values of alpha (low wave lengths), together with the ~~experi~~mentally determined particle density, the diameter of the particle was obtained. The calculated value for the particle diameter was 5.62 microns. This value compares favorably with the equivalent diameter of 5.94 microns which was calculated on the basis of an assumed dimension of the particle. Utilizing the latter method of comparing the extinction coefficient with the known value of the extinction cross section theoretical calculations, the calculated value of particle diameter of 5.62 microns forms a realistic comparison with the experimental values, and the values could be made to compare identically by adjusting the particle dimensions, since the particle dimensions were assumed on the basis of microscopic observations. The only calculated dimension was the average particle size which was the largest dimension and was based on a statistical average. However, the comparison just made is obviously a good indication of the accuracy of the results.

PARTICLE TUBE VELOCITY

The velocity in the tube from which the fluidized particles were being ejected was calculated in order to determine whether laminar or turbulent flow existed within the tube. The velocity in the tube was 29.5 feet per second, with a Reynolds number of 5,894, which indicates that the fluid in the tube was in a turbulent condition.

AEROSOL DENSITY MEASUREMENTS

Calculations of the mass extinction and mass scattering coefficients required that the density of the aerosol be known. First consideration conceived the idea that an aerosol density measurement be established for the period in which data was being taken. The original idea was to collect the particles that had passed through the specimen area for the entire period in which scattering and/or extinction data were taken on millipore filters and weigh them. Measurements of the air-flow rate, the time required to collect the particles on a filter, and the weight of the accumulated particles would provide information for the determination of the media density for a particular set of data. However, skepticism of this method was felt from the very beginning, because of the anticipated vacuum requirements necessary to collect all of the particles on the millipore filters. Other methods, such as drawing off or collecting all the

particles in an evacuated chamber, were analyzed. The scattering and extinction apparatus was being designed for the continuous collection of data to extend for periods of over ten minutes; consequently, the method of collecting the particles on a suitable filter or filters was considered the best compromise. This compromise revealed its inadequacies soon after the vacuum cleaners were purchased and the system was constructed. It soon became apparent that the vacuum system was inadequate for the filter would accumulate sufficient particles in one or two minutes to cover the filter, and an overloading of the vacuum cleaner motor followed.

A solution to this dilemma was a sampling technique, which necessitated the use of two separate vacuum systems. Instead of millipore filters, a readily available fibre-glass material that would filter particles down to 0.5 micron was purchased from The Fram Corporation, Tulsa, Oklahoma. This material proved very satisfactory and was used in all particle density measurements included in this report.

With the exception of the vacuum cleaner used, the two systems were identical in design. The collecting devices, including bell-mouth inlets, housing screens, and filters (See Figure 3), could be used alternately, and sampling could thus be conducted continuously. However, it was found later that the number of samples necessary for a given run could be reduced to one or two since the particle flow rate was comparatively steady for the period in which data was taken.

The air-flow rate was measured with a precision flowrater (included in description of air system) with 0-2.5 cfm range, calibrated in increments of 0.1 cfm. A flow rate corrected for inlet pressure and temperature was used in all measurements. The filters were weighed before and after collection of the particles on a beam balance capable of reading to 1/10,000 gram.

Calculations were made to determine the optical depth of the aerosol to see if single scattering phenomena could be considered prevalent throughout the test. The optical depth (τ) is defined as

$$\tau = \int_0^l \rho \beta \, dr \qquad \text{or} \qquad \tau = \rho \beta l \qquad (1)$$

assuming density and mass coefficient constants, and with l representing the length of path traversed by the ray of energy through the aerosol. The plot of the mass extinction coefficient as a function of wave length (Figure 39), indicates that β can be considered constant for a large range of wave lengths. Using a value of β equal to 11,350 ft^2/lb_m and the maximum and minimum density values obtained during the investigation, a range of optical depths between 0.077 and 0.01102 will result. These values fall within the range specified by Van de Hulst (156) who stated that single scattering phenomena can be considered if the optical depth is less than 1/10. Boll and

Sliepcevich (7) published a paper in which they indicated, as a result of experimental evidence, that the condition for single scattering will be fulfilled if log Io/I is less than approximately 2.5 to 3, and the half-angle of reception, Θ , for the light received is less than about 1 degree to 1.4 degree. Thus, the first of the conditions specified by Boll and Sliepcevich was satisfied in this experiment.

In addition, from the definition of single scattering, the amount of scattering will change in direct proportion to the number of particles involved. From the extinction data a curve was plotted which indicated the decrease in incident intensity per a unit incident intensity and was plotted as a function of the density of the medium. The curve plotted from this data was essentially a straight line (Figure 15). It is then obvious from this curve that the decrease in incident intensity or the extinction is, or can be considered to be, directly proportional to the density. As an example, an increase in the density by 49.5 percent will result in a decrease in the intensity by 50 percent. The above information was considered as sufficient evidence to accept the phenomena of single scattering for this experiment.

Although the information obtained and reported in this work covers the results for one substance, the versatility of the design of the equipment makes it possible to investigate other substances or media containing other types of particles. As a consequence, research is presently being continued with this equipment to obtain additional information, such as the emission function of the substance used in this investigation, as well as information on media containing other types of particles.

REDUCTION OF DATA

As pointed out in the discussion of the equipment, all data were recorded on a Leeds and Northrup Speedox strip chart recorder. Measurement of the angular distribution of intensity was recorded for all angles of Θ between 7 and 173 degrees; i.e., the aerosol specimen was scanned continuously over this range. Scattering measurements were taken for 21 wave lengths; i.e., at 0.5-micron intervals for wave lengths between 1 and 7 microns, and at 1-micron intervals between 7 and 15 microns. Extinction measurements were recorded for the same intervals of wave lengths as the scattering, with the additional wave length of 15.5 microns being recorded.

Due to the large amount of data taken, it was not feasible to include all the data in this report; therefore, representative samples have been included (photographic reduction method) as an appendage to illustrate the type of data recorded. The "raw data" for both the extinction and scattering measurements are on file at the Department of Aerospace and Mechanical Engineering, University of Oklahoma.

NORMALIZATION OF THE EXPERIMENTAL DATA

In presenting the data it is convenient to isolate the influence of radiative scattering by neglecting other effects. For the experimental work reported herein the variation of monochromatic intensity $I_s(\Theta')$ with the direction Θ' was measured. Emission from the particles was neglected. The validity of this approach is to be investigated in future work; however, for this work the approach is probably adequate since the particles were at relatively low temperatures (approximately 75° F.).

Radiative scattering for the axial-symmetric case was experimentally determined (scattering in a horizontal plane).

The energy balance per unit solid angle can be written:

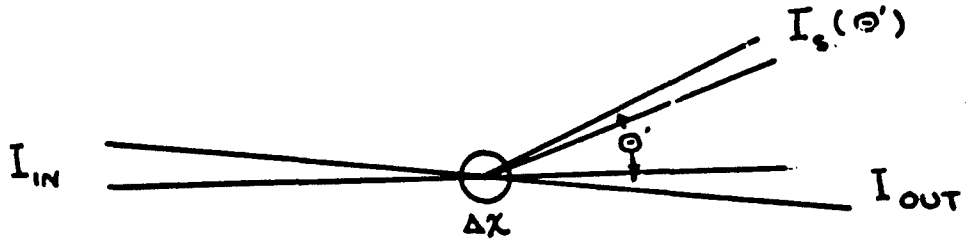

$$I_{IN} - I_{OUT} = \Delta I_{SCAT} + \Delta I_{ABS} = \Delta I_{EXT} \qquad (2)$$

where: ΔI_{SCAT} = decrease in the incident intensity due to scattering

ΔI_{ABS} = decrease in the incident intensity due to absorption

ΔI_{EXT} = decrease in the incident intensity due to extinction

$$\Delta I_{SCAT} = \frac{1}{4\pi} \int_0^{2\pi} \int_0^{\pi} I_s(\Theta') \sin\Theta' \, d\Theta' \, d\phi' \qquad (3)$$

For the axial-symmetric case, we write

$$\Delta I_{SCAT} = \frac{1}{2} \int_0^{\pi} I_s(\Theta') \sin\Theta' \, d\Theta' \qquad (4)$$

Approximating Beer's law as,

$$\frac{\Delta I_{EXT}}{I_{IN}} = \rho \beta \Delta X \qquad (5)$$

$$\frac{\Delta I_{SCAT}}{I_{IN}} = \rho \sigma \Delta x \tag{6}$$

If I_{IN}, ρ and Δx are identical in Eq (5) and Eq (6) we then have

$$\frac{\Delta I_{SCAT}}{\Delta I_{EXT}} = \frac{\sigma}{\beta} \tag{7}$$

Rewriting Eq (2) in the following manner,

$$\frac{\Delta I_{SCAT}}{\Delta I_{EXT}} + \frac{\Delta I_{ABS}}{\Delta I_{EXT}} = 1 \tag{8}$$

or

$$\frac{\sigma}{\beta} + \frac{K}{\beta} = 1 \tag{9}$$

also, from Eq (4)

$$\frac{\Delta I_{SCAT}}{\Delta I_{EXT}} = \frac{\sigma}{\beta} = \frac{1}{\Delta I_{EXT}} \left[\frac{1}{2} \int_0^{\pi} I_s(\theta') \sin\theta' d\theta' \right] \tag{10}$$

Since the scattering function $S(\theta', \phi')$ is defined as the fraction of scattered radiation directed into a unit solid angle $d\omega'$ in the direction θ', ϕ', it is evident that for the case of non-conservative scattering we can write

$$\frac{1}{4\pi} \int_0^{2\pi} \int_0^{\pi} S(\theta', \phi') \sin\theta' d\theta' d\phi' = \frac{\sigma}{\beta} \tag{11}$$

The scattering function is referred to by Van de Hulst (156) as the amplitude function, whereas Chandresekhar (14) refers to it as the phase function.

For the axial-symmetric case we have

$$\frac{\sigma}{\beta} = \frac{1}{2}\int_0^{\pi} S(\Theta') \sin\Theta' \, d\Theta' \qquad (12)$$

Upon comparing Eq (10) with Eq (12) and assuming that ΔI_{EXT} is not a function of Θ' we then have

$$S(\Theta') = \frac{I_s(\Theta')}{\Delta I_{EXT}} \qquad (13)$$

For a particular case of conservative scattering ($\sigma = \beta$) Eq (10) is identical to Eq (4) and we can, therefore, define a conservative scattering function as

$$S_{CONS}(\Theta') = \frac{I_s(\Theta')}{\Delta I_{SCAT}} \qquad (14)$$

Examining Eq (7), Eq (3), and Eq (4), one can readily see that

$$S(\Theta') = \frac{\sigma}{\beta} S_{CONS}(\Theta') \qquad (15)$$

The conservative scattering function, $S_{CONS}(\Theta')$, has been plotted as a function of Θ' for the wave length interval 1 micron to 15 microns (21 values). In addition $S_{CONS}(\Theta')$ has been tabulated between $0° < \Theta' < 180°$ for 21 values of wave length, Table 1.

The mass extinction coefficient β has been calculated from Eq (5), using the measured values of density ρ, the path length ΔX, and the percent decrease in incident energy $\frac{\Delta I_{EXT}}{I_{IN}}$. The mass scattering coefficient σ has been calculated from Eq (10) by numerically integrating $I_s(\Theta')$ over finite (1 degree) intervals. One can, therefore, determine the corresponding $S(\Theta')$ for the interval $0° < \Theta' < 180°$

Beginning with Eq (4) and considering $d\Theta$ as $\Delta\Theta$ and taking $\Delta\Theta = \frac{\pi}{180}$ radian, we write

$$\frac{1}{2}\sum_{n=1}^{180} I_s(\Theta_n) \sin\Theta_n \frac{\pi}{180} = \Delta I_{SCAT} \qquad (16)$$

Therefore, from Eq (3)

$$S_{CONS}(\Theta_n) = \frac{360\, I_s(\Theta_n)}{\pi \sum_{n=1}^{180} I_s(\Theta_n) \sin \Theta_n} \qquad (17)$$

The numerical values of $S_{CONS}(\Theta_n)$ were calculated using the IBM1410 digital computer for 21 values of wave lengths (from . micron to 7 microns in one-half-micron intervals and from 7 microns to 15 microns in one-micron intervals). The values are presented in Figures 16 to 36 ~~and in~~ tabular form in Table 1.

CALCULATION OF MASS SCATTERING COEFFICIENT

The mass scattering and mass extinction coefficients are necessary to obtain an accurate solution of the radiant transfer equation. Just as the determination of the scattering function and the mass extinction coefficient were desirable for actual media, so is the determination of the mass scattering coefficient desirable for the actual media.

With a few minor assumptions it was possible to obtain the mass scattering coefficient for the aerosol of aluminum powder used in this experiment. From Eq (7) developed earlier,

$$\sigma = \beta \frac{\Delta I_{SCAT}}{\Delta I_{EXT}}$$

In the development of Eq (7) it was assumed that ρ, I_{in} and Δx were identical for both extinction and scattering data. Since the extinction data and the scattering data were obtained independently, it is obvious that it was impossible to obtain identical conditions for both sets of data. Consequently, to apply Eq (7) the data must be corrected.

ΔI_{scat} has been determined by integration of Eq (4), assuming the finite difference technique to be justified; i.e.

$$\Delta I_{SCAT} = \frac{1}{2} \int_0^{\pi} I_s(\Theta') \sin\Theta' \, d\Theta'$$

Where $I_s(\theta')$ has been measured at a particular set of conditions. These conditions include the wave length of the radiation, the mass density of the cloud, and the path length of the radiation.

The mass scattering coefficient has been determined in the following manner.

1. Obtain the value of, β, the monochromatic mass extinction coefficient from the graph in Figure 39, for the wave length corresponding to the experimental data for $I_s(\theta')$

2. Compute $\frac{\Delta I_{EXT}}{I_{IN}}$ by multiplying β by the value of $\rho \Delta x$ corresponding to the experimental data for $I_s(\theta')$

3. I_{IN} is determined by assuming $I_{IN} \cong I_s(0)$. This approximation is valid because the optical thickness of the samples was small. ΔI_{EXT} is then computed as follows:

$$\Delta I_{EXT} = \left[\frac{\Delta I_{EXT}}{I_{IN}}\right] \times I_{IN}$$

4. Obtain ΔI_{SCAT} from integration of

$$\Delta I_{SCAT} = \frac{1}{2} \int_0^{\pi} I_s(\theta') \sin\theta' d\theta'$$

5. Calculate

$$\sigma = \beta \frac{\Delta I_{SCAT}}{\Delta I_{EXT}}$$

The above procedure has been followed in the calculation of the mass scattering coefficients for 15 wave lengths, the results of which are plotted in Figures 37 and 38. However, the average density was used in the calculations. As can be seen from Figure 37, considerable dispersion of the calculated points occurred. Possibly this dispersion could be improved if additional points were used in the calculations. Aerosol density measurements were not recorded for all measurements of scattered intensity recorded for purposes of calculating the scattering function since the scattering function per se is independent of density. Unfortunately it was not planned that the mass scattering coefficient would be calculated by the above procedure prior to the accumulation of the scattering and extinction data. Consequently, calculation of the mass scattering coefficient and the resulting plot are based on a minimum of data.

It can be seen from the figure that the media upon which

measurements were made should not be considered as a non-absorbing media, i.e. $\sigma \neq \beta$.

RELATIONSHIP BETWEEN $S_{cons}(\mu_i, \pm\mu_j)$ AND $S_{cons}(\Theta')$

In solving the heat transfer equation by approximation methods, it has been found convenient to express the equations in a particular form. Similarly, in order to expand the utility of the experimental data, it is desirable to express the data in a form which is convenient for use in these types of problems. The problem is one of ascertaining the relationship between $I_s(\mu_i, \pm\mu_j)$ and $I_s(\Theta')$. $S_{cons}(\mu_i, \pm\mu_j)$ can be obtained directly if its relationship with $S_{cons}(\Theta')$ is known.

If we consider scattering into discrete directions (j) from a particular incident direction (i), we can write

$$S(\mu_i, \mu_j) = \frac{1}{2\pi} \int_0^{2\pi} S(\Theta_{ij})\, d\phi' \tag{18}$$

where Θ_{ij} is the angle between the directions of the incident and leaving rays, and from solid geometry,

$$\cos\Theta_{ij} = \mu_i \mu_j + (1-\mu_i^2)^{\frac{1}{2}}(1-\mu_j^2)^{\frac{1}{2}} \cos(\phi - \phi') \tag{19}$$

Equation (18) has been evaluated using the finite difference integration. Azimuthal increments of 10 degrees were selected, i.e., $\Delta\phi = 10^\circ$. In addition, discrete values of $\mu_i, \pm\mu_j$ as dictated by the fourth order approximation were used to calculate values of Θ_{ij}. Sixteen values of ~~$S(\mu_i, \mu_j)$~~ and sixteen values of $S(\mu_i, -\mu_j)$ are tabulated in Table 2. The calculated values of Θ_{ij} are tabulated in Appendix B.

Since σ is the probability that a photon will be deflected from its original direction or scattered as it encounters an elemental mass, we can write

$$\frac{1}{4\pi} \int_{-1}^{+1} \int_0^{2\pi} S(\Theta)\, d\phi' d\mu' = \frac{\sigma}{\beta} \tag{20}$$

or

$$\frac{1}{2} \int_{-1}^{+1} S(\mu, \mu')\, d\mu' = \frac{\sigma}{\beta}$$

In the absence of absorption, the total flux scattered in all directions equals the incident flux, i.e., for the case of conservative scattering,

$$\frac{1}{2}\int_{-1}^{+1} S(\mu,\mu')\,d\mu' = 1 \tag{21}$$

Rewriting Eq (21)

$$\frac{1}{2}\left[\int_{0}^{1} S(\mu,-\mu')\,d\mu' + \int_{0}^{1} S(\mu,\mu')\,d\mu'\right] = 1 \tag{22}$$

Equation (22) is now rewritten in a form suitable for integration by an approximation method, i.e.,

$$\frac{1}{2}\sum_{n=1}^{N} a_j S(\mu_i,\mu_j') + \frac{1}{2}\sum_{n=1}^{N} a_j S(\mu_i,-\mu_j') = 1 \tag{23}$$

For the case of fourth approximation Eq (23) becomes

$$\frac{1}{2}\sum_{n=1}^{4} a_j S(\mu_i,\mu_j') + \frac{1}{2}\sum_{n=1}^{4} a_j S(\mu_i,-\mu_j') = 1 \tag{24}$$

Due to the fact that intervals of $\Delta\phi = 10$ and a fourth order approximation were used in the calculation of the functions $S(\mu_i \pm \mu_j)$, it seemed advisable to check the accuracy of the computations. Equation (24) was used to make this check.

It should be noted that only the positive directions of μ_i need be considered in Eq (24) since the Hemholtz reciprocity law is valid; i.e.,

$$S(\mu_i,\mu_j) = S(-\mu_i,-\mu_j)$$

$$S(-\mu_i,\mu_j) = S(\mu_i,-\mu_j)$$

To provide a comparison of the experimental results with a theoretical result, 32 values of $S(\mu_i,\pm\mu_j)$ were calculated using the work of Chu, Clark, Churchill (17, 21) and Love (96). These

alculations for the Mie theory considered a real refractive index of 1.6 and $\alpha = 2$ and $\alpha = 3$. Calculations for values of α larger than 3 were not attempted, due to the tremendous amount of work invclved. These values are tabulated in Table 5. Checking the computations using Eq (24) indicated that the accuracy was sufficiently close for most engineering work. However, the experimental results did not agree too closely with Eq (24) as indicated in Table 6. The following is offered as an explanation of this disagreement.

The scattering function calculated from the Mie theory does not change as rapidly in the region for small values of Θ as that calculated from the experimental data. The scattering in the neighborhood of 0° (forward scattering) was much higher for the experimental data when compared to that calculated from the Mie theory. Since a fourth approximation quadrature formula was used to express this function and discrete values of μ_i, μ_j were dictated by this relation, it seems reasonable to assume that the approximation method used did not express this function adequately in the neighborhood of 0°. Another possible explanation is that an insufficient number of azimuthal increments were used and possibly $\Delta\phi$ of 5° or even 1° should be used.

In order to improve the accuracy in the calculation of from the experimental data, two alternatives are suggested:

1. Increase the number of intervals of $\Delta\phi$ used in Eq (18), that is, use values of $\Delta\phi$ of 5° or 2°. This may improve the accuracy for an individual point.

2. Increase the degree of approximation so that more points can be considered in regions having steep gradients. In this respect the accuracy could be improved by considering the approach suggested earlier; i.e., to extend the application of the quadrature formula in normalizing the scattering data. However, there is one serious difficulty with this approach. Increasing the degree of approximation will present many difficulties in solving the heat transfer equation, utilizing the approximation techniques.

Since the first suggestion has not been attempted due to the obvious amount of work involved, the influence on the accuracy of the calculation can only be assumed. Therefore, for the present it is suggested that the calculated values of $S(\mu_i, \mu_j)$ be accepted as being sufficiently accurate for engineering applications.

It should be kept in mind that a direct comparison between the experimental work reported here and the theoretical calculations mentioned above cannot be made. The particles used in the experimental work were neither spherical nor of uniform size and they had a complex refractive index (an estimated, not a known value), while the calculations for the theoretical particles considered only the real refractive index.

DISCUSSION OF EXTINCTION DATA

A total of 87 calculated values of beta for 22 different wave lengths was used to plot the extinction curve. At each of the 22 wave lengths plotted the calculated values of beta were averaged arithmetically to obtain the average extinction coefficient for the wave length. Consequently, a curve was plotted for the average mass extinction coefficient as a function of wave length for the 22 wave lengths. (Refer to Figure 39).

The extinction curve was plotted as a function of wave length, since it is rather difficult to determine a value of particle size parameter (α) for irregular-shaped particles. However, one could possibly use an equivalent diameter to establish pseudo particle size parameters.

As can be seen from Figure 39, the extinction curve is relatively flat for the average line drawn through the plotted points. Possibly due to inaccuracies in measurement or to the fact that an insufficient number of points was recorded, the plotted points failed to indicate the maxima and minima observed for the Mie curves; consequently, there was no justification for not representing the extinction coefficient as a smooth function. From the extinction plot, the curve does "drop off" at a wave length larger than 10 microns. If the effective particle diameter were accepted as a correct value, and an equivalent alpha value were determined on this basis, the "drop-off" of the extinction curve would occur at values of alpha smaller than 2. Since an insufficient number of points was evaluated for equivalent values of alpha between 0 and 3, this experiment did not predict the maxima and minima as predicted by the Mie theory for this range of alpha values. As has been explained earlier, however, there is no justification for comparing the results of this experiment with the Mie theory, primarily due to the fact that the Mie theory considers scattering from single spherical particles. Also, the calculated values showing these distinct maxima and minima are, essentially, for non-absorbing spheres.

For extinction measurements the angle of reception must be small. This requisite was pointed out by the experiments of Sinclair and LaMer (134) and by the investigations of Boll and Sliepcevich (7). Due to the large value of forward scattering intensity obtained in this experimental work, especially at the low wave lengths, it was necessary to reduce the monochromator slit width in order to keep the solid angle very small. As experience pointed out, a large angle of reception would include so much forward scattering, primarily from refraction and reflection, that the amount of extinction (ΔT) would be so small that accuracy would be poor; consequently, by decreasing the cone of reception the percentage of extinction was kept between 8 and 20 percent, with a consequential improvement in the accuracy. The large amount of variation in the data can be attributed primarily to the density measurement. It is believed that the particle flow density, or particle distribution, was quite uniform, since this was confirmed by the scattering data and the investigations of the

particle generator itself. The error in the density measurement can be attributed to two factors:

1. A stopwatch was used to determine the time for sampling the flow. Any error in the measurement of the time would create a large error in the density calculation. The number of particles counted per unit of time, of course, varies with the accuracy for the period of sampling; for example, a 5-second variation in time for the one-minute sampling period could result in approximately 8 percent error in the density measurement. Consequently, improvement of the density measurement would require longer periods of sampling, which were impossible with the equipment designed for this experiment.

2. A variable area flowrater was used to measure the airflow which could be determined to within 1/10 cfm. Consequently, the accuracy of such a device was insufficient for the density measurements necessary for this type of experiment. It is suggested that a calibrated orifice plate and a manometer be used to obtain a more accurate determination of the airflow.

These two factors contributed greatly to the accuracy of the density measurements taken. Since the extinction data varied with, or was influenced directly by, the density measurement, the extinction measurements were obviously in error and it was difficult to obtain reproducible values. This error was minimized by taking a minimum of three extinction measurements at each wave length, and in some instances by taking as many as 7.

DISCUSSION OF ANGULAR DISTRIBUTION OF INTENSITY DATA

In order to have a complete set of scattering data at a particular wave length, it was necessary to have the measured scattered intensity for all angles between 0 and 180 degrees. The information at the endpoints was the most difficult to obtain, particularly in the neighborhood of 0 degrees. The backward scattering, or the scattering in the region of 180 degrees, can be extrapolated with a certain degree of accuracy. A device to measure backward scattering is more easily constructed or designed than one that would be capable of measuring the scattered intensity in the neighborhood of 0 degrees; i.e., forward scattering. The results of the data in this experiment indicated that there exists a very strong forward scattering at nearly all wave lengths, and that the ratio of the scattered intensity of 0 degrees to that at 90 degrees was at least a hundred for the high wave lengths and more than a thousand for the low wave lengths. Since there is a steep gradient in the region between 20 degrees and 0 degrees, it is quite obvious that difficulty would arise in trying to extrapolate the scattered intensity in this region. Some authors have indicated that data can satisfactorily be extrapolated to the zero point and have reported experimental data with the last measured value as high as 40 degrees being extrapolated to

the zero point. However, they offer no basis for this extrapolation. Others, for example W.E.K. Middleton (106), have recognized that errors exist in extrapolating the information to the zero position, but they did not suggest a more suitable procedure for the extrapolation of the data. Light scattering devices have been devised which will measure the scattered intensity in the neighborhood close to zero, in fact, for a value of less than 1 degree (1). Such desirable characteristics have not been incorporated in the particular design described herein, due to the fact that compromises were necessary in designing and constructing a versatile piece of equipment that could be used for scattering measurements on other powders.

Due to the physical limitations of the design reported herein, the smallest angle, theta, in which the scattered intensity can be measured is 7 degrees. Consequently, it was necessary to locate a point in the neighborhood of 0 degrees, in order to extrapolate the data in this region. The data reported herein for the scattered intensity in the neighborhood of 0 degrees was obtained from the extinction data.

It was recognized early in the experiment that the intensity in the 0-degree position was at least a hundred times more intense than the scattered intensity at the 90-degree position. Consequently, a procedure for taking data had to be considered by which the recording of data could be kept on the chart paper. It was found that recording of the angular distribution of the scattered intensity could be retained within the limits of the chart paper if the amplification of the thermocouple signals could be controlled or kept within certain magnitudes. A control of the amplification can be obtained with the equipment used through the control of the gain.

The procedure used in this experiment was to record the angular distribution of the scattered intensity beginning with the largest possible angle θ, which was approximately 173° and scanning the specimen to an angle in the neighborhood of 20 degrees. In this region, the scattered intensity was usually of such magnitude as to run off the chart paper, especially for data recorded for the lower wave lengths. For the higher wave lengths it was possible to record the scattered intensity over a larger angular range before exceeding the limits of the chart paper, i.e., from 173 to 7 degrees. Therefore, for each wave length the scattered intensity was recorded for an angular range which could be retained on the chart with one gain setting, and the remaining angular range to 0° was recorded on another portion of the chart. In this way, the ratio of the scattered intensity at 0 degrees to the scattered intensity at another angle, somewhere in the region between 20 and 30 degrees, could be established. For example, ratios could be found between the intensities at 0 and 7 degrees, between 0 and 20 degrees, or between 0 and 30 degrees. Since several ratios of the angular intensities could be established, there was sufficient information to locate the scattered intensity at the 0-degree position. There is obviously some error in this procedure, especially for the wave lengths of 1, 1.5, and 2 microns, due to the large ratios of the scattered intensity at

0 degrees to the scattered intensity at 10 degrees. Any error in reading the intensity at 10 degrees could result in a large error at the 0-degree point. For example, if the intensity measured at the 0 point was 100, and the intensity at the 10-degree point was recorded at 4, the ratio of the intensity at 0 degrees to the intensity at 10 degrees would be 25. However, if an error had been made in recording the intensity at 10 degrees, say at a value of 3.5 rather than 4, an error of approximately 14 percent would result. Even though these errors are possible, the procedure will establish the intensity at 0 degrees within 20 percent, which is a much better approach to obtaining accurate data than any attempt to extrapolate the curve beyond the last measured intensity. If such a procedure were used, errors greater than 500 percent would result, particularly for scattering measurements at the low wave lengths, for it is at these wave lengths that the scattered intensity in the forward direction is the greatest.

It is also recognized that an error exists in the scattering intensity in the backward direction, or the 180-degree direction. To obtain the 180-degree point the curve was extended beyond the 173-degree point. Consequently, it is obvious that errors could result in this region, due to the arbitrariness that would result in extending the curve. However, it was felt that this procedure was adequate for this experiment since the intensity in a backward direction was small as compared to the scattering intensity at values smaller than 20 degrees; i.e., the curve was relatively flat for angles between 70 and 180 degrees. It is estimated that the accuracy of the scattering data for the region between 0 and 10 degrees is within 10 percent, which is considered a conservative value, based on the fact that the measurements were taken on several different occasions and an average of the results was used in presenting the data. For a given wave length data were taken a minimum of 3 times and in some instances 11 times, and none were taken consecutively, but were taken in a random fashion. Comparison of the scattering data taken for a given wave length on different occasions indicated that reproducibility was very good. It was, of course, impossible to generate the same density of the aerosol consistently; therefore, the scattered intensities measured on different occasions would obviously not have identical values. However, since conditions for single scattering phenomena were prevalent, the ratio of the intensities for any two fixed angles would be the same, independent of the density of the test specimen. For example, for a given wave length the ratio of the intensity at 20 degrees to the intensity at 90 degrees, or any other combination, should be identical for two sets of data regardless of their aerosol densities. These ratios for the various scattering measurements were found to be identical for all intents and purposes.

It was also found that on comparing the normalized curve for two sets of data at a given wave length the results were identical. The results presented in normalized form were a result of the average values of all the data taken, except in those instances where the data recorded had no obvious error, for example, an error that resulted from improper operation of the particle generator, such as

clogging in the particle flow or aggregates that formed. In all cases for which these influences were disregarded the influences were noted through continuous monitoring of the equipment during the periods in which data were being recorded.

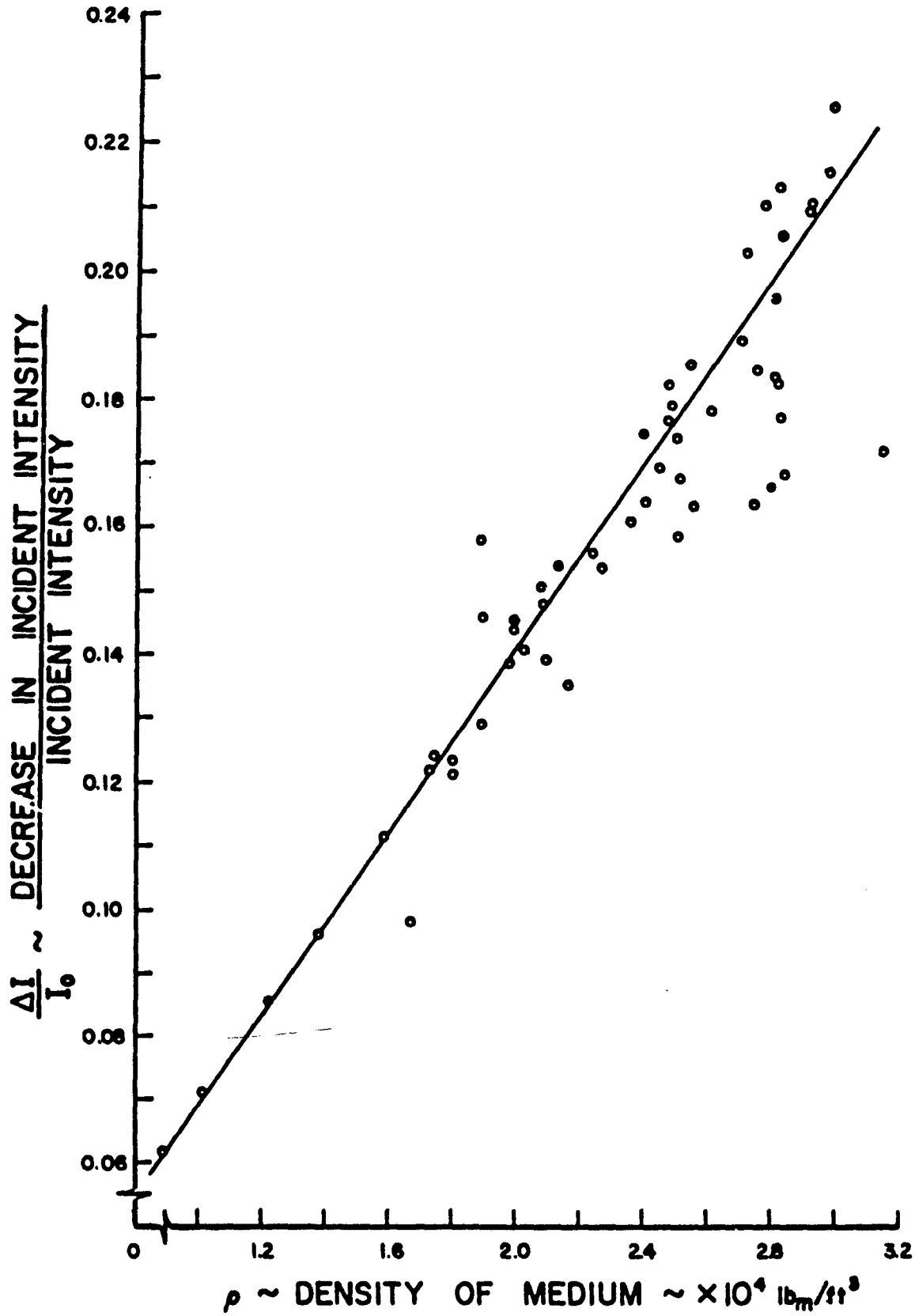

Figure 15 Percent Attentuation Variation with Media Density

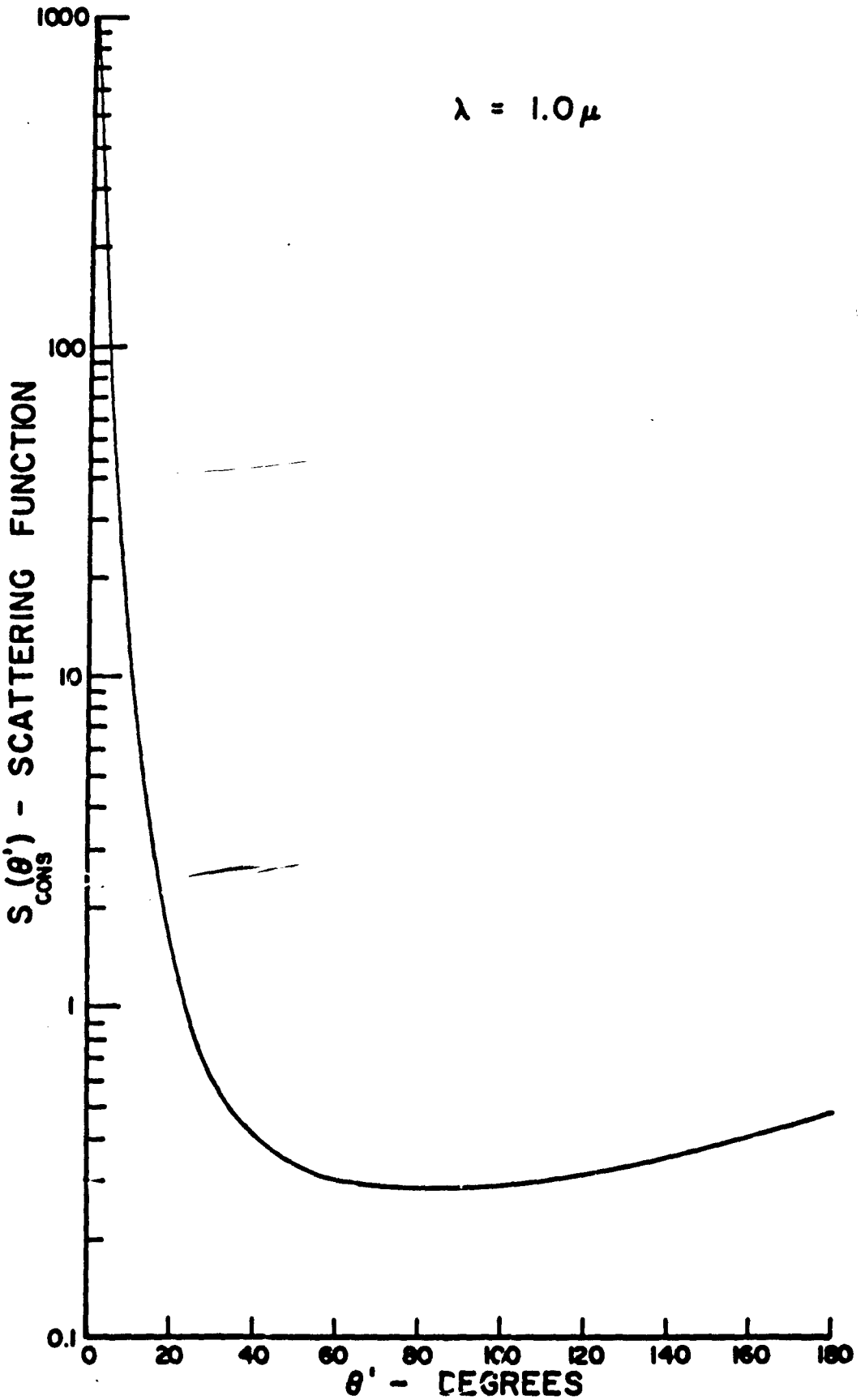

Figure 16. Angular Distribution of Scattering Function--Experimental Data

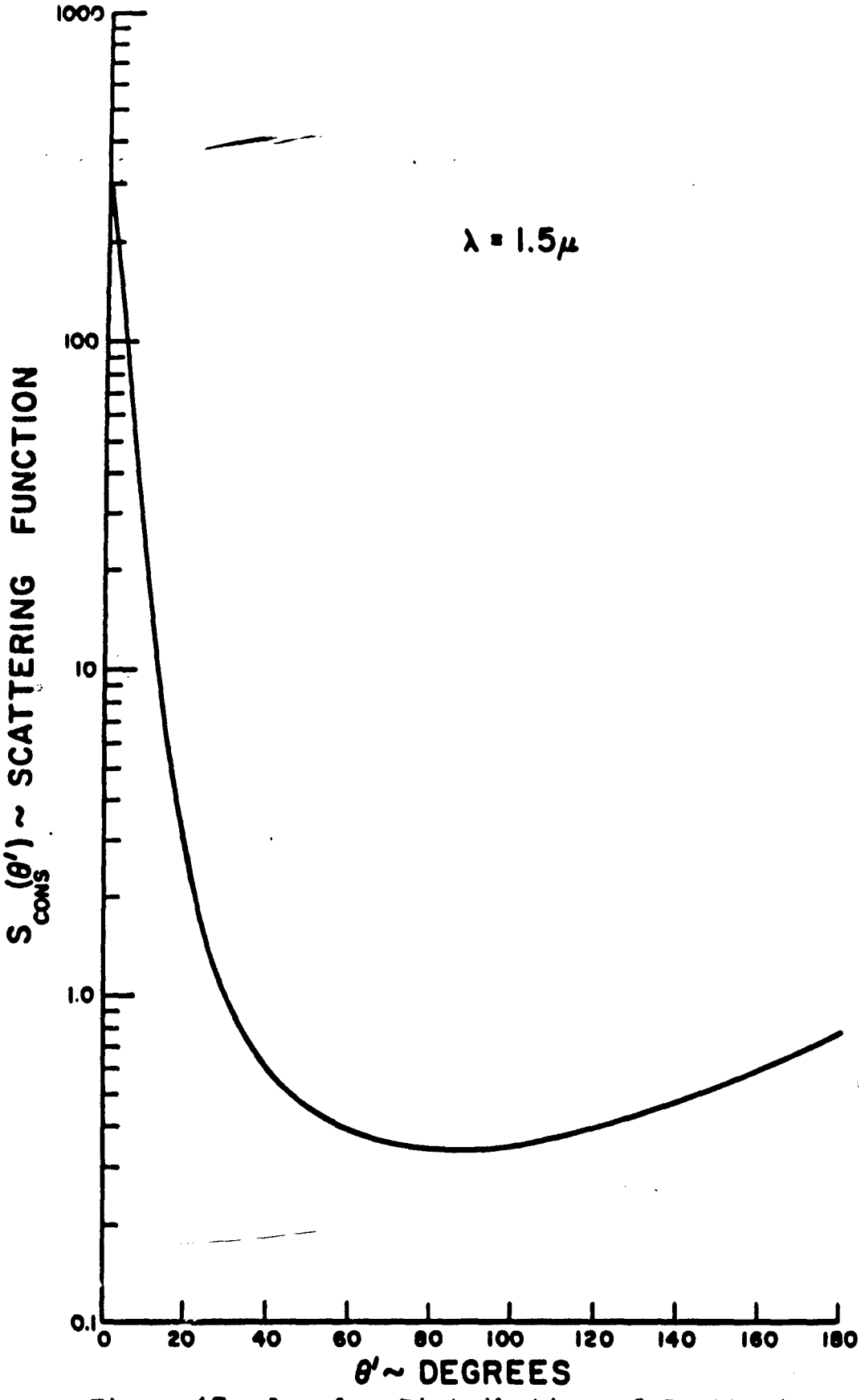

Figure 17. Angular Distribution of Scattering Function--Experimental Data

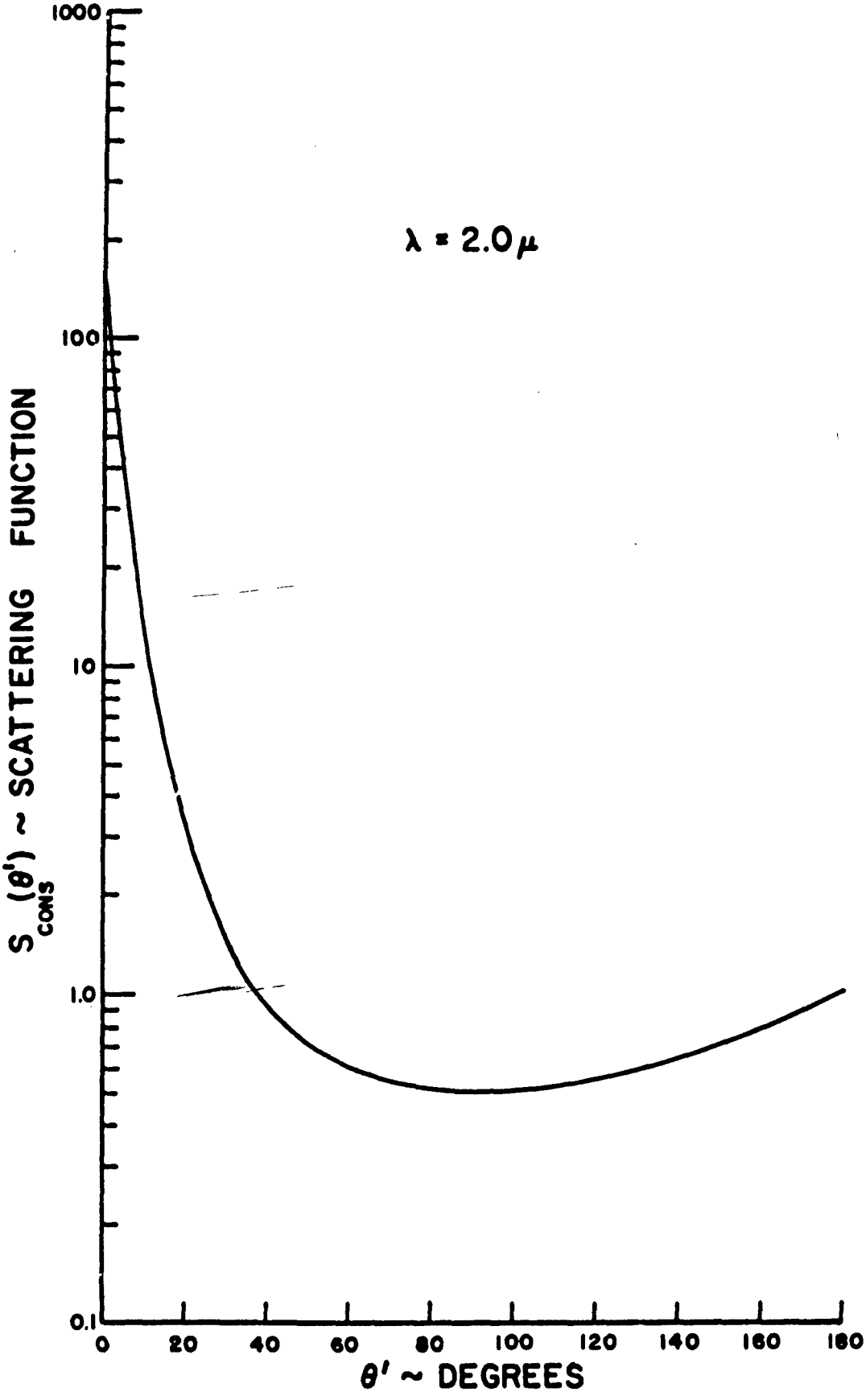

Figure 18. Angular Distribution of Scattering Function--Experimental Data

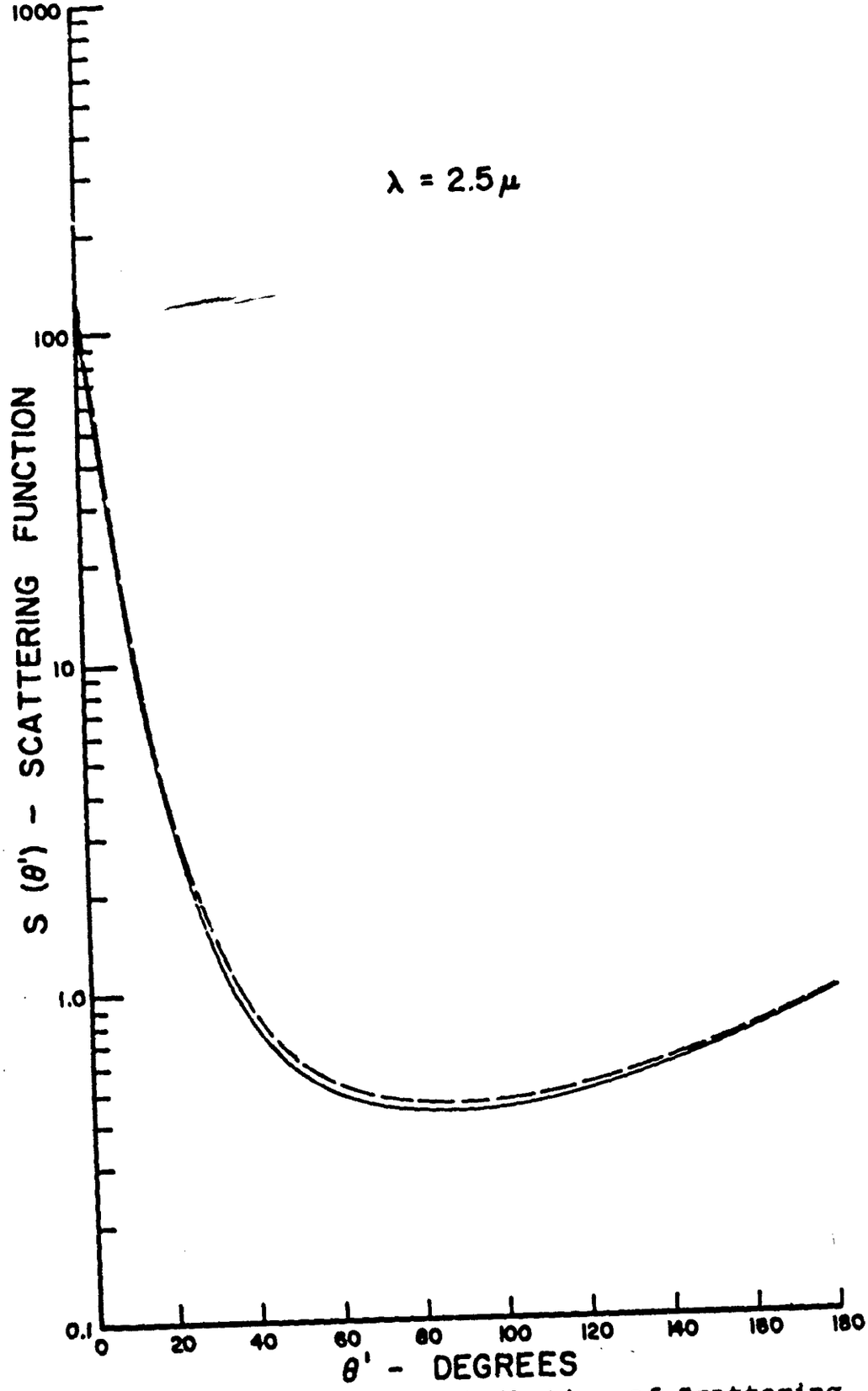

Figure 19. Angular Distribution of Scattering Function--Experimental Data

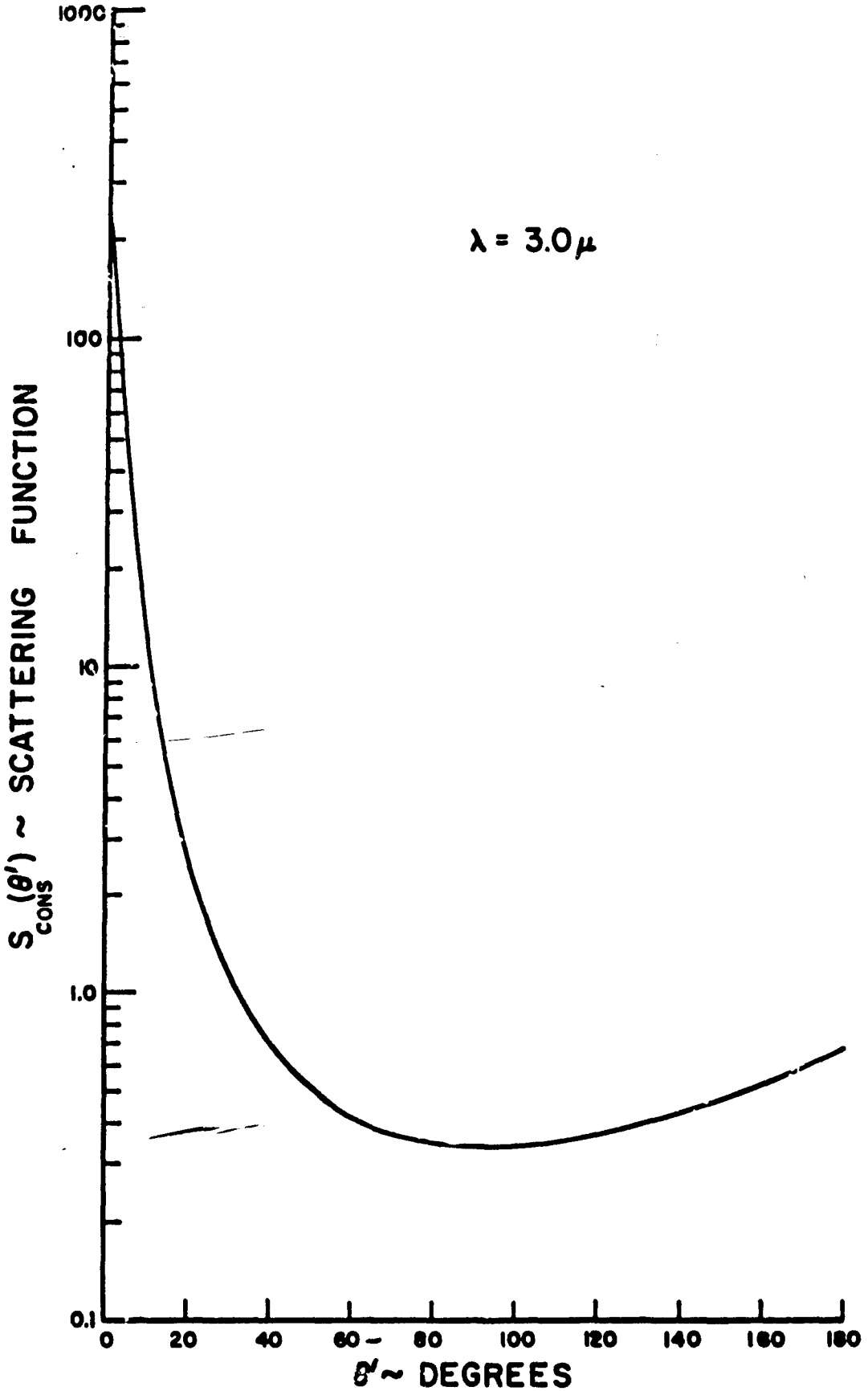

Figure 20. Angular Distribution of Scattering Function--Experimental Data

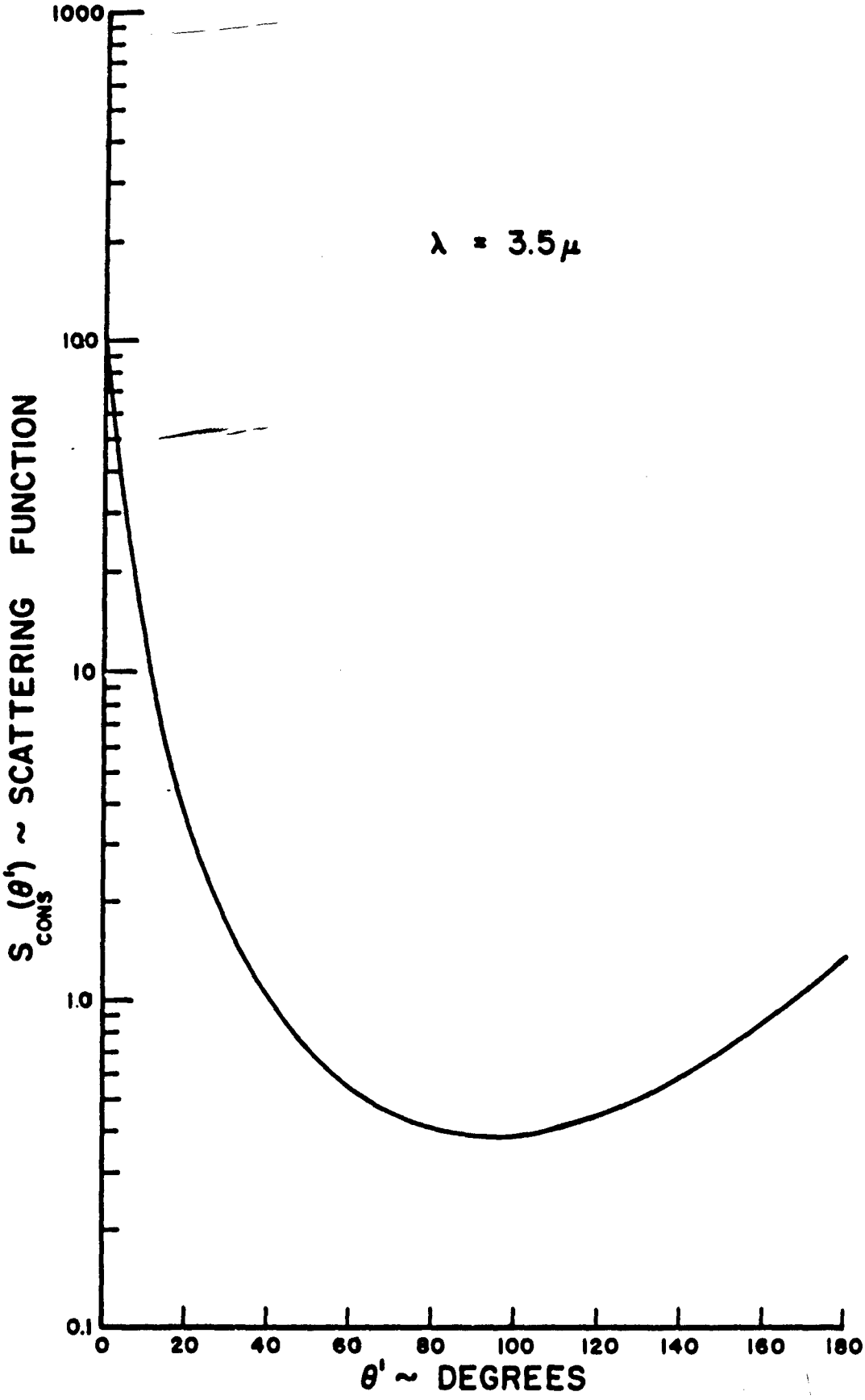

Figure 21. Angular Distribution of Scattering Function--Experimental Data

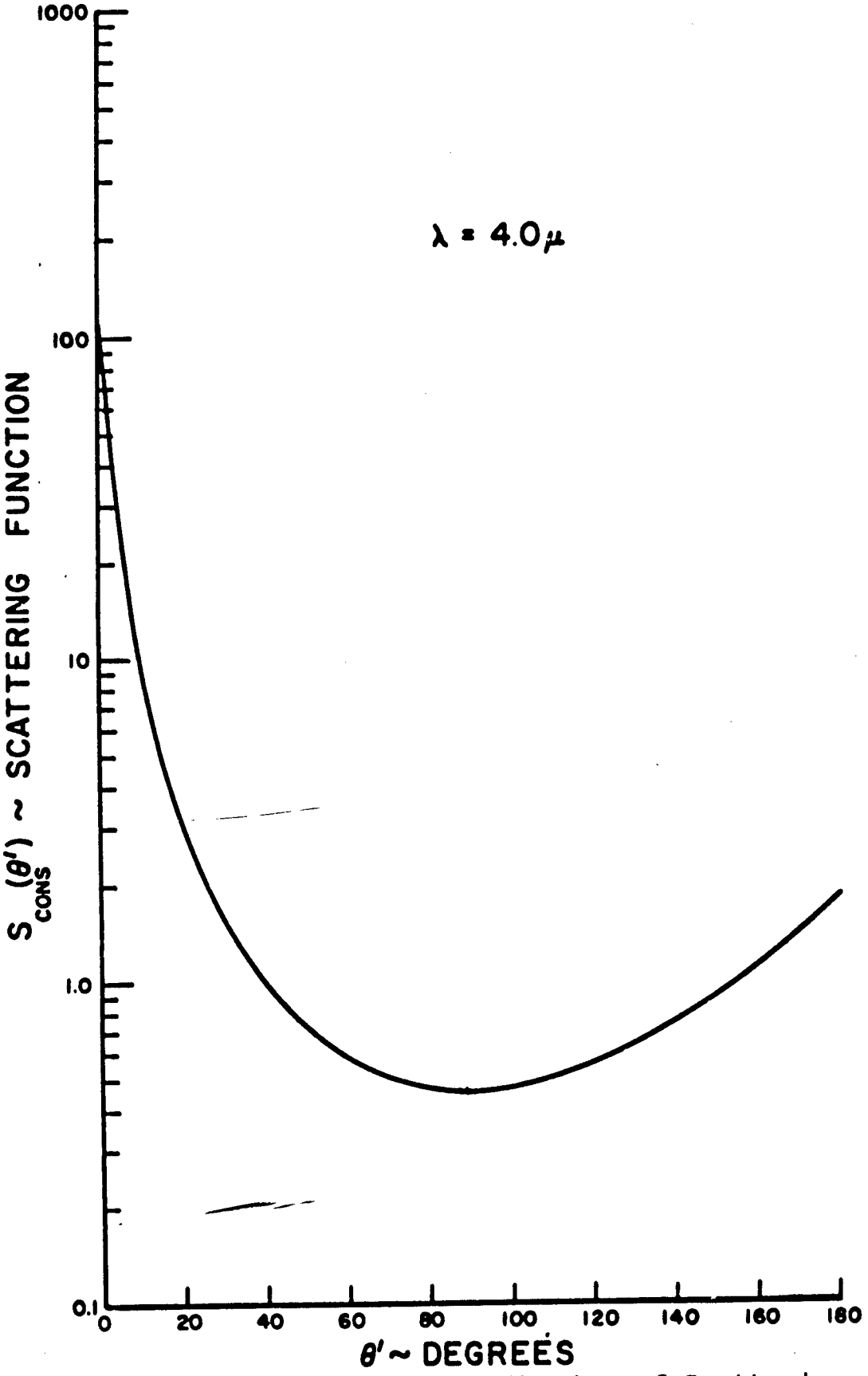

Figure 22. Angular Distribution of Scattering Function--Experimental Data

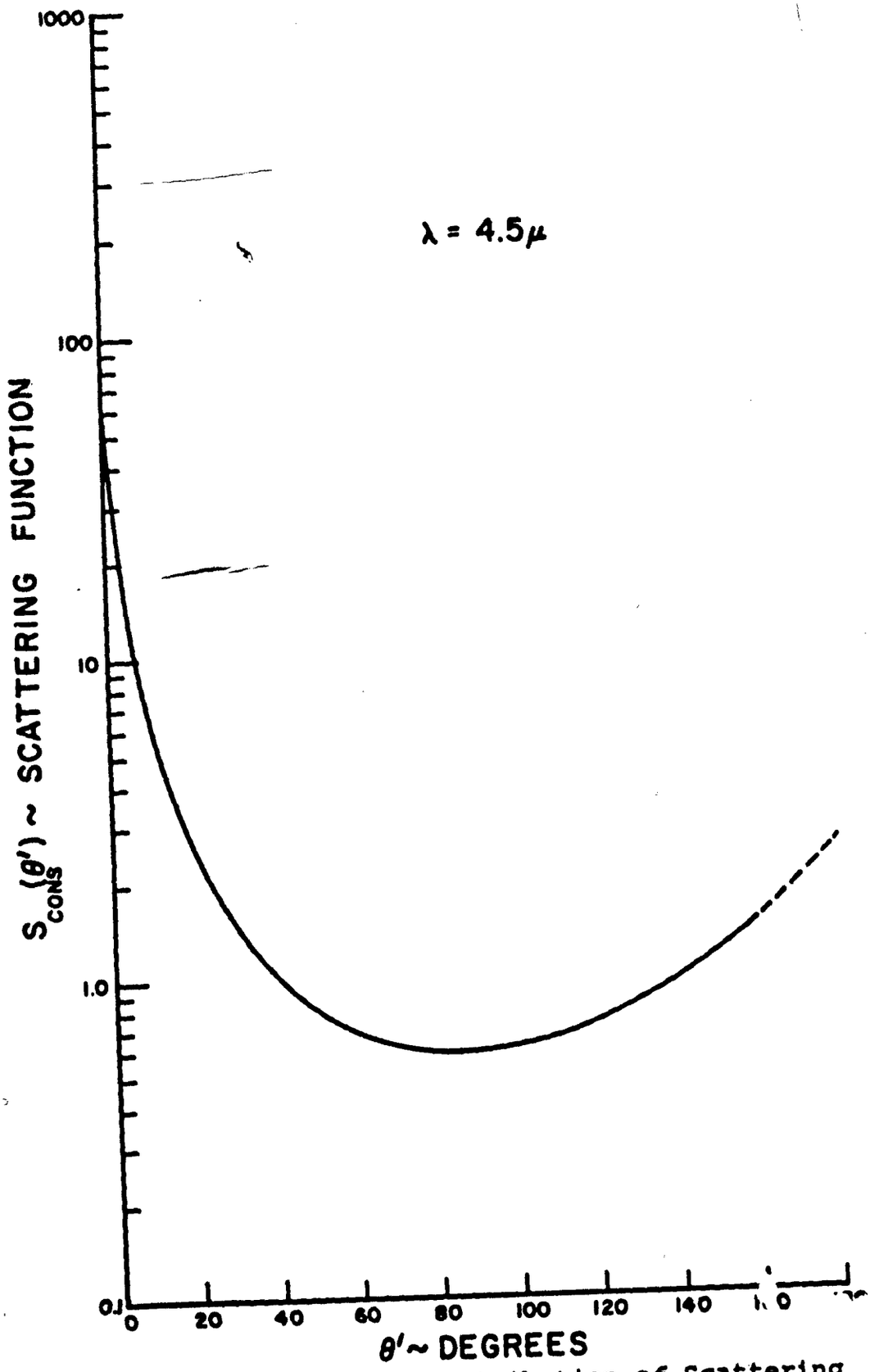

Figure 23. Angular Distribution of Scattering Function--Experimental Data

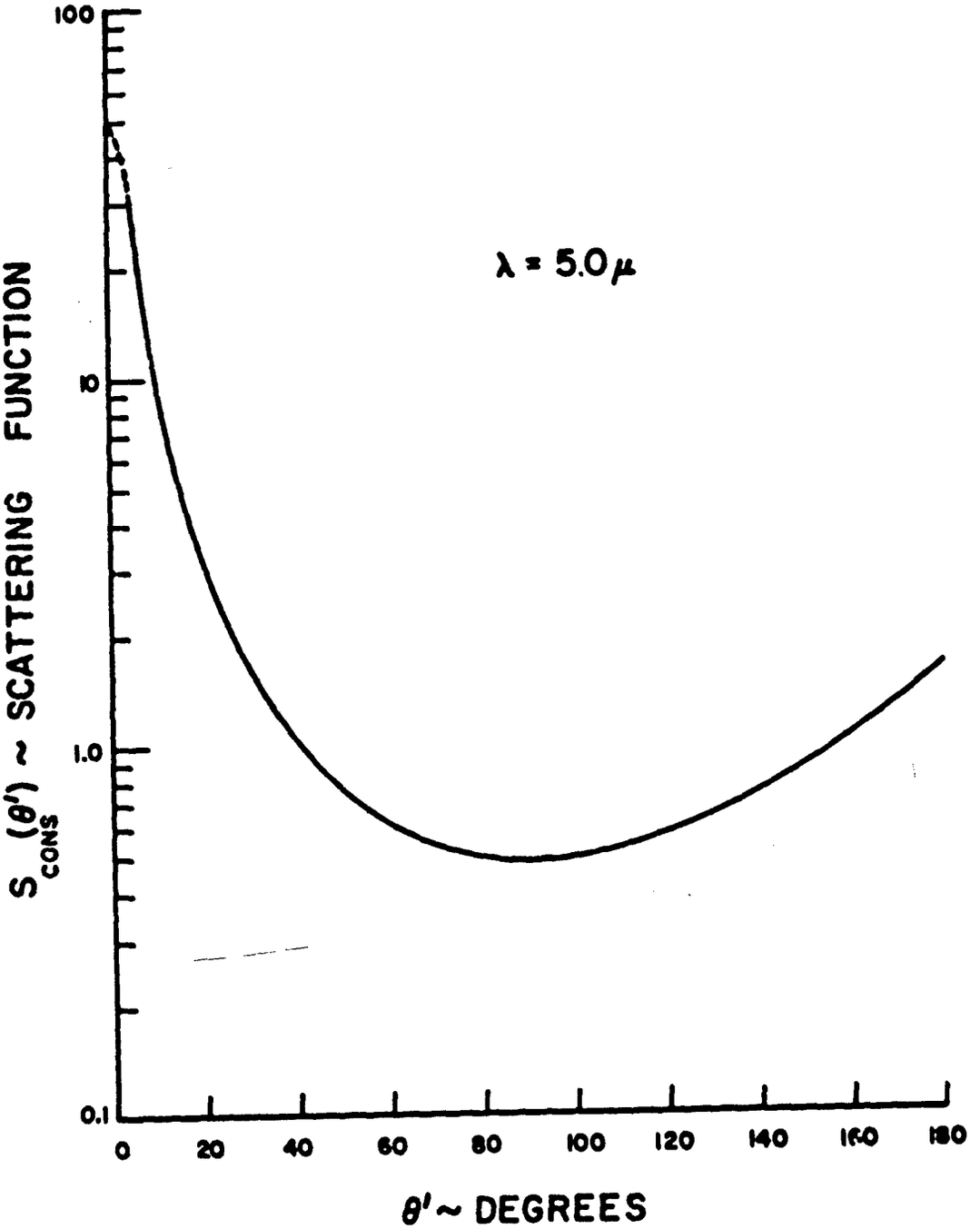

Figure 24. Angular Distribution of Scattering Function--Experimental Data

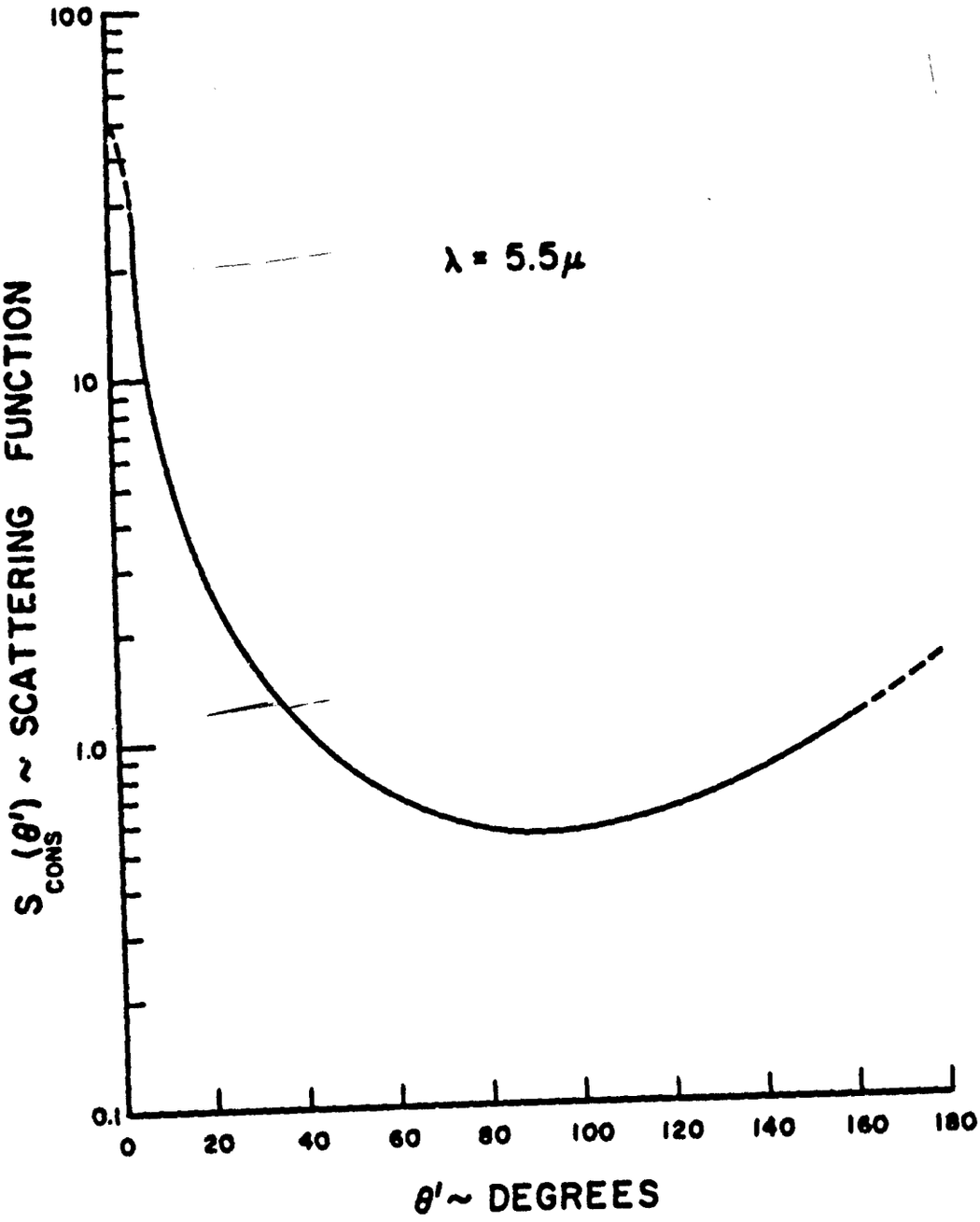

Figure 25. Angular Distribution of Scattering Function--Experimental Data

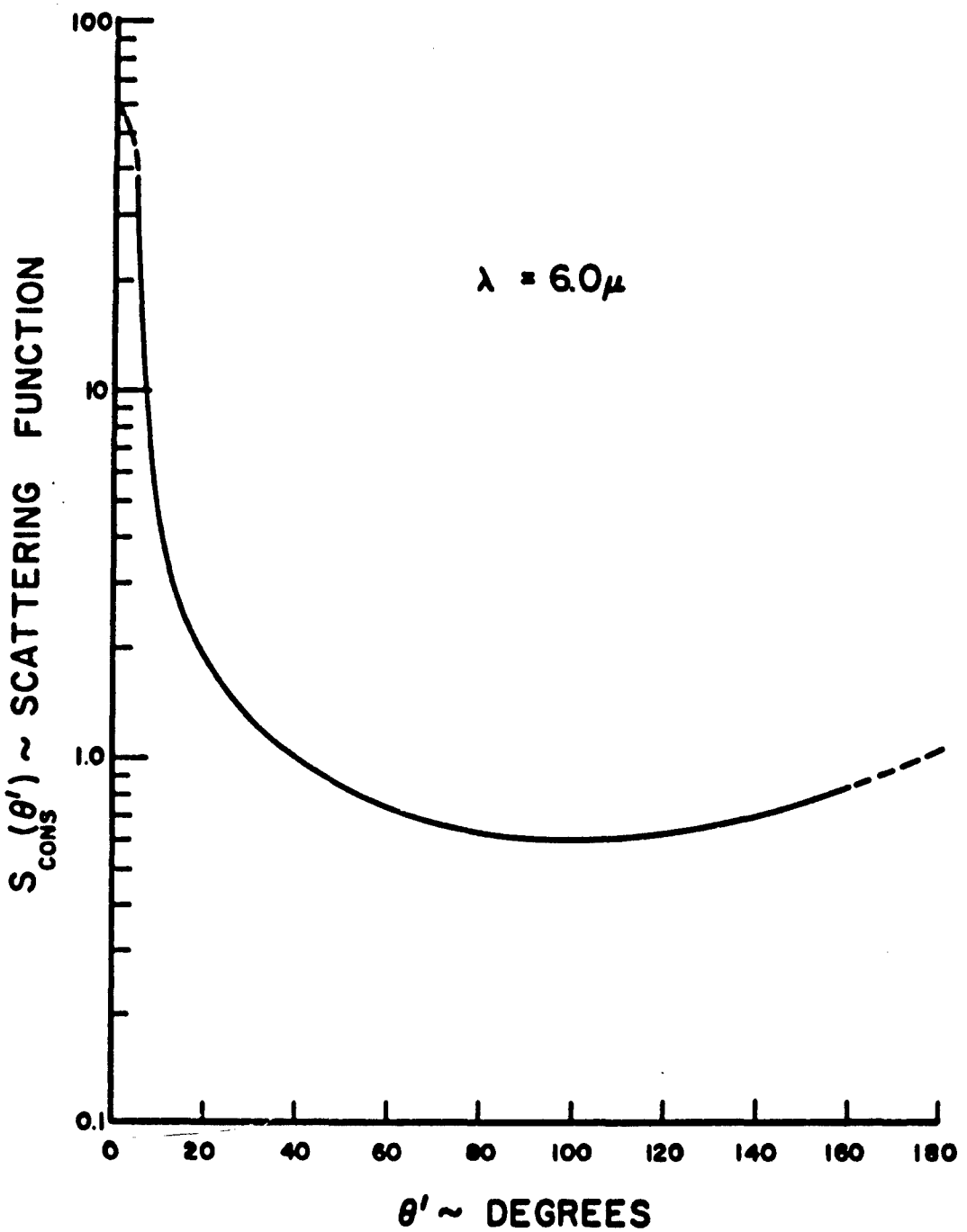

Figure 26. Angular Distribution of Scattering Function--Experimental Data

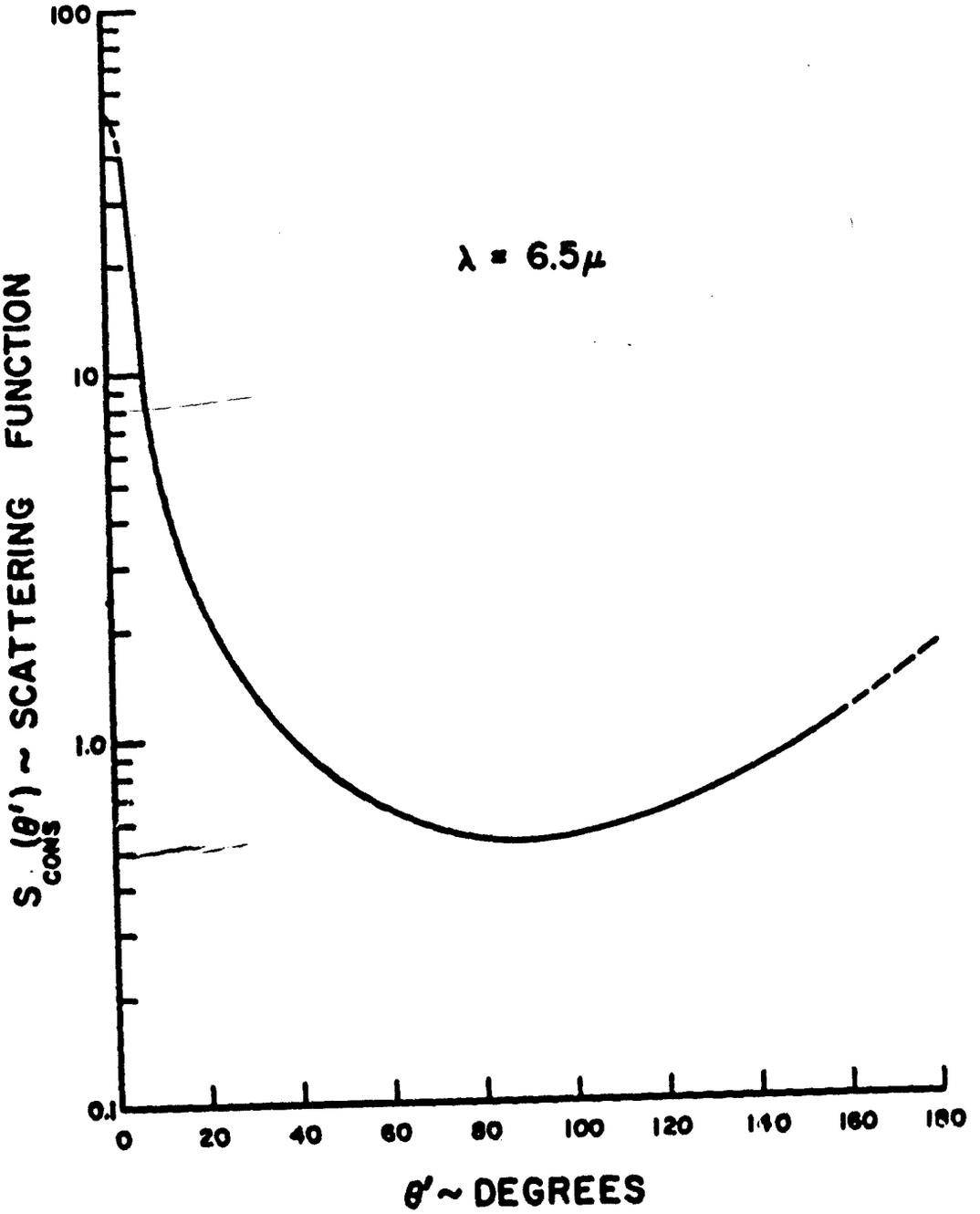

Figure 27. Angular Distribution of Scattering Function--Experimental Data

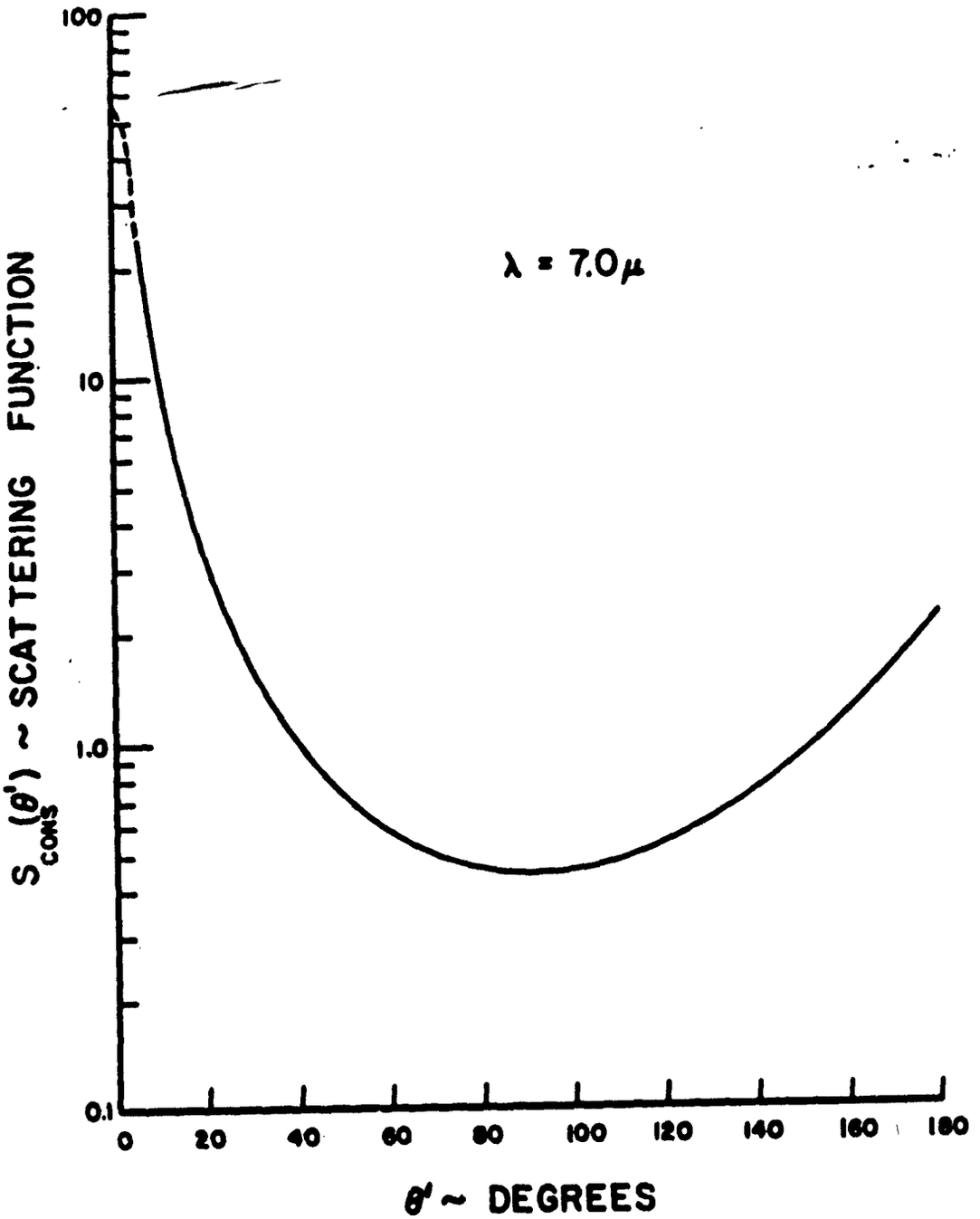

Figure 28. Angular Distribution of Scattering Function--Experimental Data

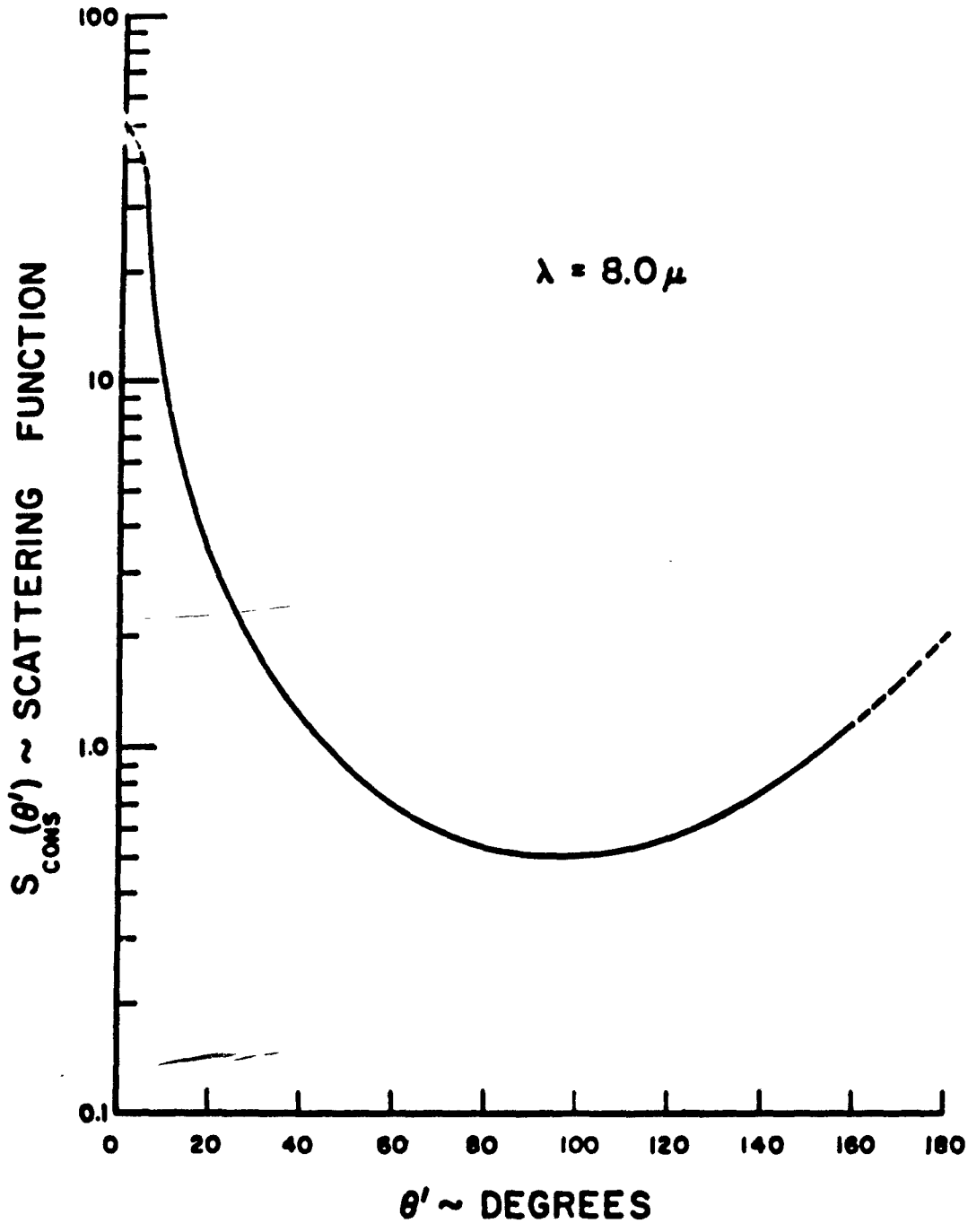

Figure 29. Angular Distribution of Scattering Function--Experimental Data

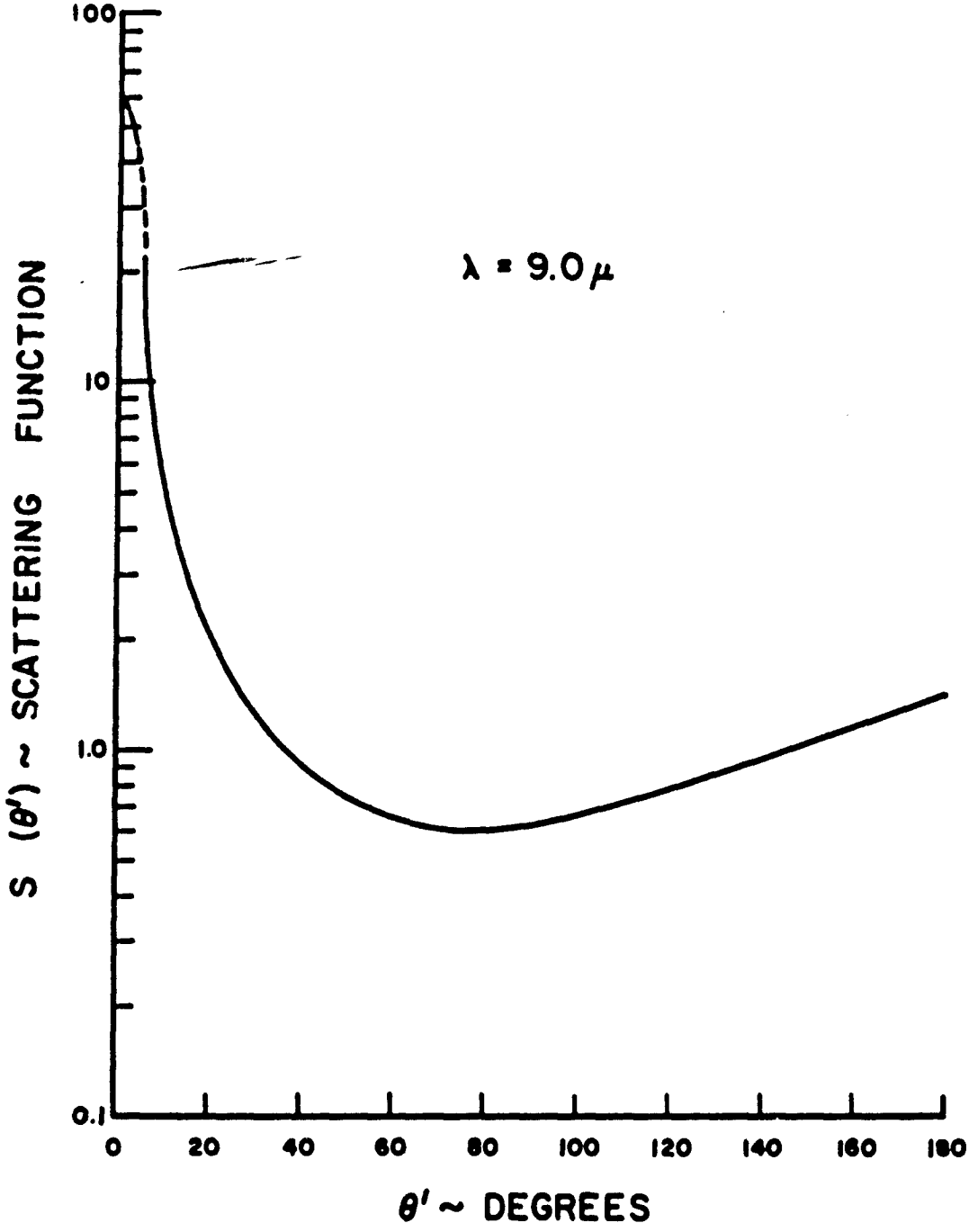

Figure 30. Angular Distribution of Scattering Function--Experimental Data

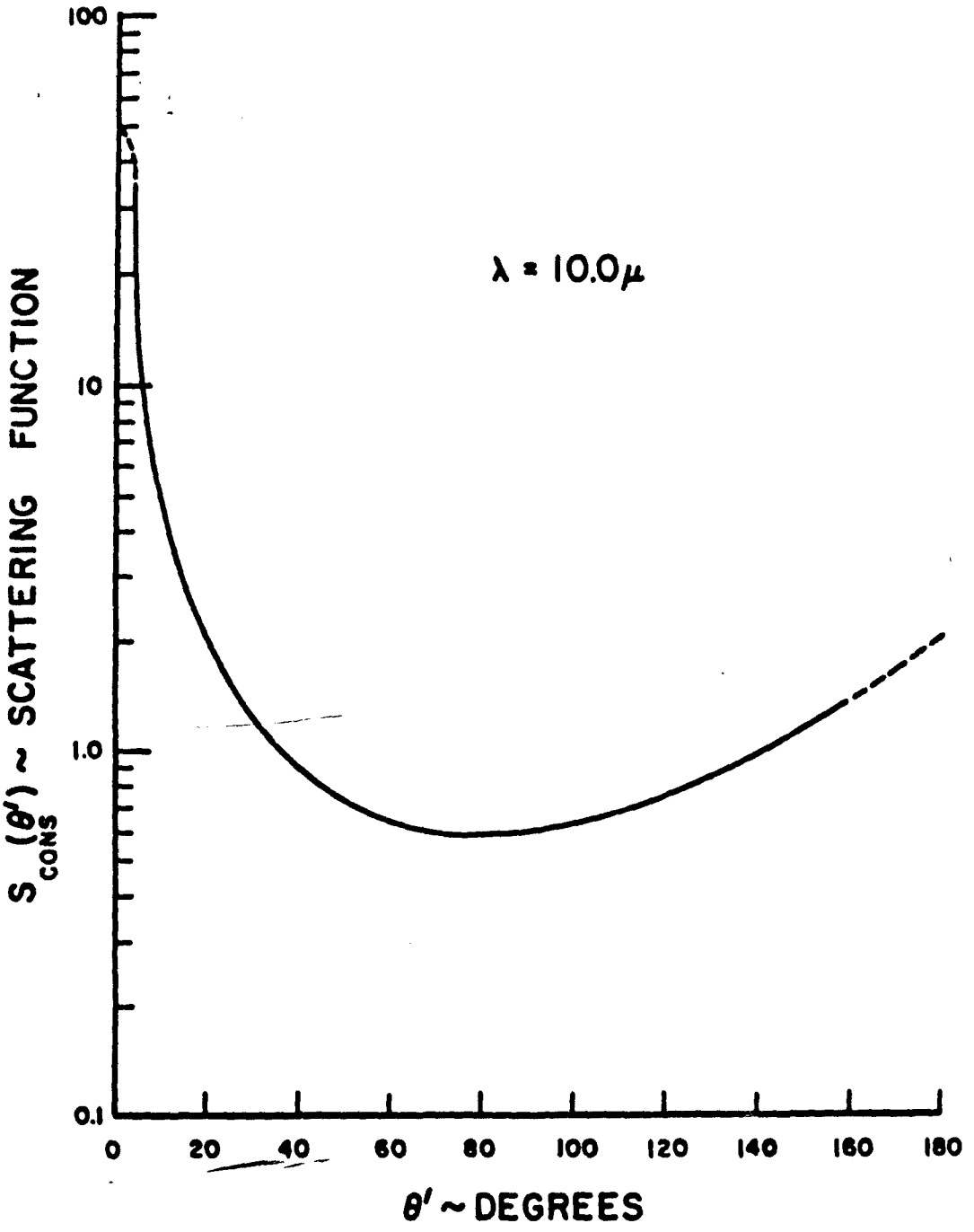

Figure 31. Angular Distribution of Scattering Function--Experimental Data

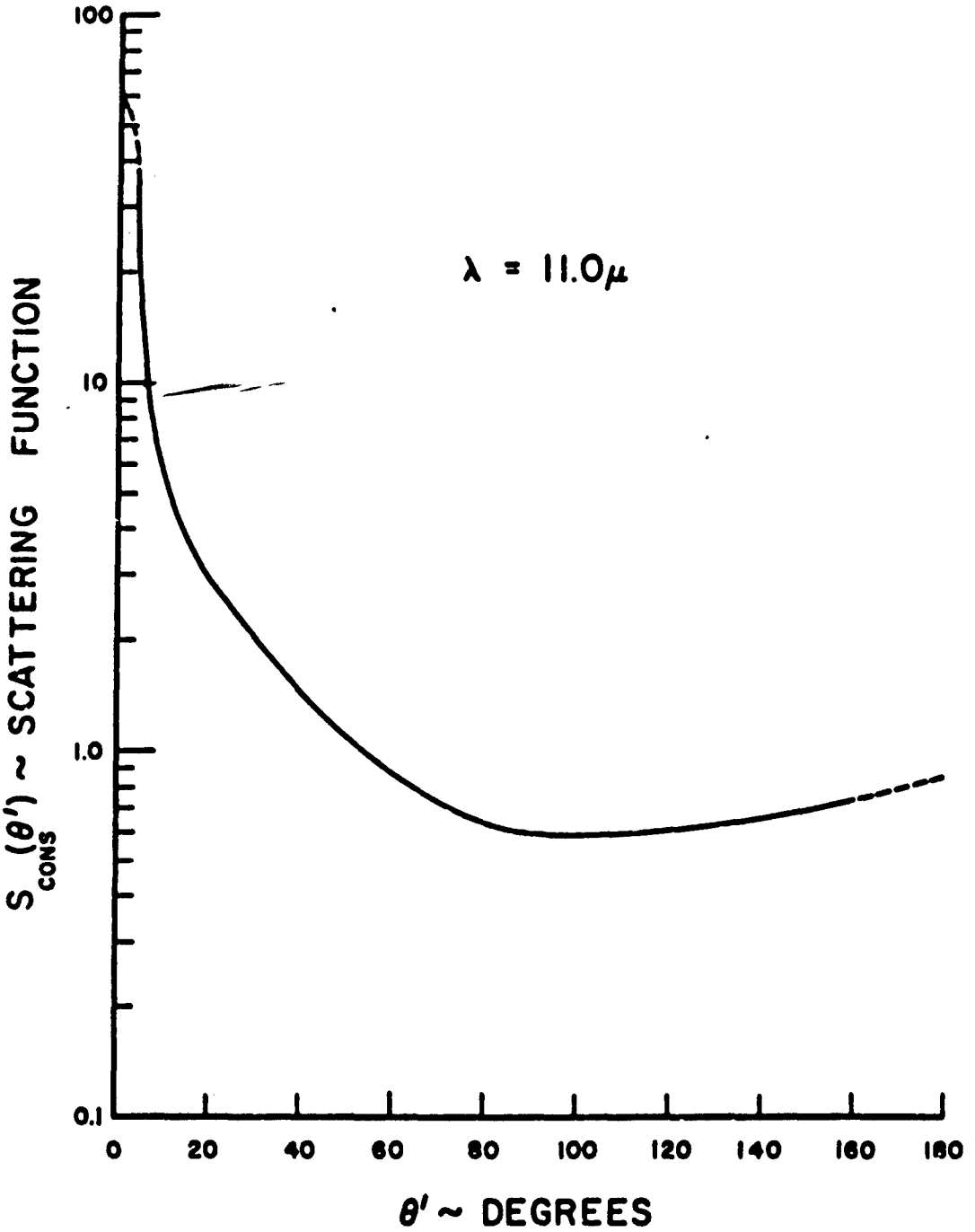

Figure 32. Angular Distribution of Scattering Function--Experimental Data

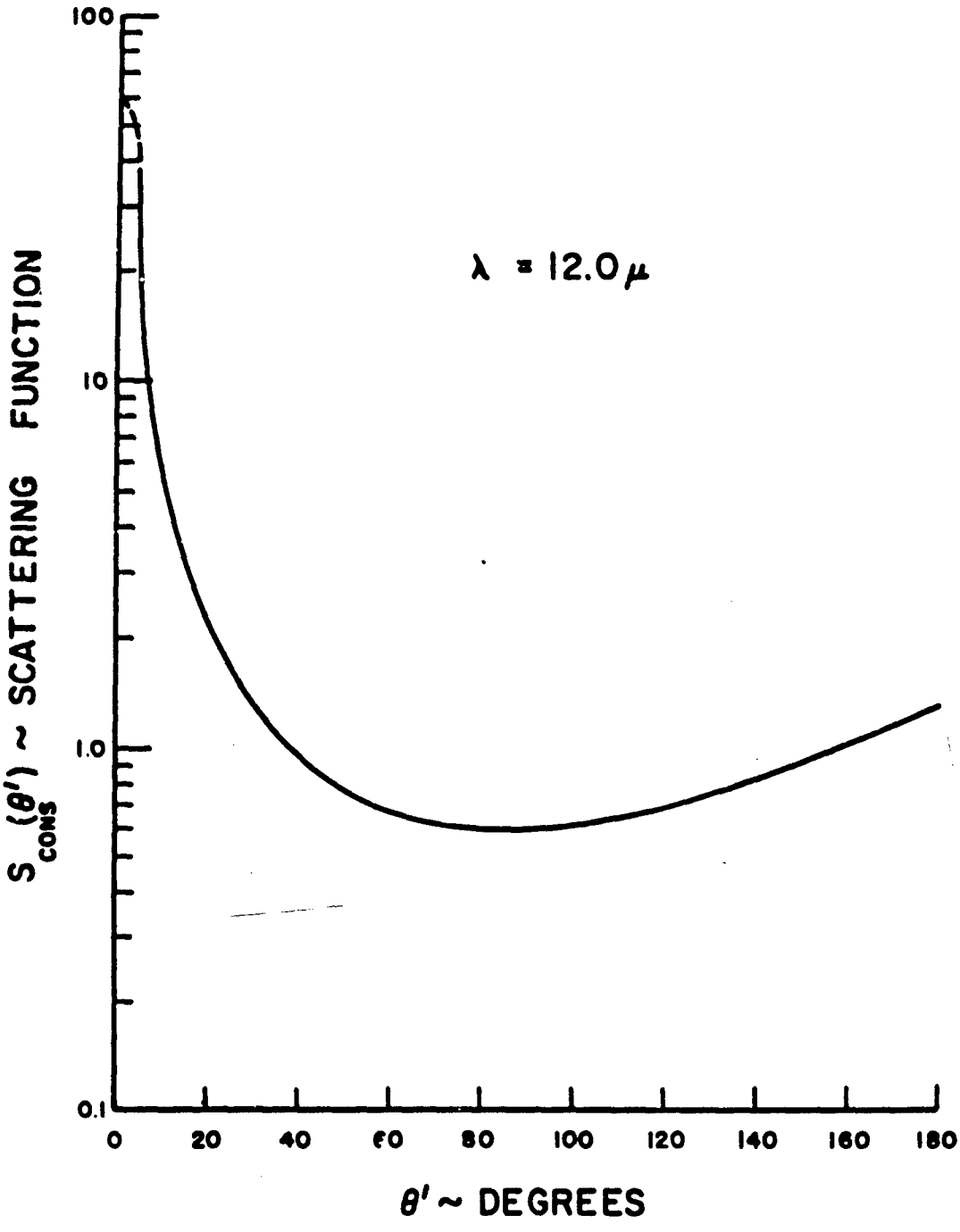

Figure 33 Angular Distribution of Scattering Function--Experimental Data

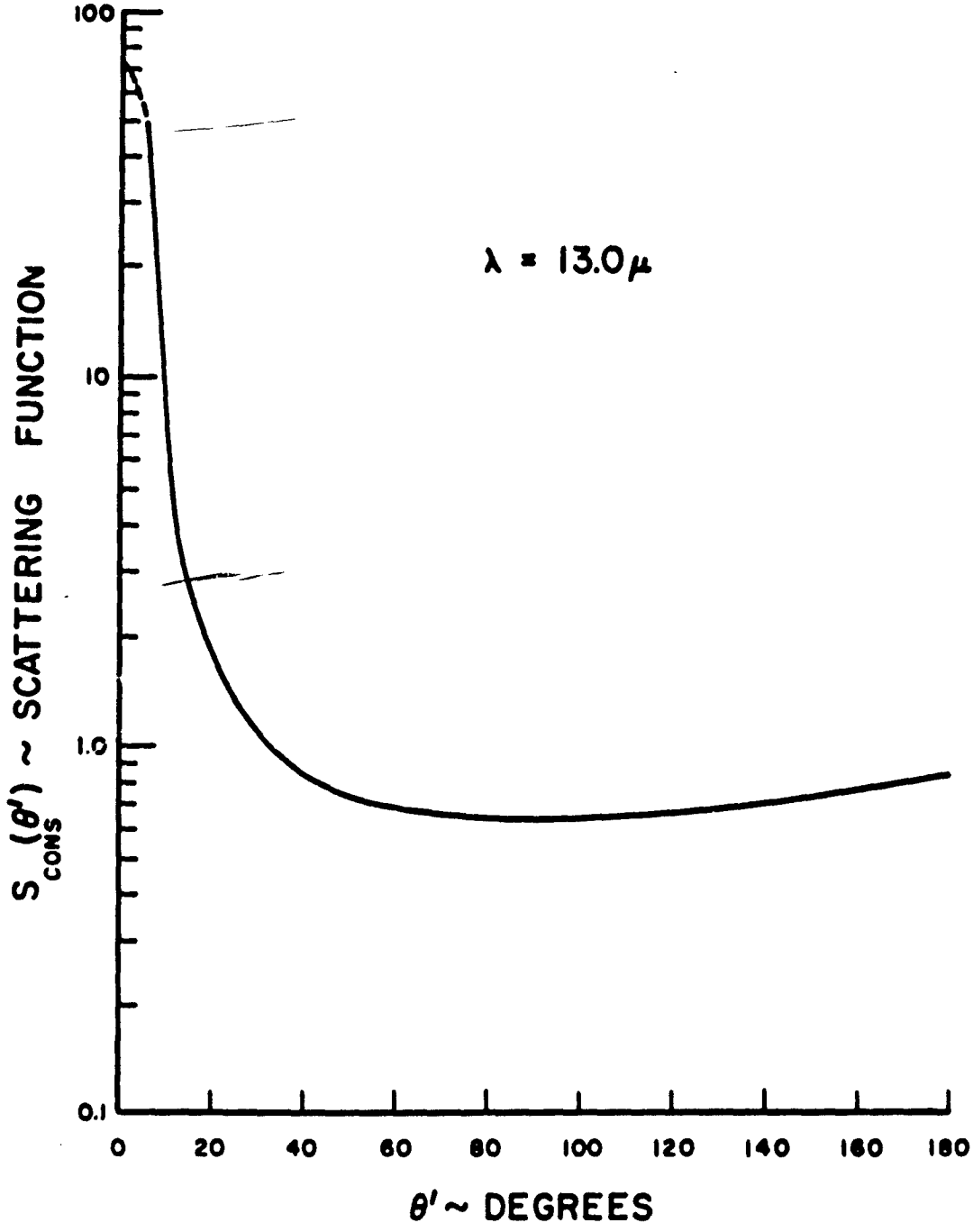

Figure 34. Angular Distribution of Scattering Function--Experimental Data

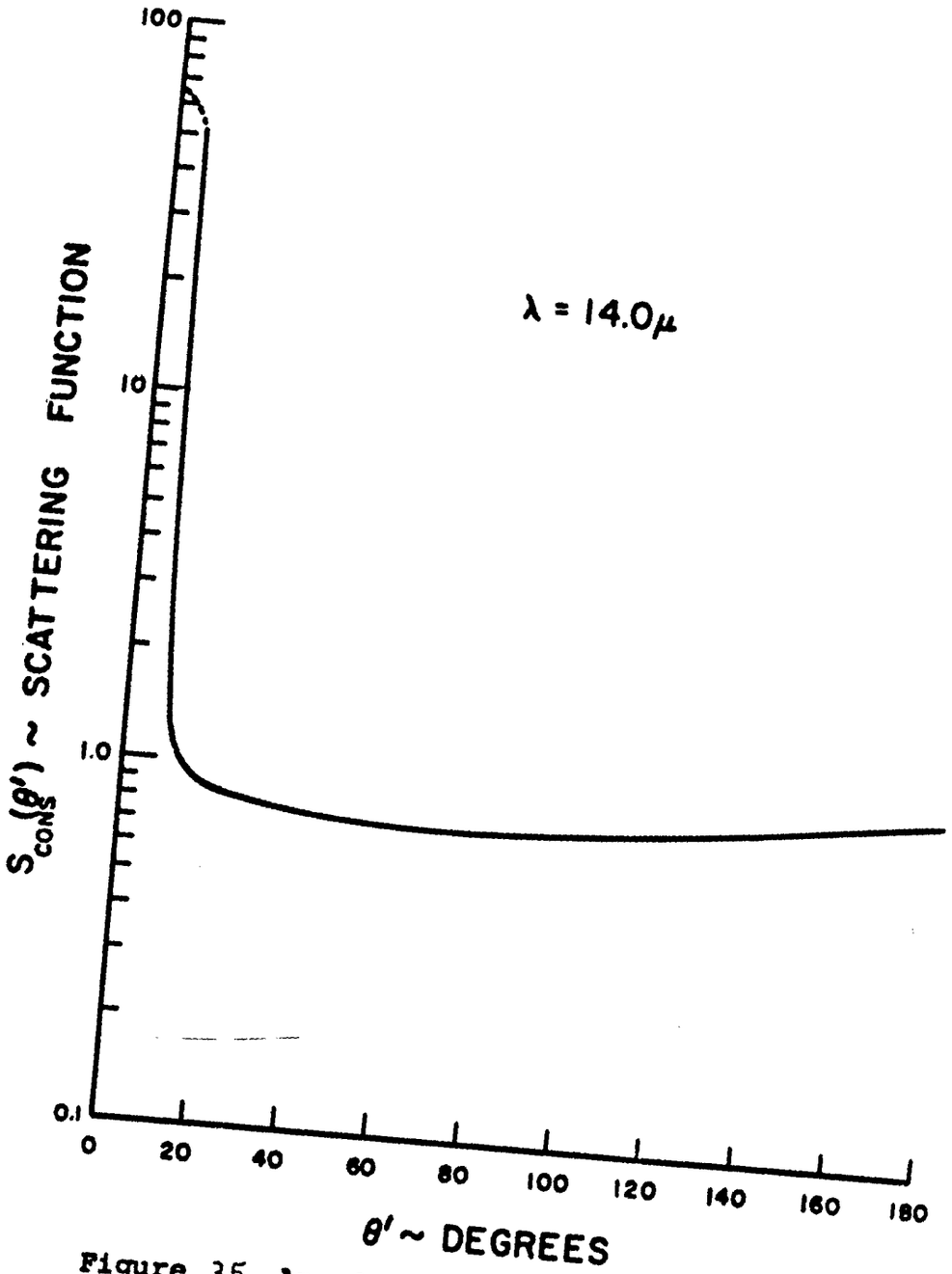

Figure 35. Angular Distribution of Scattering Function--Experimental Data

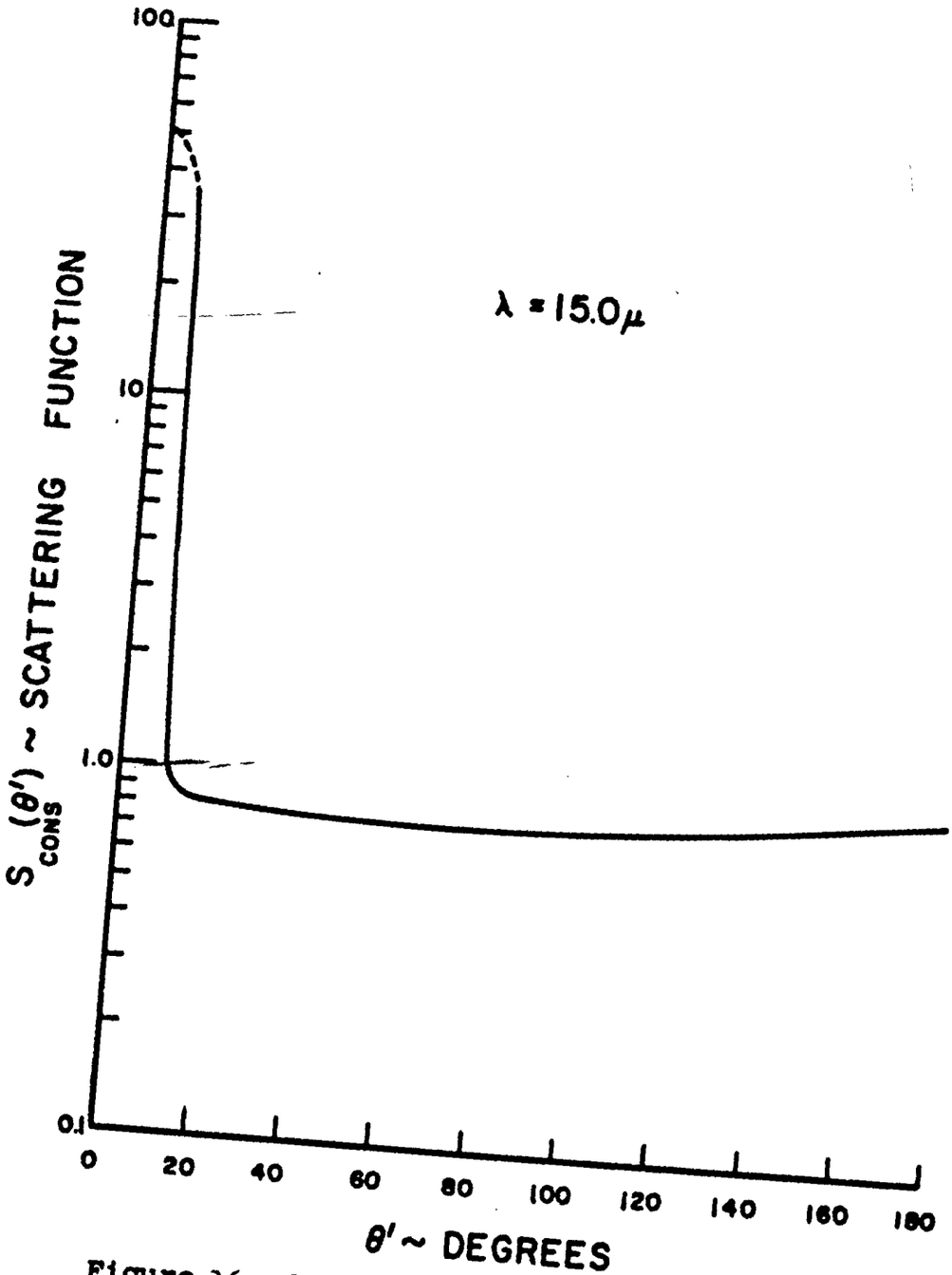

Figure 36. Angular Distribution of Scattering Function--Experimental Data

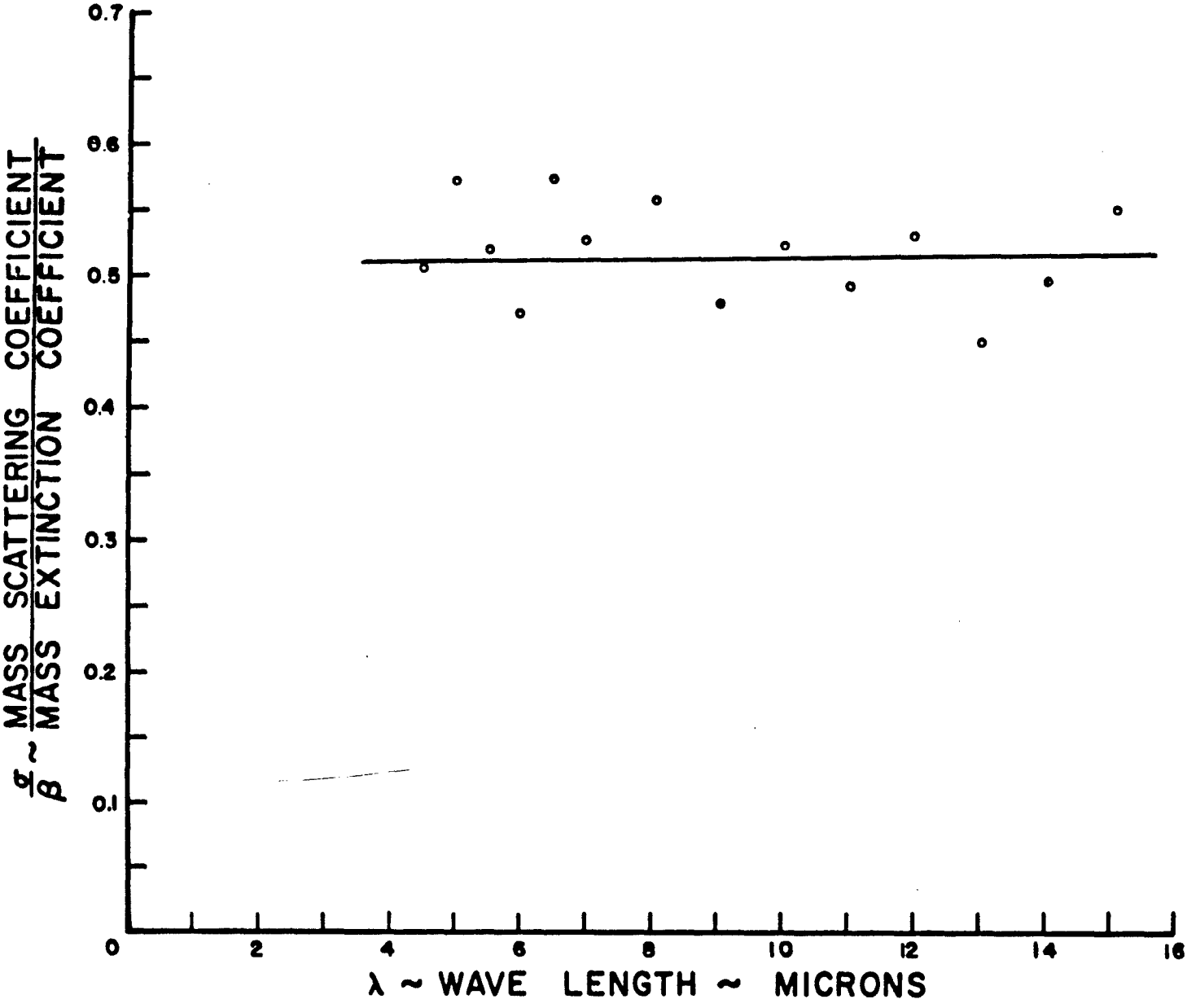

Figure 37. Variation of σ/β with Wave Length

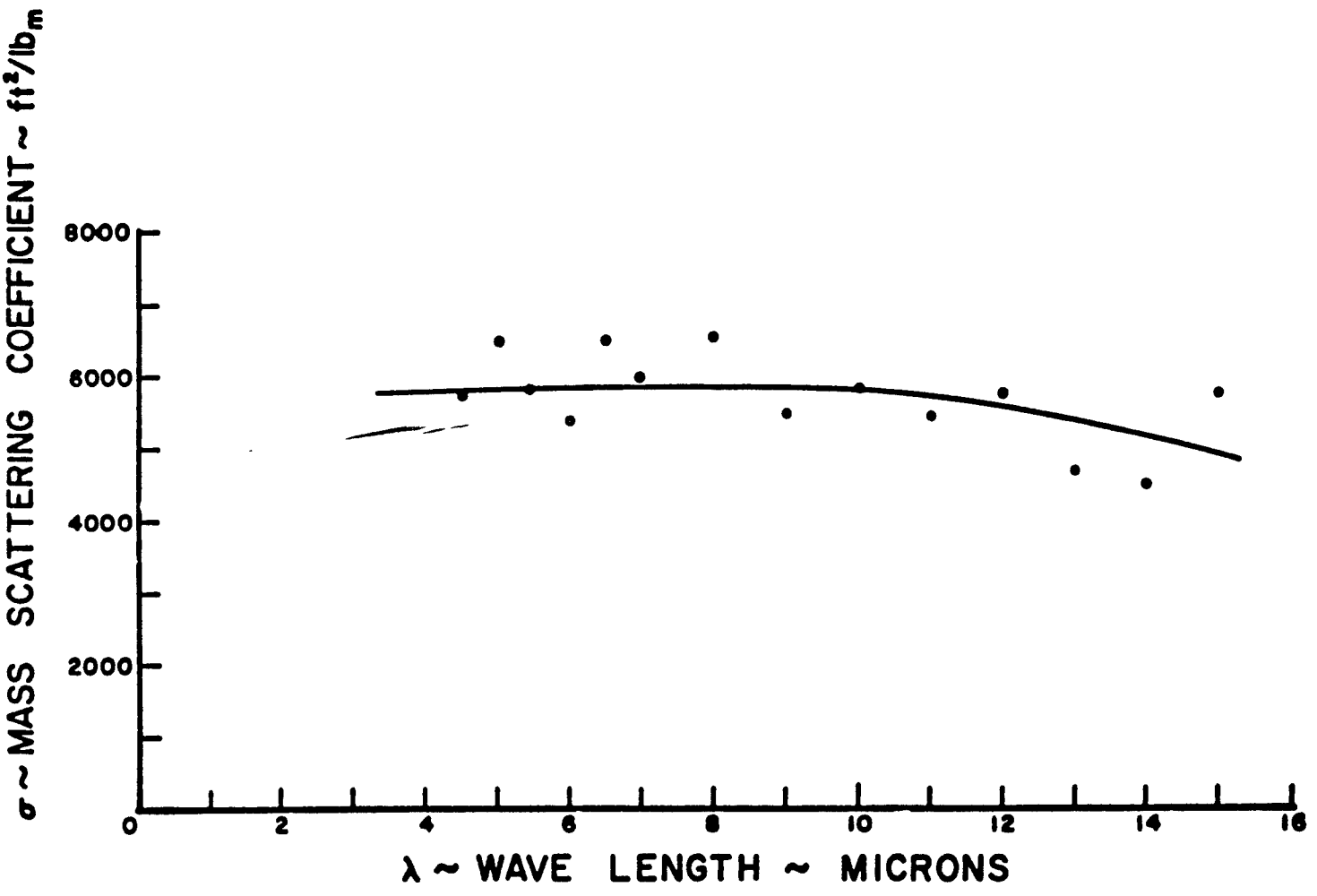

Figure 38

Mass Scattering Coefficient with Wave Length

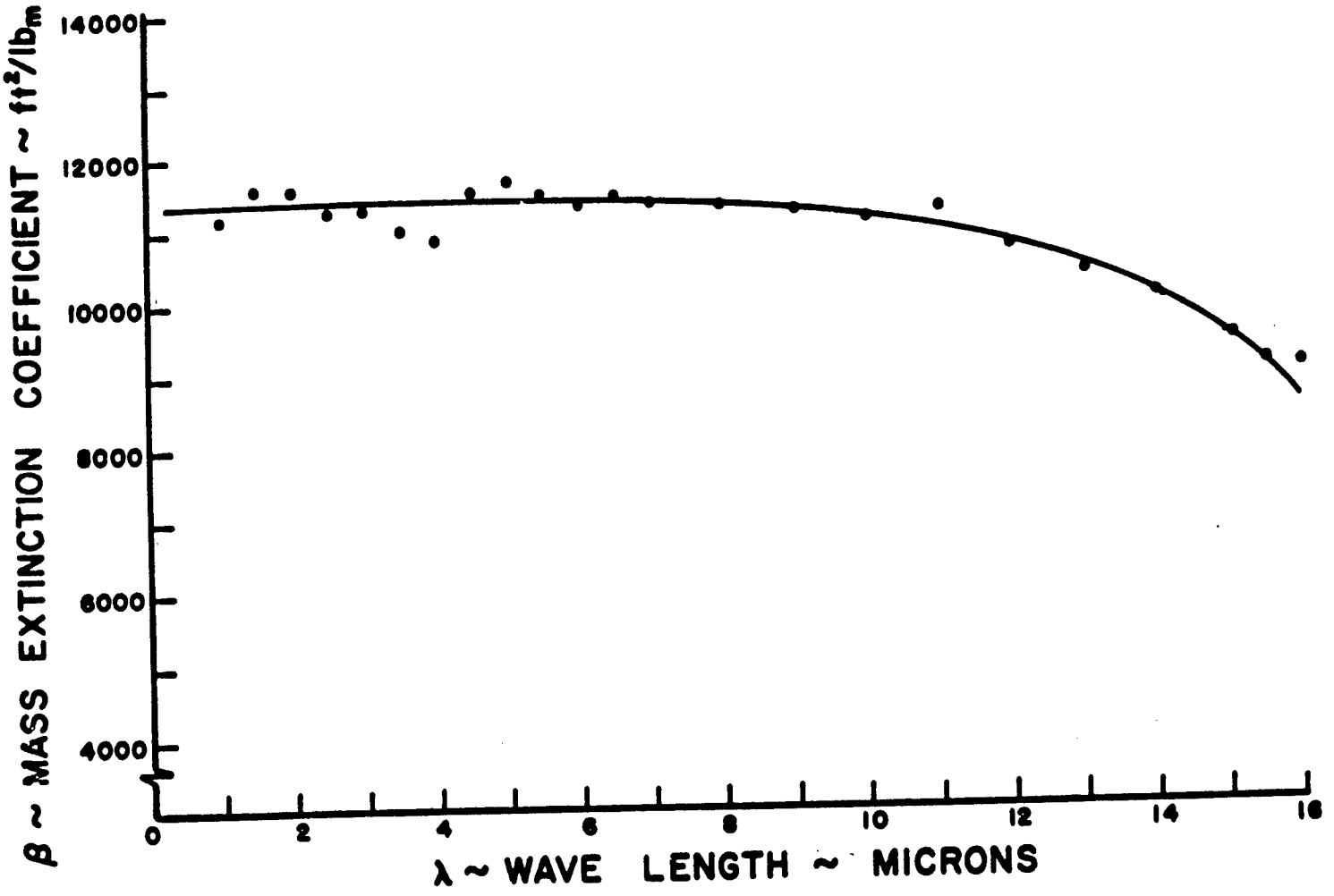

Figure 39

Variation of Mass Extinction with Wave Length

SECTION III

RESULTS AND CONCLUSIONS

COMPARISON OF EXPERIMENTAL RESULTS WITH THEORY

In any experimental work it is possible to gain a great deal of confidence and perhaps to obtain personal satisfaction if it can be stated simply that the experimental results compared quite favorably with the theoretical investigations. However, this is not possible for the experimental work reported herein, since the only existing theory with which a comparison could possibly be made is the classical theory of Mie, and Mie's theory is limited to spherical particles of known refractive index. As stated earlier, no theory has been established for the case of scattering from non-homogeneous systems containing irregular-shaped particles.

If the scattering function obtained through computations of the Mie theory for spherical particles of a known refractive index and particle-size parameter (α) were plotted as a function of scattered angle (Θ), the resulting curve would not be a smooth function. Such a curve would include several maxima and minima plus, in some instances, secondary maxima and minima, with an increase in the number of maxima and a corresponding increase in the particle-size parameter, i.e., with a decreasing value of wave length. It is also known that the maxima and minima do not occur at the same angle (Θ) with variation in the particle-size parameter, and there is a variation in the location of these maxima for particles of different refractive indicies.

Therefore, the only comparison that can be made between the Mie theory and the results of this investigation are the "general trends" of the regular distribution curves. A comparison of this type has been made assuming the refractive index of the aerosol to be 1.6, which is approximately the refractive index of aluminum oxide. The angular distribution of the scattering function was calculated using the IBM1410 Computer for a refractive index of 1.6 and particle size parameters (α) of 2, 3, 4, 5, 6, 8, and 15, with the aid of tables of the Legendre polynomials (21) and the angular distribution coefficient (17).

The Mie scattering functions were calculated and plotted for angles of Θ between 1 and 180 degrees at 5-degree intervals and are included as an Appendix E. A cursory comparison between the angular distribution curves plotted from this investigation and the Mie curves will show that the trends are the same. As an example, for decreasing values of wave length (large α) the ratio of the scattered intensity at 0 degrees compared to that at 90 degrees increases for both the experimental and the theoretical curves. Similarly, variations of the forward and backward scattering with variations in wave length will display the same trend. An examination of both the theoretical and experimental curves will also emphasize the influence of irregular shaped particles on the angular distribution

curves. The experimental curves will not depict the maxima and minima as illustrated by the theoretical curves based on media containing non-absorbing spherical particles.

It might be expected that a solution to the problem of scattering from irregular-shaped particles could be obtained by superimposing the results of the computations for scattering from particles of a variety of sizes. This approach to the solution of the problem would undoubtedly provide some interesting answers and might provide answers that would be sufficiently accurate for most engineering work. However, this approach would be extremely difficult and would obviously require a great expenditure of time. If this approach were taken, one would intuitively feel that the results would indicate that for irregular shaped particles of various sizes and orientations the scattering function, when plotted as a function of scattering angle (Θ) would approach a smooth curve; i.e., the maxima and minima for the case of spherical particles would tend to dampen out, resulting in a smooth function.

As has been shown by Van de Hulst (156), the imaginary component of the refractive index, which must be included when considering absorbing particles, can be considered a dampening component which would also tend to reduce the large amplitudes that occur in Mie curves for non-absorbing particles.

The results of the experimental data indicate that this is true; however, there is little information through which the experimental results of this investigation can be compared with experimental results of other investigations, as very little information has been reported in the literature. However, there has been an agreement with measurements recorded as a result of experiments on light scattering in the atmosphere (41). Light scattering measurements on fogs and dust particles in the atmosphere result in smooth functions when data are plotted. Hodkinson of Great Britain reported in a paper (79) based on his Ph.D. thesis results of his angular distribution of intensity experiments on dusts of quartz, diamond, bituminous and anthracite coal. These results indicated that a smooth function was obtained for the scattering from irregular-shaped particles. His data, however, considered only the angular range between 0 and 90 degrees and was limited to wave lengths 0.546 and 0.526 microns.

No method or equation has been developed which permits the calculation of the scattering function, the mass scattering coefficient, and mass extinction coefficient for media containing particles having irregular shapes, sizes and orientations. To obtain a realistic solution to the radiative heat transfer equation for problems considering scattering and absorbing media, laboratory equipment must be designed to evaluate these functions experimentally. The experimental approach to the determination of these functions is not only feasible, but it appears to be the most promising. Once the equipment is designed and developed, accurate scattering data can be obtained with relative ease.

The angular distribution of intensity and the mass scattering and mass extinction coefficients were obtained for a media containing particles of aluminum oxide of irregular size and shape suspended in air. The data was obtained for 21 wave lengths over a range of 1 to 15 microns at 0.5-micron intervals between wave lengths of 1 and 7 microns and at 1-micron intervals between wave lengths of 7 and 15 microns.

The results of this investigation indicate that the scattering from irregular shaped particles will produce angular distribution of intensity curves which are smooth functions. This further supports the experiments of those few who have attempted to measure the scattered intensity for poly-disperse media.

No exact theory exists with which to compare the experimental results: however, a cursory comparison with the Mie theory as well as a study of the literature covering scattering measurements indicate that no irregularities have occurred during the investigation which would raise any doubt as to the reliability of the data.

The mass scattering coefficient calculated from the experimental data indicates that the scattering media contained absorbing particles; i.e., the ratio of the mass scattering coefficient to the mass extinction coefficient ($\frac{\sigma}{\beta}$) was approximately 0.52 for all wave lengths.

The refractive index of the media has a marked influence on any theoretical calculation of the scattering function even when spherical particles are assumed. To the knowledge of the author, no satisfactory method exists for determining the refractive index of powders composed of particles having irregular size, shape and orientation; however, knowledge of the refractive index is not necessary for an experimental determination of the scattering function.

This investigation also revealed a stronger forward scattering for all wave lengths than that indicated by the Mie theory for scattering from spherical particles.

The design of the equipment was sufficiently versatile that data similar to that obtained during this investigation can be obtained for other types of media. It is anticipated that only a modification in technique and procedure would be required to investigate media containing other types of particles. The following improvements are suggested before ~~future~~ investigations are attempted:

1. The present method of measuring airflow rate should be modified through use of a more sensitive device, such as a manometer and calibrated orifice plate.

2. An improved vacuum system would allow longer periods of time for the collection of particles to be weighed for the density calculations, unless an alternate method of obtaining media density could be developed.

3. An auxiliary optical system should be provided to investigate the angular distribution of intensity for the angular range 0 to 10 degrees.

This latter suggestion would require a major modification in the present equipment, which was, of course, the primary reason that it was not incorporated in the present design. As stated earlier, it was the angular region 0 to 10 degrees that required alternate techniques in obtaining data, and skepticism toward the accuracy of the data occurred.

It can be concluded that equipment of a design such as described herein will provide scattering data for actual media and will aid in obtaining a more realistic solution to the radiative heat transfer equation when applied to problems considering scattering and absorbing media.

SECTION IV

REFERENCES

1. Aughey, W. Henry and F. J. Baum, "Angular-Dependence Light Scattering--A High-Resolution Recording Instrument for the Angular Range 0.05-140°," J. Opt. Soc. Am., XLIV (1954), pp. 833-837.

2. Barnes, Marion D., and Victor K. LaMer, "Monodispersed Hydrophobic Colloidal Dispersions and Light Scattering Properties. II. Total Scattering from Transmittance as a Basis for the Calculation of Particle Size and Concentration," J. Colloid Sci., I (1946), pp. 79-91.

3. Barnes, Marion D., A. S. Kenyon, E. M. Zaiser, "Monodispersed Sulfur Sols. IV. Comparison of the Particle Radius Determined by Transmittance and by the Angular Positions of Higher Order Tyndall Spectra from the Mie Theory," J. Colloid Sci., II (1947), pp. 349-359.

4. Bateman, J. B., E. J. Weneck, and D. C. Eshler, "Determination of Particle Size and Concentration from Spectrophotometric Transmission," J. Colloid Sci., XIV (1959), pp. 308-329.

5. Blevin, W. R. and W. J. Brown, "Light Scattering Properties of Pigment Suspensions," J. Opt. Soc. Am., LI (1961), p. 975.

6. Boll, R. H., R. O. Gumprecht, and C. M. Sliepcevich, "Theoretical Light-Scattering Coefficients for Relative Refractive Indices Less than Unity and for Totally Reflecting Spheres," J. Opt. Soc. Am., XLIV (1954), p. 18.

7. Boll, R. H. and C. M. Sliepcevich, "Evaluation of Errors of Optical Origin Arising in the Size Analysis of a Dispersion by Light Transmission," J. Opt. Soc. Am., XLVI (1956), pp. 200-208.

8. Bonnelycke, Byrg E. and W. B. Dandliker, "Light Scattering of Colloidal Silica," J. Colloid Sci., XIV (1959), pp. 567-571.

9. Born, Max and E. Wolf. Principles of Optics, London: Pergamon Press, 1959.

10. Brackett, Frederick S. and Elliot Charney, "Apparatus for Measuring the Spectral Dependence of Light Scattering from Large Particles," J. Opt. Soc. Am., L (1960), pp. 811-812.

11. Bugnolo, D. S., "Transport Equation for the Spectral Density of a Multiple-Scattered Electromagnetic Field," J. Appl. Phys., XXXI (1960), pp. 1176-1182.

12. Butler, Warren L., "Absorption of Light by Turbid Materials," J. Opt. Soc. Am., LII (1962), pp. 292-299.

13. Carr, C. I., Jr., and B. H. Zimm, "Absolute Intensity of Light Scattering from Pure Liquids and Solutions," J. Chem. Phys., XVIII (1950), pp. 1616-1626.

14. Chandrasekhar, S. Radiative Transfer, Oxford University Press (1950), Dover Publications (1960).

15. Chromey, F. C., "Evaluation of Mie Equations for Colored Spheres," J. Opt. Soc. Am., L (1960).

16. Chu, C. M. and S. W. Churchill, "Numerical Solution of Problems in Multiple Scattering of Electromagnetic Radiation," J. Phys. Chem., LIX (1955), pp. 855-863.

17. Chu, C. M., C. C. Clark, and S. W. Churchill. Tables of Angular Distribution Coefficients for Light-Scattering by Spheres. University of Michigan Press, Engineering Research Institute (1957).

18. Churchill, S. W., C. M. Chu, L. B. Evans, L. C. Tien, and S. C. Pang. Exact Solutions for Anisotropic, Multiple Scattering by Parallel Plane Dispersions, DASA - 1257 (1961).

19. Churchill, S. W., G. C. Clark, and C. M. Sliepcevich, "Light-Scattering by Very Dense Monodispersions of Latex Particles," Faraday Society Discussions, XXX (1960), pp. 192-199.

20. Clark, Geo. C., Chiao-Min Chu and Stuart W. Churchill, "Angular Distribution Coefficients for Radiation Scattered by a Spherical Particle," J. Opt. Soc. Am., XLVII (1957), pp. 81-84.

21. Clark, G. C. and S. W. Churchill. Legendre Polynomials, University of Michigan Press, Engineering Research Institute (1957).

22. Cleveland, E. Lynn, and Richard C. Raymond, "Scattering of Visible and Near Infra-red Radiation by Layered Distributions of Small Metal Spheres," J. Opt. Soc. Am., XLII (1952), pp. 183-186.

23. Corn, M., "Orientation of Dust Particles During and After Settling in Water," J. Colloid Sci. (to be published).

24. Coumou, D. J., "Apparatus for the Measurement of Light Scattering in Liquids. Measurement of the Rayleigh Factor of Benzene and of Some Other Pure Liquids," J. Colloid Sci., XV (1960), pp. 408-417.

25. Dandliker, Walter B., "Light Scattering Studies of a Polystyrene Latex," J. Am. Chem. Soc., LXXII (1950), pp. 5110-5116.

26. Debye, P., "Light Scattering in Soap Solutions," J. Colloid Sci., III (1948), pp. 407-409.

27. Deirmendjian, D., R. Clasen, and W. Viezee, "Mie Scattering with Complex Index of Refraction," J. Opt. Soc. Am., LI (1961), pp. 620-633.

28. Denman, H., W. Heller, and W. J. Pangonis. Angular Scattering Functions for Spherical Particles II, Detroit: Wayne State University Press, 1963.

29. DeVore, J. R. and A. H. Pfund, "Optical Scattering by Dielectric Powders of Uniform Particle Size," J. Opt. Soc. Am., XXXVII (1947), pp. 826-832.

30. Dezelic, Gjuro, and Josip P. Kratohvil, "Determination of Particle Size of Polystyrene Latexes by Light Scattering," J. Colloid Sci., XVI (1961), pp. 561-580.

31. Doty, Paul and Robert F. Steiner, "Light Scattering and Spectrophotometry of Colloidal Solutions," J. Chem. Phys., XVIII (1950), pp. 1211-1220.

32. Drude, Paul. The Theory of Optics, (Translated from the German by C. Riborg Mann and Robert A. Millikan) New York: Dover Publications, Inc., 1959.

33. Duntley, Seibert Q., "The Optical Properties of Diffusing Materials," J. Opt. Soc. Am., XXXII (1942), pp. 61-69.

34. Ellison, J. McK., "Extinction of Light by Suspensions of Silica Dust," Proc. Phys. Soc. Brit., LXX (1957), pp. 102-111.

35. Erlander, Stig R., and Dexter French, "Dispersion of Starch Granules and the Validity of Light Scattering Results on Amylopectin," J. Am. Chem. Soc., LXXX (1958), pp. 4413-4420.

36. Filler, A. S. and L. Indyk, "Calibration of Infra-Red Prism Spectrometers," J. Opt. Soc. Am., LI (1961).

37. Fishman, M. M. Light Scattering by Colloidal Systems - An Annotated Billiography, River Edge, New Jersey: Technical Service Laboratories, 1957.

38. Forsythe, W. E. Measurement of Radiant Energy, New York: McGraw-Hill Book Company, Inc., 1932.

39. Frei, K. and Hs. H. Gunthard, "Distortion of Spectral Line Shapes by Recording Instruments," J. Opt. Soc. Am., LI (1961), pp. 83-86.

40. Gibbons, Mathew G., Frank I. Laughridge, John R. Nichols, and Nicholas A. Krause, "Transmission and Scattering Properties of a Nevada Desert Atmosphere under Cloudy Conditions," J. Opt. Soc. Am., LII (1962), pp. 38-43.

41. Gibbons, Mathew G., John R. Nichols, Frank I. Laughridge, and Ralph L. Rudkin, "Transmission and Scattering Properties of a Nevada Desert Atmosphere," J. Opt. Soc. Am., Ll (1961), pp. 633-640.

42. Goldstein, M., "Depolarized Components of Light Scattered by Glasses," J. Appl. Phys., XXX (1959), pp. 493-506.

43. Greenberg, J. Mayo, "Scattering by Nonspherical Particles," J. Appl. Phys., XXXI (1960), pp. 82-84.

44. Greenberg, J. Mayo, Norman E. Pedersen, and Jeanne C. Pedersen, "Microwave Analog to the Scattering of Light by Nonspherical Particles," J. Appl. Phys., XXXII (1961), pp. 233-242.

45. Gucker, Frank T. and James J. Egan, "Measurement of the Angular Variation of Light Scattered from Single Aerosol Droplets," J. Colloid Sci., XVI (1961), pp. 68-84.

46. Gucker, F. T. and R. L. Rowell, "The Angular Variation of Light Scattered by Single Dioctyl Phthalate Aerosol Droplets," Faraday Society Discussions, XXX (1960), pp. 185-191.

47. Gumprecht, R. O. and C. M. Sliepcevich. Tables of Light Scattering Functions for Spherical Particles, University of Michigan Press, Engineering Research Institute (1951).

48. Gumprecht, R. O. and C. M. Sliepcevich, "Scattering of Light by Large Spherical Particles," J. Phys. Chem., LVII (1953), pp. 90-95.

49. Gumprecht, R. O., and C. M. Sliepcevich, "Measurement of Particle Sizes in Polydispersed Systems by Means of Light Transmission Measurements Combined with Differential Settling," J. Phys. Chem., LVII (1953), pp. 95-97.

50. Gumprecht, R. O., N. L. Sung, J. H. Chin, and C. M. Sliepcevich, "Angular Distribution of Intensity of Light Scattered by Large Droplets of Water," J. Opt. Soc. Am., XLII (1952), pp. 226-231.

51. Hardy, A. C., and F. M. Young, "In Defense of Beer's Law," J. Opt. Soc. Am., XXXVIII (1948), pp. 854-858.

52. Harrison, J. A. and C. D. Reid, "Infra-Red Absorptiometer, Using Interference Filters, for Analysis of Hydrogen Fluoride in Gaseous Mixtures," J. Sci. Instr., XXXVI (1959), p. 240.

53. Hart, Robert W. and Elliott W. Montroll, "On the Scattering of Plane Waves by Soft Obstacles. I. Spherical Obstacles," J. Appl. Phys., XXII (1951), pp. 376-386.

54. Hart, R. W., and E. W. Montroll, "Sound Scattering of a Plane Wave from a Nonabsorbing Sphere," J. Acoust. Soc. Am., XXIII (1951), pp. 323-329.

55. Heller, W., "Tyndall Spectra, Their Significance and Applications," J. Chem. Phys., XIV (1946), p. 565.

56. Heller, Wilfried, "Theoretical Investigations on the Light Scattering of Colloidal Spheres. II. Accurate Interpolations of Theoretical Turbidity-Data," J. Chem. Phys., XXVI (1957), pp. 920-922.

57. Heller, Wilfried, "Theoretical Investigations on the Light Scattering of Colloidal Spheres. III. Analytical Expressions for Turbidity Approximating the Performance of the Mie Equations Prior to the First Maximum," J. Chem. Phys., XXVI (1957), pp. 1258-1264.

58. Heller, Wilfried, Hari L. Bhatnagar, and Masayaki Nakagaki, "Theoretical Investigat'ons on the Light Scattering of Spheres. XIII. The 'Wavelength Exponent' of Differential Turbidity Spectra," J. Chem. Phys., XXXVI (1962), pp. 1163-1170.

59. Heller, W. and H. James McCarty, "Theoretical Investigations on the Light Scattering of Colloidal Spheres. IV. Specific Turbidities in the Lower Microscopic Range and Fine Structure Phenomena," J. Chem. Phys., XXIX (1958), pp. 78-80.

60. Heller, Wilfried and Masayuki Nakagaki, "Theoretical Investigations on the Light Scattering of Colloidal Spheres. VII. Dissymmetry in Unpolarized and Polarized Light," J. Chem. Phys., XXXI (1959), pp. 1188-1195.

61. Heller, Wilfried, Masayuki Nakagaki, and Morton L. Wallach, "Theoretical Investigations on the Light Scattering of Colloidal Spheres. V. Forward Scattering," J. Chem. Phys., XXX (1959), pp. 444-450.

62. Heller, Wilfried and William J. Pangonis, "Theoretical Investigations on the Light Scattering of Colloidal Spheres. I. The Specific Turbidity," J. Chem. Phys., XXVI (1957), pp. 498-506.

63. Heller, Wilfried and Thomas L. Pugh, "Experimental Investigations on the Effect of Light Scattering Upon the Refractive Index of Colloidal Particles," J. Colloid Sci., XII (1957), pp. 294-307.

64. Heller, Wilfried, and Richard M. Tabibian, "Experimental Investigations on the Light Scattering of Colloidal Spheres. II. Sources of Error in Turbidity Measurements," J. Colloid Sci., XII (1957), pp. 25-39.

65. Heller, W., and Richard Tabibian, "Experimental Investigations on the Light Scattering of Colloidal Spheres. IV. Scattering Ratio," J. Phys. Chem., LXVI (1962), pp. 2059-2065.

66. Henry, R. L., "The Transmission of Powder Films in the Infra-Red," J. Opt. Soc. Am., XXXVIII (1948), pp. 775-789.

67. Hill, F. B. and R. H. Wilhelm, "Radiative and Conductive Heat Transfer in a Quiescent Gas-Solid Bed of Particles," J. Am. Inst. Chem. Engr., V (1957).

68. Hughes, W. J., and P. Johnsen, "The Construction and Testing of a 'Universal' Light Scattering Apparatus," J. Sci. Instr., XXXV (1958), pp. 57-59.

69. Hutchinson, Eric, Physical Chemistry, Philadelphia (London): W. B. Saunders Co., 1962.

70. Jakob, M. Heat Transfer, I. J. Wiley and Sons (1949).

71. Jakob, M. Heat Transfer, II. J. Wiley and Sons (1957).

72. Jenkins, Francis A., and Harvey E. White. Fundamentals of Optics, 2nd ed., New York: McGraw-Hill Book Company, Inc., 1950.

73. Johnson, Irving, and Victor K. LaMer, "The Determination of the Particle Size of Monodispersed Systems by the Scattering of Light," J. Am. Chem. Soc., LXIX (1957), pp. 1184-1192.

74. Jones, J. F., "Method of Double Beam Spectrophotometry in the Vacuum Ultra-Violet," J. Sci. Instr., XXXVI.

75. Kahn, A. H., "Phase-Shift Method for One Dimensional Scattering," Am. J. Phys., XXIX (1961), pp. 77-80.

76. Kauzman, Walter. Quantum Chemistry, New York: Academic Press, Inc., 1957.

77. Keith, C. H., and J. C. Derrick, "Measurement of the Particle Size Distribution and Concentration of Cigarette Smoke by the 'Conifuge,'" J. Colloid Sci., XV (1960), pp. 340-356.

78. Keller, Joseph B., "Geometrical Theory of Diffraction," J. Opt. Soc. Am., LII (1962), pp. 116-130.

79. Kerker, Milton, Electromagnetic Scattering, Proceedings of the Inter-disciplinary Conference held at Clarkson College of Technology, Potsdam, New York. New York: Pergamon Press, 1963.

80. Kerker, M., "The Use of White Light in Determining Particle Radius by the Polarization Ratio of the Scattered Light," J. Colloid Sci., V (1950), pp. 165-167.

81. Kerker, Milton, and Merle I. Hampton, "The Use of Unfiltered Light in Determining Particle Radius by the Polarization Ratio of the Scattered Light," J. Opt. Soc. Am., XLIII (1953), pp. 370-372.

82. Kerker, Milton, and Victor K. LaMer, "Particle Size Distribution in Sulfur Hydrosols by Polarimetric Analysis of Scattered Light," J. Am. Chem. Soc., LXXII (1950), pp. 3516-3525.

83. Kerker, M., D. Lee, and A. Chou, "The Molecular Weight of Phosphotungstic Acids by Light Scattering," J. Am. Chem. Soc., LXXX (1958), pp. 1539-1545.

84. Kerker, Milton and Egon Matijevio, "Light Scattering of Monodispersed Polystyrene Latexes," J. Opt. Soc. Am., L (1960), pp. 722-729.

85. Kourganoff, V. Basic Methods in Heat Transfer Problems, Oxford University Press (1952).

86. Kratohvil, J. P., Gj. Dezelic, M. Kerker, and E. Matijevic, "Calibration of Light-Scattering Instruments: A Critical Survey," J. Polymer Sci., LVII (1962), pp. 59-78.

87. Kubelka, Paul, "New Contributions to the Optics of Intensely Light-Scattering Materials. Part I." J. Opt. Soc. Am., XXXVIII (1948), pp. 448-457.

88. Kunz, K. S. Numerical Analysis, New York: McGraw-Hill Book Company, 1957.

89. LaMer, Victor K., and Marion D. Barnes, "Monodispersed Hydrophobic Colloidal Dispersions and Light Scattering Properties. I. Preparation and Light Scattering Properties of Monodispersed Colloidal Sulfur," J. Colloid Sci., I (1946), pp. 71-76.

90. LaMer, Victor K., and Marion D. Barnes, "A Note on the Symbols and Definitions Involved in Light Scattering Equations," J. Colloid Sci., II (1947), pp. 361-363.

91. LaMer, V. K., and I. W. Plesner, "Letters to the Editor," J. Polymer Sci., XXIV (1957), pp. 147-150.

92. Langer, G., and A. Lieberman, "Anomalous Behavior of Aerosol Produced by Atomization of Monodisperse Polystyrene Latex," J. Colloid Sci., XV (1960), pp. 357-360.

93. Larkin, B. K., and S. W. Churchill, "Scattering and Absorption of Electromagnetic Radiation by Infinite Cylinders," J. Opt. Soc. Am., XLIX (1959), pp. 188-190.

94. Larkin, B. K. and S. W. Churchill, "Heat Transfer by Radiation through Porous Insulations," J. Am. Inst. Chem. Engr., V (1959), pp. 467-474.

95. Lindsey, R. B. Mechanical Radiation, New York: McGraw-Hill Book Company, Inc., 1960.

96. Love, Tom J., Jr. An Investigation of Radiant Heat Transfer in Absorbing, Emitting and Scattering Media, Norman, Oklahoma: University of Oklahoma Research Institute, 1963. (Contract AF 33 (657)-8859) (ARL63-3).

97. Lowan, A. Tables of Scattering Functions for Spherical Particles, National Bureau of Standards (U.S.), Applied Mathematics Series 4 (1949).

98. McCartney, J. T. and S. Ergun, "Refractive Index and Thickness of Ultrathin Sections of Coals and Graphite by Interferometry," J. Opt. Soc. Am., LII (1962).

99. McIntyre, D., and G. C. Doderer, "Absolute Light-Scattering Photometer: Design and Operation," J. Res. Natl. Bur. Std., LXII (1959), pp. 153-159. (Research Paper 2946)

100. Mallette, F. S. Air Pollution, New York: Reinhold Publishing Corporation, 1955.

101. Maron, Samuel H., and Richard L. H. Lou, "Calibration of Light Scattering Photometers with Ludox," J. Polymer Sci., XIV (1954), pp. 29-36.

102. Matijevic, E., M. Kerker, and K. F. Schulz, "Light Scattering of Coated Aerosols. Part I - Scattering by the AgCl Cores," Faraday Soc. Discussions, XXX (1960), pp. 178-184.

103. Matijevic, E., R. H. Ottewill, and M. Kerker, "Light Scattering by Infinite Cylinders. Spider Fibers," J. Opt. Soc. Am., LI (1961), pp. 115-116.

104. Matijevic, E., K. F. Schulz, and M. Kerker, "Light Scattering of Coated Aerosols. II. Scattering by Linolenic Acid Aerosols," J. Colloid Sci., XVII (1962), pp. 26-38.

105. Meehar, E. J., and Z. Z. Hugas, "Light Scattering Functions for Spherical Particles with m = 1.65 (0.05) 185," J. Opt. Soc. Am., LI (1961), p. 260.

106. Middleton, W. E. Knowles. Vision Through the Atmosphere, Toronto: University of Toronto Press, 1952.

107. Middleton, W. E. Knowles, "Diffusion of Ultraviolet and Visible Light by Ground Surfaces of Fused Quartz," J. Opt. Soc. Am., L (1960), pp. 747-749.

108. Millikan, R. C., "Measurement of Particle and Gas Temperatures in a Slightly Luminous Premixed Flame," J. Opt. Soc. Am., LI (1961), p. 535.

109. Montroll, E. W., and J. M. Greenberg, "Scattering of Plane Waves by Soft Obstacles. III. Scattering by Obstacles with Spherical and Circular Cylindrical Symmetry," Phys. Rev., LXXXVI (1952), pp. 889-898.

110. Nakagaki, Masayuki, and Wilfried Heller, "Theoretical Investigations on the Light Scattering of Colloidal Spheres. VI. Backward Scattering," J. Chem. Phys., XXX (1959), pp. 783-786.

111. Nakagaki, Masayuki, and Wilfried Heller, "Theoretical Investigations on the Light Scattering of Colloidal Spheres. VIII. Angular Location of Intensity Maxima and Minima in the Radiation Diagram of Colloidal Spheres," J. Chem. Phys., XXXII (1960), pp. 835-842.

112. Olson, Donald R., "Research Proposal on Self-Ignition of Fuel Droplets," submitted to National Science Foundation by Department of Mechanical Engineering, Pennsylvania State University.

113. Osborne, A. B., "7 KW Plasma Jet for Laboratory Use," J. Sci. Instr., XXXVI (1959), p. 317.

114. Pangonis, William J., Wilfried Heller, and Nicolaos A. Economou, "Theoretical Investigations on the Light Scattering of Colloidal Spheres. IX. Lateral Scattering at 90° from Incident Natural and Linearly Polarized Light," J. Chem. Phys., XXXIV (1961), pp. 960-970.

115. Pangonis, W. M., W. Heller, and A. Jacobson. Tables of Light Scattering Functions of Spherical Particles, Detroit: Wayne State University Press, 1957.

116. Penndorf, R. New Tables of Mie Scattering Functions, Geophysics Research Directorate, Air Force Cambridge Research Center, (Parts 1, 2, 3, 4, 5, 6; m = 1.33, 1.40, 1.44, 1.486, and 1.50).

117. Penndorf, R., "Scattering Coefficients for Absorbing and Nonabsorbing Aerosols," Research on Aerosol Scattering in the Infrared, Scientific Report No. 3, Bedford, Massachusetts: Air Research and Development Command, United States Air Force, 1960. (Avco Corp., Tech. Rept. RAD-TR-60-27).

118. Penndorf, Rudolf B., "Atlas of Scattering Diagrams for n = 1.33," Research on Aerosol Scattering in the Infrared, Scientific Report No. 5, Bedford, Massachusetts, Office of Aerospace Research, United States Air Force, 1961 (AFCRL-1044; Avco RAD-TR-61-32) 69 pages.

119. Penndorf, Rudolf B., "An Approximation Method to the Mie Theory for Colloidal Spheres," J. Phys. Chem., LXII (1958), pp. 1537-1542.

120. Penndorf, Rudolf B., "Angular Mie Scattering," J. Opt. Soc. Am., LII (1962), pp. 402-408.

121. Planck, M. Theory of Heat, London: MacMillan and Company, Limited, 1932.

122. Planck, M. Theory of Light, London: MacMillan and Company, Limited, 1932.

123. Planck, Max. The Theory of Heat Radiation, New York: Dover Publications, Inc.

124. Pritchard, B. S. and W. G. Elliott, "Two Instruments for Atmospheric Optics Measurements," J. Opt. Soc. Am., L (1960), pp. 191-202.

125. Roof, R. B., Jr., "Experimental Determination of Atomic Scattering Factors," J. Appl. Phys., XXX (1959), pp. 1599-1603.

126. Sato, T., and R. Matsumoto, "Radiant Heat Transfer from Luminous Flame," Intern. Heat. Transfer Conference Proc. (1961).

127. Saunderson, J. L., "Calculation on the Color of Pigmented Plastics," J. Opt. Soc. Am., XXXII (1942), pp. 727-736.

128. Schiff, L. I., "Approximation Method for Short Wave-length or High-Energy Scattering," Phys. Rev., CIV (1956), pp. 1481-1485.

129. Schiff, L. I., "Scattering of Waves and Particles by Inhomogeneous Regions," J. Opt. Soc. Am., LII (1962), pp. 140-144.

130. Schuster, A., "Radiation Through a Foggy Atmosphere," Astrophys. J., XXI (1905), pp. 1-22.

131. Sekera, Z., "Light Scattering in the Atmosphere and the Polarization of Sky Light," J. Opt. Soc. Am., XLVII (1957), pp. 484-490.

132. Sinclair, David, "Light Scattering by Spherical Particles," J. Opt. Soc. Am., XXXVII (1947), pp. 475-480.

133. Sinclair, D. Physical Properties of Aerosols, New York: McGraw-Hill Book Company, Inc., 1952.

134. Sinclair D., and V. K. LaMer, "Light Scattering as a Measure of Particle Size in Aerosols," Chem. Rev., XLIV (1949), pp. 245-267.

135. Slavin, Walter, R. W. Mooney, and D. T. Palumbo, "Energy-Recording Spectrofluorimeter," J. Opt. Soc. Am., LI (1961), 93.

136. Sleator, F. B., "A Variational Solution to the Problem of Scalar Scattering by a Prolate Spheroid," J. Math Phys., XXXIX (1960), pp. 105-120.

137. Sliepcevich, C. M., and Gumprecht, R. O., "Scattering of Light by Large Spherical Particles," J. Phys. Chem., LVII (1953), p. 90.

138. Slutsker, A. I., and V. A. Marikin, "Certain Problems in the Theory of the Scattering of Electromagnetic Radiation by Submicroscopic Nonspherical Particles," Opt. and Spectroscopy, X (1961), p. 116.

139. Slutsker, A. I., and V. A. Marikin, "Measurement of the Transmittance of a Light-Scattering Medium as a Method of Studying Inhomogeneities in it," Opt. and Spectroscopy, X (1961), pp. 263-266.

140. Stacey, K. A. Light Scattering in Physical Chemistry, New York: Academic Press, 1956.

141. Stavropoulos, Napoleon, "Deposition of Particles from Turbulent Gas Streams," a thesis submitted in partial fulfillment of the requirements for the degree of Master of Science to the Faculty of Engineering, Columbia University (1954).

142. Stegun, Irene A., and Milton Abramowitz, "Generation of Coulomb Wave Functions by Means of Recurrence Relations," Phys. Rev., XCVIII (1955), pp. 1851-1852.

143. Stein, R. S., P. R. Wilson, and S. N. Stidham, "Scattering of Light by Heterogeneous Spheres," J. Appl. Phys., XXXIV (1963), pp. 46-50.

144. Stevenson, A. F., "Electromagnetic Scattering by an Ellipsoid in the Third Approximation," J. Appl. Phys., XXIV (1953), pp. 1143-1151.

145. Stevenson, A. F., "Note on Krishman's Reciprocity Relation in Light Scattering," J. App. Phys., XXVIII (1957), pp. 1015-1016.

146. Stevenson, Arthur F., Wilfried Heller, and Morton L. Wallach, "Theoretical Investigations on the Light Scattering of Colloidal Spheres. XI. Determination of Size Distribution Curves from Spectra of the Scattering Ratio or from Depolarization Spectra," J. Chem. Phys., XXXIV (1961), pp. 1789-1795.

147. Stratton, J. A. Electromagnetic Theory, 1st ed., New York: McGraw-Hill Book Company, Inc., 1941.

148. Sykes, J. B., "Approximate Integration of the Equation of Transfer," Monthly Notes of Royal Astronomical Society, III (1951).

149. Tabibian, Richard M., and Wilfried Heller, "Experimental Investigations on the Light Scattering of Colloidal Spheres. III. The Specific Scattering @ 90^{o}," J. Colloid Sci., XIII (1958), pp. 6-23.

150. Tabibian, Richard M., Wilfried Heller, and Joseph N. Epel, "Experimental Investigations on the Light Scattering of Colloidal Spheres. I. The Specific Turbidity," J. Colloid Sci., XI (1956), pp. 195-213.

151. Theimer, O., and J. Canfield, "Theoretical Analysis of Light Scattering Irregular Dislocation Networks," J. Appl. Phys., XXXIII (1962), pp. 570-574.

152. Thring, M. W., R. J. Foster, I. A. McGrath, and J. S. Ashton, "Prediction of the Emissivity of Hydrocarbon Flames," Intern. Heat Transfer Conference Proc. (1961).

153. Tobias, R. Stuart and S. Young Tyree, Jr., "Application of Light Scattering to the Study of the Hydrolytic Aggregation of Ions," J. Am. Chem. Soc., LXXXI (1959), pp. 6385-6389.

154. Tobias, R. S., and S. Y. Tyree, Jr., "Studies on Hydrolyzed Bismuth (III) Solutions, II. Light Scattering," J. Am. Chem. Soc., LXXXII (1960), pp. 3244-3249.

155. Twersky, V., "Multiple Scattering of Waves and Optical Phenomena," J. Opt. Soc. Am., LII (1962), p. 145.

156. Van de Hulst, H. C., Light Scattering by Small Particles, New York: J. Wiley and Sons, 1957.

157. Verba, J. and R. Hawrylak, "Continuous Rotation Scattering Chamber of New Design," Rev. Sci. Instr., XXXII (1961), pp. 1037-1039.

158. Verschoor, J. D. and P. Greebler, "Heat Transfer by Gas Conduction and Radiation in Fibrous Insulation," Transactions, Am. Soc. Mech. Engr., LXXIV (1952), pp. 961-962.

159. Viskanta, Raymond. Heat Transfer in Thermal Radiation Absorbing and Scattering Media, Argonne, Illinois: Argonne National Laboratory, 1960. (Based on a thesis submitted to the faculty of Purdue University in partial fulfillment of the requirements for the degree of Doctor of Philosophy.) ANL-6170.

160. Wallach, Morton L., Wilfried Heller, and Arthur F. Stevenson, "Theoretical Investigations on the Light Scattering of Colloidal Spheres. XII. The Determination of Size Distribution Curves from Turbidity Spectra," J. Chem. Phys., XXXIV (1961), pp. 1796-1802.

161. Walton, W. A., "Supplement on Particle-Size Analysis," Transactions, Inst. Chem. Engr., XXV (1947), pp. 141-142.

162. Williams, C. S., "Discussion of the Theories of Cavity-Type Sources of Radiant Energy," J. Opt. Soc. Am., LI (1961), p. 564.

163. Wyatt, Philip J., "Scattering of Electromagnetic Plane Waves from Inhomogeneous Spherically Symmetric Objects," Phys. Rev., CXXVII (1962), pp. 1837-1843.

164. Yokobori, S., "Study on the Emissivity of a Gas Which Contains Particles," Intern. Heat Transfer Conference Proc. (1961).

165. Zabrodsky, S. S., "Heat Transfer by a Fluidized Bed," Intern. Heat Transfer Conference Proc. (1961), p. 737.

166. Zimm, Bruno H., "The Scattering of Light and the Radial Distribution Function of High Polymer Solutions," J. Chem. Phys., XVI (1948), pp. 1093-1099.

167. Zimm, Bruno H., "Apparatus and Methods for Measurement and Interpretation of the Angular Variation of Light Scattering; Preliminary Results on Polystyrene Solutions," J. Chem. Phys., XVI (1948), pp. 1099-1116.

TABLE 1

ANGULAR DISTRIBUTION OF SCATTERING FUNCTION, $s_{CONS}(\theta')$
BASED ON EXPERIMENTAL DATA

θ'	θ' (In Degrees)--λ, Wave Length, in Microns				
	$\lambda = 1.0$	$\lambda = 1.5$	$\lambda = 2.0$	$\lambda = 2.5$	$\lambda = 3.0$
1	721.708800	250.629180	132.575980	115.072760	228.020020
2	320.759460	159.491300	70.346442	82.194831	167.214680
3	184.436690	96.834003	48.701383	55.187958	121.610680
4	104.246820	69.777443	35.173221	42.271627	83.607343
5	80.189867	54.113119	27.056323	33.112774	64.605674
6	56.934805	41.296854	23.430776	28.181084	45.604005
7	32.877845	32.752677	18.668863	24.188764	36.483204
8	22.052213	25.632530	15.692667	20.666128	28.502503
9	17.240821	21.645247	13.528161	17.848020	22.041936
10	12.830378	17.657965	11.363656	15.734439	17.101502
11	9.823258	13.670682	9.740276	13.151172	13.301168
12	8.018986	11.392235	8.522742	11.037591	9.880867
13	6.415189	9.683400	7.575770	9.863379	7.600667
14	5.212341	8.116967	6.899362	8.924010	6.080534
15	3.929303	6.550535	6.006503	7.514955	4.940433
16	3.207594	5.525234	5.411264	6.340744	4.180367
17	2.566075	4.841700	4.870138	5.636216	3.572313
18	2.084936	4.129685	4.329011	5.049111	3.192280
19	1.724082	3.474631	3.923166	4.462005	2.888253
20	1.523607	3.132864	3.571434	3.945351	2.546223
21	1.383275	2.620214	3.246758	3.358245	2.280200
22	1.222895	2.335408	2.976195	3.052950	2.128186
23	1.106620	1.993641	2.705632	2.700687	1.900166
24	1.002373	1.794277	2.489181	2.442360	1.748153
25	.922183	1.623393	2.272731	2.254486	1.634143
26	.862041	1.480990	2.137449	2.090097	1.520133
27	.781851	1.338587	2.002167	1.878738	1.406123
28	.701661	1.210425	1.812773	1.714349	1.311115
29	.661566	1.139223	1.731604	1.620412	1.235108
30	.633499	1.110742	1.596323	1.467764	1.159101

TABLE 1--Continued

θ'	λ = 1.0	λ = 1.5	λ = 2.0	λ = 2.5	λ = 3.0
31	.601424	1.053781	1.488097	1.362085	1.102096
32	.561329	.968340	1.379872	1.291633	1.045091
33	.537272	.911378	1.298703	1.221180	1.007088
34	.513215	.854417	1.217534	1.150727	.950083
35	.489158	.817392	1.163421	1.080274	.904479
36	.473120	.726255	1.109309	1.009822	.855075
37	.457082	.703470	1.055196	.962853	.820872
38	.441044	.669293	1.001083	.915885	.798070
39	.425006	.640813	.946971	.880658	.760066
40	.412977	.620876	.906386	.833690	.729664
41	.400949	.598092	.879330	.798464	.714462
42	.392930	.575307	.852274	.774979	.684060
43	.380901	.563915	.811689	.739753	.649857
44	.372882	.541131	.798161	.716269	.627055
45	.364863	.532587	.771105	.692785	.608053
46	.356844	.518346	.744048	.657558	.589051
47	.348825	.504106	.730520	.634074	.570050
48	.340806	.484170	.711581	.622332	.551048
49	.336797	.475625	.698053	.610590	.539647
50	.332787	.467081	.676408	.587105	.532046
51	.328778	.458537	.662879	.575363	.520645
52	.324768	.449993	.649351	.558924	.494043
53	.320759	.435753	.641234	.551879	.490243
54	.316749	.430056	.630412	.540137	.486442
55	.312740	.427208	.622295	.528395	.475041
56	.308730	.421512	.608757	.516653	.463640
57	.304721	.415816	.603356	.511956	.456040
58	.302716	.410120	.597944	.504911	.444639
59	.300712	.404424	.589827	.493168	.437038
60	.298707	.401576	.581710	.486123	.425637

TABLE 1--Continued

θ'	λ = 1.0	λ = 1.5	λ = 2.0	λ = 2.5	λ = 3.0
61	.297504	.400152	.576299	.476730	.421837
62	.296702	.398728	.568182	.464987	.418036
63	.295499	.395880	.562771	.460291	.410436
64	.294697	.393032	.557360	.457942	.399035
65	.293494	.390184	.554654	.454419	.391434
66	.292693	.387336	.551949	.450897	.387634
67	.291891	.384487	.549243	.448548	.385733
68	.290688	.381639	.543832	.446200	.383833
69	.289485	.378791	.542479	.443852	.381933
70	.288683	.375943	.541126	.441503	.380033
71	.286678	.374519	.538420	.439155	.376233
72	.285475	.373095	.535715	.436806	.372432
73	.285074	.370247	.530303	.434458	.368632
74	.284674	.367399	.524892	.432109	.364832
75	.284674	.364551	.522187	.429761	.361031
76	.283872	.358855	.519481	.427413	.357231
77	.283471	.357431	.516775	.426708	.355331
78	.283070	.356007	.515964	.426238	.354191
79	.282669	.354583	.515422	.425769	.353431
80	.282268	.353159	.514881	.425064	.352670
81	.281867	.351735	.514340	.423890	.351530
82	.281466	.350311	.514070	.422716	.350770
83	.281065	.348887	.514070	.423890	.349630
84	.281065	.347463	.514070	.425064	.349630
85	.280664	.346893	.514340	.425769	.349250
86	.280664	.346608	.514611	.426238	.348870
87	.281065	.346039	.515152	.426708	.348490
88	.281466	.345469	.515693	.427413	.348110
89	.281867	.345184	.516234	.427413	.347730
90	.282268	.344615	.516775	.428587	.347350

TABLE 1--Continued

θ°	λ = 1.0	λ = 1.5	λ = 2.0	λ = 2.5	λ = 3.0
91	.282669	.344615	.517046	.429761	.346970
92	.283070	.344615	.517316	.430935	.346590
93	.283471	.344615	.517587	.432109	.346210
94	.283872	.346039	.517858	.433284	.345830
95	.284273	.347463	.518128	.434458	.345830
96	.284674	.350311	.519481	.436806	.346590
97	.285475	.351735	.522187	.439155	.347350
98	.286277	.353159	.524892	.441503	.348110
99	.287881	.356007	.527598	.443852	.348870
100	.288683	.358855	.530303	.446200	.349630
101	.289084	.360279	.533009	.448548	.350390
102	.289886	.361703	.534362	.450897	.351150
103	.290287	.364551	.535715	.453245	.351910
104	.290688	.367399	.537068	.455594	.352290
105	.291490	.368823	.538420	.457942	.352670
106	.291891	.370247	.539773	.460291	.353051
107	.292693	.373095	.541126	.462639	.353431
108	.293895	.375943	.543832	.464987	.354191
109	.295098	.380215	.545184	.467336	.354951
110	.296702	.384487	.546537	.469684	.355711
111	.297504	.388760	.547890	.472033	.356471
112	.298306	.393032	.549243	.476730	.357231
113	.298707	.395880	.550596	.479078	.357991
114	.300712	.398728	.551949	.481426	.359511
115	.302716	.403000	.553301	.483775	.360271
116	.304721	.407272	.554654	.486123	.361031
117	.306726	.412114	.558713	.490820	.362931
118	.307929	.414392	.561418	.493168	.364832
119	.308730	.417810	.564124	.495517	.364832
120	.311617	.421512	.568182	.497865	.370532

TABLE 1--Continued

θ'	λ = 1.0	λ = 1.5	λ = 2.0	λ = 2.5	λ = 3.0
121	.311738	.424360	.570888	.504911	.372432
122	.312740	.427208	.573594	.511956	.374332
123	.314745	.432904	.576299	.516653	.376233
124	.316749	.438601	.579005	.519001	.380033
125	.318754	.441449	.581710	.521350	.381933
126	.320759	.444297	.584416	.528395	.383833
127	.321561	.449993	.587122	.533092	.385733
128	.322764	.452841	.589827	.540137	.387634
129	.323967	.454265	.592533	.542485	.389534
130	.324768	.455689	.595239	.544834	.391434
131	.326773	.461385	.597944	.549531	.395234
132	.328778	.465657	.600650	.551879	.399035
133	.330783	.469929	.606061	.556576	.402835
134	.332787	.475625	.611472	.563621	.406635
135	.334792	.479897	.616884	.570666	.410436
136	.336797	.484170	.622295	.573015	.414236
137	.338802	.489866	.627706	.577712	.418036
138	.340806	.495562	.633117	.582409	.421837
139	.342811	.501258	.638529	.587105	.423737
140	.346821	.506954	.643940	.596499	.425637
141	.348825	.509802	.649351	.603544	.429437
142	.350830	.512650	.654763	.610590	.433238
143	.352835	.518346	.660174	.617635	.437038
144	.354840	.524042	.662879	.622332	.440838
145	.355642	.529738	.669644	.628203	.444639
146	.356844	.535435	.676408	.634074	.448439
147	.358849	.538283	.683172	.652861	.452239
148	.360854	.541131	.689936	.662255	.456040
149	.362859	.546827	.696700	.669300	.463640
150	.364863	.552523	.703464	.676346	.471241

TABLE 1--Continued

θ°	λ = 1.0	λ = 1.5	λ = 2.0	λ = 2.5	λ = 3.0
151	.366868	.558219	.708875	.669300	.478842
152	.368873	.566763	.711581	.676346	.486442
153	.368873	.569611	.714286	.681042	.490243
154	.372882	.572459	.716992	.692785	.494043
155	.374887	.575307	.730520	.699830	.497843
156	.376892	.581004	.744048	.704527	.501644
157	.378897	.586700	.752165	.713920	.505444
158	.380901	.592396	.762988	.720966	.509244
159	.384911	.598092	.773810	.728011	.513045
160	.388920	.606636	.784633	.739753	.520645
161	.390925	.618028	.791397	.746798	.532046
162	.392930	.626572	.798161	.751495	.535847
163	.396939	.632269	.811689	.763237	.539647
164	.400949	.637965	.822512	.774979	.551048
165	.404958	.643661	.827923	.779676	.558649
166	.408968	.647933	.838746	.793767	.570050
167	.412977	.650781	.846862	.803160	.573850
168	.416987	.655053	.857685	.810206	.577650
169	.420996	.663597	.865802	.817251	.581451
170	.425006	.672141	.879330	.821943	.589051
171	.429015	.679262	.892858	.833690	.608053
172	.433025	.683534	.906386	.845432	.611853
173	.435030	.689230	.919915	.854826	.615654
174	.437034	.694926	.933443	.864219	.623254
175	.439039	.700622	.946971	.873613	.634655
176	.441044	.709166	.960499	.880658	.646056
177	.443049	.717710	.974027	.892401	.653657
178	.445053	.729103	.987555	.904143	.699261
179	.447058	.734799	1.001083	.915885	.710662
180	.449063	.740495	1.014612	.927627	.684060

TABLE 1--Continued

θ'	λ = 3.5	λ = 4.0	λ = 4.5	λ = 5.0	λ = 5.5
1	188.651600	74.753295	55.131701	48.915822	53.723397
2	104.806440	68.523854	35.733510	48.263611	51.484922
3	68.124192	52.327306	24.502978	46.959189	49.246447
4	46.114837	39.868424	18.377233	43.045923	44.769497
5	35.634192	33.638982	14.803882	35.219392	40.292548
6	28.297741	26.163653	12.047297	27.392860	24.623223
7	22.533386	20.557156	10.209574	19.566329	14.326239
8	18.341128	16.196547	8.678138	14.348641	9.849289
9	14.672902	13.081826	7.555085	12.783334	8.058509
10	12.576773	10.590050	6.738319	10.174491	6.715424
11	10.480644	8.409745	6.023648	8.348300	6.043882
12	9.013354	7.475329	5.308978	7.304762	5.372339
13	7.860483	6.540913	4.696404	6.130783	4.812721
14	6.812419	5.855674	4.288021	5.478572	4.409795
15	5.764354	4.983553	3.981734	4.956803	3.894946
16	5.240322	4.422903	3.624398	4.369813	3.626329
17	4.821096	4.111431	3.471255	4.043707	3.469636
18	4.401870	3.675370	3.164968	3.652381	3.201019
19	3.982645	3.363898	2.909728	3.391497	2.932402
20	3.615822	3.114720	2.705537	3.065391	2.753324
21	3.301403	2.865542	2.501345	2.804507	2.641400
22	3.039387	2.616365	2.348202	2.608843	2.462322
23	2.829774	2.429482	2.195058	2.426224	2.283244
24	2.567758	2.211451	2.062334	2.269694	2.171320
25	2.410548	2.055715	1.950028	2.100119	2.104166
26	2.253338	1.931126	1.847932	1.982721	1.969857
27	2.043725	1.806537	1.745837	1.917500	1.857934
28	1.938919	1.713096	1.653951	1.826190	1.790779
29	1.834112	1.619654	1.551855	1.695748	1.678856
30	1.703104	1.557360	1.511017	1.643571	1.611701

TABLE 1--Continued

θ'	λ = 3.5	λ = 4.0	λ = 4.5	λ = 5.0	λ = 5.5
31	1.624499	1.463918	1.439549	1.565306	1.544547
32	1.519693	1.401624	1.368082	1.473996	1.455008
33	1.441088	1.320641	1.327244	1.434864	1.399046
34	1.362483	1.258347	1.255777	1.356598	1.343084
35	1.283879	1.183593	1.214939	1.304421	1.298315
36	1.231475	1.133758	1.163891	1.252245	1.242353
37	1.179072	1.090152	1.123053	1.213112	1.208776
38	1.100467	1.059005	1.072005	1.173979	1.152814
39	1.058545	1.002940	1.031167	1.121802	1.119237
40	1.021862	.965563	1.020957	1.069625	1.085660
41	.979940	.934416	.990328	1.043537	1.052083
42	.938017	.903268	.959699	.991360	1.007313
43	.901335	.872121	.918061	.965272	.984928
44	.859412	.840974	.908652	.926139	.962544
45	.838451	.809827	.878023	.913095	.928967
46	.801769	.778680	.857604	.873962	.906582
47	.775567	.759991	.826975	.860918	.884197
48	.744125	.747532	.816765	.821785	.850620
49	.733645	.716385	.796346	.808741	.839428
50	.696962	.691467	.775927	.782653	.828235
51	.681241	.672779	.765718	.756564	.794658
52	.660280	.654091	.745298	.743520	.783466
53	.639319	.641632	.735089	.730476	.761081
54	.628838	.629173	.724879	.704387	.749889
55	.613117	.622944	.714670	.691343	.727504
56	.597396	.610485	.704460	.678299	.716311
57	.581675	.598026	.694251	.665255	.705119
58	.576435	.585567	.684041	.652210	.693927
59	.560714	.573108	.673831	.639166	.682734
60	.539753	.566879	.663622	.626122	.671542

TABLE 1--Continued

θ'	λ = 3.5	λ = 4.0	λ = 4.5	λ = 5.0	λ = 5.5
61	.529272	.560649	.658517	.613078	.660350
62	.524032	.548190	.653412	.600034	.644680
63	.513551	.535731	.648307	.586989	.637965
64	.503070	.529502	.643203	.580467	.626772
65	.492590	.523273	.632993	.573945	.622296
66	.487349	.517043	.627888	.560901	.615580
67	.476869	.510814	.622784	.554379	.604388
68	.471629	.507699	.617679	.547857	.599911
69	.466388	.501470	.614616	.541335	.593195
70	.461148	.498355	.612574	.534812	.588718
71	.455908	.492125	.610532	.528290	.582003
72	.450667	.485896	.607469	.521768	.577526
73	.445427	.482781	.602364	.515246	.573049
74	.440187	.479666	.598281	.508724	.568572
75	.434946	.476552	.596239	.504811	.566334
76	.429706	.474683	.595218	.502202	.564095
77	.424466	.473437	.594197	.498289	.561857
78	.419225	.470322	.592155	.495680	.559618
79	.413985	.468453	.592155	.493071	.557380
80	.412937	.467208	.592155	.489158	.555141
81	.410841	.464093	.592155	.487853	.554470
82	.408745	.460978	.592155	.486549	.553574
83	.406124	.460978	.592155	.485244	.552903
84	.404552	.460978	.592155	.482636	.552231
85	.403504	.460978	.593176	.480027	.551336
86	.400884	.460978	.594197	.478722	.550664
87	.399836	.460978	.595218	.477418	.549545
88	.398788	.460978	.596239	.476114	.548426
89	.398264	.460978	.597260	.474809	.547307
90	.397740	.460978	.598281	.474809	.546187

TABLE 1--Continued

θ°	λ = 3.5	λ = 4.0	λ = 4.5	λ = 5.0	λ = 5.5
91	.395644	.460978	.599302	.474809	.547307
92	.395120	.464093	.600322	.474809	.548426
93	.394596	.465962	.602364	.474809	.549545
94	.393024	.467208	.604406	.474809	.550664
95	.393548	.468453	.606448	.476114	.551784
96	.394072	.469076	.608490	.477418	.552903
97	.394596	.470945	.610532	.478722	.554022
98	.395120	.473437	.612574	.480027	.555141
99	.395644	.474683	.616658	.481331	.557380
100	.396168	.475929	.620742	.482636	.559618
101	.396692	.476552	.624825	.483940	.560737
102	.397216	.479666	.626867	.485244	.561857
103	.397740	.485896	.629930	.486549	.562976
104	.398264	.492125	.632993	.487853	.564095
105	.400884	.495240	.635035	.489158	.565214
106	.403504	.498355	.638098	.491767	.566334
107	.406124	.504584	.640140	.495680	.568572
108	.408745	.510814	.643203	.502202	.570811
109	.411365	.517043	.648307	.506115	.577526
110	.413985	.520158	.653412	.508724	.582003
111	.416605	.523273	.658517	.515246	.586480
112	.419225	.526387	.663622	.521768	.589838
113	.421845	.529502	.665664	.525682	.593195
114	.424465	.535731	.668727	.530899	.597672
115	.427086	.541961	.673831	.534812	.599911
116	.429706	.548190	.678936	.541335	.602149
117	.432326	.554420	.684041	.547857	.604388
118	.434946	.560649	.694251	.554379	.606626
119	.437566	.566879	.699355	.560901	.608865
120	.440187	.573108	.704460	.567423	.611103

TABLE 1--Continued

θ°	λ = 3.5	λ = 4.0	λ = 4.5	λ = 5.0	λ = 5.5
121	.442807	.579338	.709565	.579163	.613342
122	.445427	.585567	.724979	.580467	.617819
123	.450667	.594911	.735089	.586989	.626772
124	.455908	.604255	.745298	.593511	.631249
125	.461148	.613599	.755508	.600034	.635726
126	.466388	.622944	.765718	.606556	.640203
127	.471629	.629173	.775927	.613078	.644680
128	.476869	.635403	.786137	.619600	.649157
129	.482109	.647861	.796346	.626122	.654753
130	.487349	.660320	.806556	.632644	.660350
131	.492590	.672779	.816765	.645688	.665946
132	.497830	.685238	.837185	.652210	.671542
133	.503070	.691467	.847394	.665255	.682734
134	.508311	.697697	.857604	.678299	.693927
135	.513551	.710156	.872918	.687430	.705119
136	.518791	.722615	.888232	.697865	.716313
137	.521412	.735074	.898442	.704387	.727504
138	.524032	.747532	.918861	.717432	.738696
139	.537133	.753762	.939280	.730476	.744292
140	.550233	.759991	.959699	.743520	.749889
141	.560714	.772450	.969909	.750042	.761081
142	.576435	.791139	.980119	.756564	.774512
143	.581675	.809827	.990328	.769608	.783466
144	.586916	.822286	1.020957	.782653	.794658
145	.597396	.834745	1.031167	.795697	.805850
146	.607877	.853433	1.041376	.808741	.821520
147	.618358	.872121	1.061795	.821785	.828235
148	.628838	.897039	1.092424	.834830	.839428
149	.639319	.915727	1.123053	.847874	.855097
150	.655040	.934416	1.133262	.860918	.873005

TABLE 1—Continued

θ'	λ = 3.5	λ = 4.0	λ = 4.5	λ = 5.0	λ = 5.5
151	.670761	.946875	1.153681	.873962	.895389
152	.681241	.959333	1.194520	.887006	.906582
153	.691722	.978022	1.225148	.900051	.917774
154	.707443	.996710	1.245568	.913095	.940159
155	.717924	1.015398	1.276196	.926139	.951351
156	.733645	1.040316	1.306825	.939183	.969931
157	.744125	1.059005	1.327244	.952228	.984928
158	.754606	1.077693	1.388502	.965272	.998359
159	.770327	1.102611	1.429340	.991360	1.011790
160	.791288	1.121299	1.459969	1.043537	1.040890
161	.817490	1.139987	1.500807	1.056581	1.052083
162	.838451	1.164905	1.531436	1.069625	1.074467
163	.854172	1.183593	1.562064	1.095714	1.096852
164	.875133	1.208511	1.602903	1.121802	1.119237
165	.890854	1.245888	1.633531	1.147891	1.141622
166	.922296	1.270806	1.694789	1.173979	1.164006
167	.943258	1.308182	1.735627	1.200068	1.186391
168	.958979	1.326870	1.796885	1.226156	1.208776
169	.979940	1.351788	1.837723	1.245722	1.231161
170	.995661	1.370477	1.898980	1.265289	1.253545
171	1.027103	1.395394	1.939819	1.304421	1.275930
172	1.048064	1.432771	2.001076	1.317466	1.298315
173	1.074266	1.457689	2.041914	1.330510	1.365469
174	1.100467	1.495065	2.103172	1.356598	1.387854
175	1.152870	1.557360	2.144010	1.395731	1.410239
176	1.184312	1.582278	2.205268	1.434864	1.432623
177	1.205274	1.619654	2.246106	1.460952	1.455008
178	1.226235	1.644572	2.348202	1.487041	1.477393
179	1.257677	1.681949	2.450297	1.526173	1.522162
180	1.310080	1.713096	2.511555	1.591394	1.566932

TABLE 1--Continued

θ'	λ = 6.0	λ = 6.5	λ = 7.0	λ = 8.0	λ = 9.0
1	59.002318	48.714768	53.030448	48.332710	58.432443
2	57.939213	47.916165	51.990635	46.685004	56.506099
3	55.813004	45.121056	46.791572	43.938828	54.579755
4	53.686794	43.923152	38.473070	40.643416	51.369181
5	31.627368	42.725247	29.114755	27.461767	38.526885
6	31.095816	40.728740	22.875879	19.772472	23.116131
7	26.577621	31.944110	17.676816	15.378589	14.126524
8	11.162600	9.982534	14.557377	12.083177	8.989606
9	6.112852	7.187424	12.217799	9.886236	6.421147
10	4.518195	5.989520	9.982202	8.238530	5.329552
11	3.720866	4.871476	8.578454	7.140059	4.623226
12	3.269047	4.232594	8.058548	6.041588	4.173745
13	3.003271	3.833293	6.758782	5.272659	3.788477
14	2.737494	3.513852	6.134895	4.613576	3.467419
15	2.498296	3.274271	5.303044	4.174188	3.210573
16	2.312253	2.994760	4.939110	3.899570	2.921622
17	2.179364	2.874969	4.575175	3.570029	2.632670
18	2.073054	2.675319	4.159250	3.350335	2.504247
19	1.966743	2.555528	3.795316	3.075717	2.311613
20	1.860433	2.395808	3.431381	2.910947	2.183190
21	1.780700	2.276017	3.119438	2.691253	2.054767
22	1.714256	2.116297	2.911475	2.526482	1.894238
23	1.647812	2.036437	2.703513	2.389173	1.797921
24	1.568079	1.936611	2.495550	2.279326	1.701604
25	1.528213	1.836786	2.339578	2.142017	1.605286
26	1.488346	1.756926	2.183606	2.032170	1.528233
27	1.435191	1.697030	2.079625	1.977247	1.425494
28	1.382036	1.637135	1.949648	1.894861	1.361283
29	1.355458	1.577240	1.845667	1.812476	1.322756
30	1.315592	1.497380	1.715690	1.730091	1.252123

TABLE 1--Continued

θ°	λ = 6.0	λ = 6.5	λ = 7.0	λ = 8.0	λ = 9.0
31	1.275725	1.437484	1.637705	1.675167	1.175070
32	1.249148	1.397554	1.559719	1.620244	1.142964
33	1.222570	1.337659	1.481733	1.565329	1.091595
34	1.195992	1.297729	1.429742	1.493920	1.040225
35	1.169415	1.245820	1.351756	1.435473	1.014541
36	1.142837	1.201897	1.273770	1.400550	.976014
37	1.129548	1.177939	1.221779	1.356611	.956751
38	1.110944	1.122036	1.169789	1.301687	.911802
39	1.089682	1.078113	1.117798	1.274226	.898960
40	1.063104	1.046169	1.065808	1.219302	.866854
41	1.049816	1.030197	1.039812	1.197333	.841170
42	1.036527	.990267	.998220	1.153394	.834749
43	1.015265	.950337	.946229	1.109455	.796222
44	.996660	.918393	.915035	1.087485	.783380
45	.986029	.898428	.889039	1.054531	.770537
46	.970083	.866483	.852646	1.032562	.751274
47	.956794	.838532	.811053	.988623	.725589
48	.935532	.806588	.785058	.961161	.719168
49	.924901	.794609	.774660	.933700	.712747
50	.916927	.770651	.748665	.906238	.699905
51	.903639	.750686	.727868	.878776	.674220
52	.898323	.726728	.691475	.834837	.661378
53	.890350	.718742	.685276	.823853	.654957
54	.877061	.710756	.675079	.812868	.648535
55	.871745	.686798	.639484	.779914	.645325
56	.855799	.674819	.629086	.768929	.642114
57	.850483	.666833	.618688	.752452	.635693
58	.837195	.658847	.597892	.730483	.634409
59	.829221	.646868	.582295	.714005	.632483
60	.818590	.634889	.577096	.697528	.629272

TABLE 1--Continued

θ'	λ = 6.0	λ = 6.5	λ = 7.0	λ = 8.0	λ = 9.0
61	.810617	.626903	.566697	.686544	.626061
62	.802644	.614924	.556299	.664574	.622851
63	.797328	.602945	.535503	.659082	.621567
64	.789355	.594959	.530304	.642605	.620924
65	.781382	.586973	.525105	.631620	.620282
66	.770751	.574993	.514707	.615143	.619640
67	.762777	.571000	.509508	.609651	.618998
68	.757462	.567007	.504309	.604158	.618356
69	.749488	.563014	.499110	.593174	.617714
70	.746831	.561018	.493911	.576697	.617072
71	.738857	.559021	.488711	.565712	.616430
72	.730884	.555028	.483512	.560220	.615788
73	.722911	.551035	.478313	.554727	.615145
74	.717595	.547042	.473114	.551981	.614503
75	.712280	.543049	.467915	.549235	.613861
76	.706964	.539056	.462716	.538250	.613219
77	.701649	.535063	.457517	.532758	.612577
78	.696333	.531070	.454918	.527265	.611293
79	.691018	.527077	.452318	.524519	.610009
80	.685702	.523084	.449718	.521773	.608724
81	.680387	.522286	.448679	.516281	.607440
82	.675071	.521886	.448159	.513535	.606156
83	.669756	.521487	.447639	.510788	.607440
84	.664440	.521088	.447639	.505296	.608724
85	.661782	.520689	.447119	.499804	.610009
86	.659125	.520289	.446599	.497057	.611293
87	.653809	.519890	.446079	.494311	.612577
88	.648493	.519491	.445559	.493213	.613861
89	.643178	.519091	.446079	.491565	.615145
90	.640520	.519491	.446599	.491016	.616430

TABLE 1--Continued

θ°	λ = 6.0	λ = 6.5	λ = 7.0	λ = 8.0	λ = 9.0
91	.637862	.519090	.447119	.490467	.618356
92	.635205	.520289	.447639	.489917	.620282
93	.632547	.520689	.448159	.489368	.622209
94	.629889	.521487	.448679	.488819	.624135
95	.627231	.522286	.449718	.488819	.627988
96	.624574	.523084	.450758	.488819	.633125
97	.621916	.525081	.452318	.489368	.638262
98	.619258	.527077	.454918	.489917	.642114
99	.616600	.529074	.455957	.491016	.648535
100	.613943	.531070	.457517	.492114	.651746
101	.613411	.535063	.460117	.492664	.654957
102	.612879	.539056	.462716	.493213	.658167
103	.612348	.543049	.465316	.493762	.661378
104	.611816	.547042	.467915	.494311	.664588
105	.611285	.551035	.473114	.497057	.667799
106	.611019	.553032	.478313	.499804	.671009
107	.611019	.555028	.483512	.502550	.674220
108	.611019	.557025	.486112	.505296	.677431
109	.610753	.559021	.488711	.508042	.680641
110	.610487	.563014	.491311	.510788	.642114
111	.610753	.567007	.493911	.516281	.706326
112	.611019	.571000	.499110	.521773	.709536
113	.611285	.574993	.501709	.524519	.712747
114	.612348	.582980	.506908	.527265	.719168
115	.613411	.590966	.514707	.532758	.725589
116	.614474	.598952	.519906	.538250	.732010
117	.615006	.606938	.525105	.540996	.738431
118	.616600	.614924	.530304	.543742	.744853
119	.619258	.622910	.535503	.549235	.751274
120	.621916	.630896	.540702	.554727	.757695

TABLE 1--Continued

θ'	λ = 6.0	λ = 6.5	λ = 7.0	λ = 8.0	λ = 9.0
121	.624574	.638882	.551100	.560220	.764116
122	.627231	.646868	.561498	.565712	.770537
123	.629889	.654854	.571896	.571204	.773748
124	.632547	.662840	.577096	.576697	.776958
125	.635205	.670826	.582295	.587681	.783380
126	.637862	.678812	.592693	.604158	.789801
127	.643178	.686798	.603091	.609651	.796222
128	.648493	.694784	.613489	.615143	.802643
129	.651151	.702770	.623887	.620635	.809064
130	.653809	.710756	.634285	.626128	.821906
131	.659125	.718742	.644683	.637113	.834749
132	.661782	.726728	.655082	.659082	.837959
133	.664440	.734714	.665480	.664574	.841170
134	.669756	.742700	.675878	.670067	.847591
135	.675071	.750686	.681077	.681051	.854012
136	.680387	.758672	.686276	.692034	.860433
137	.685702	.770651	.707072	.7140	.866854
138	.691018	.782630	.727868	.719692	.879697
139	.696333	.794609	.738267	.725215	.898960
140	.701649	.806588	.759063	.752452	.905381
141	.706964	.818567	.774660	.763437	.911802
142	.712280	.838532	.785058	.774421	.918224
143	.717595	.850511	.795456	.785406	.924645
144	.720253	.862490	.821452	.801883	.937487
145	.725569	.874470	.831850	.823853	.950329
146	.730884	.886449	.800655	.834837	.956751
147	.744173	.898428	.826651	.845822	.969593
148	.749488	.910407	.837049	.867791	.976014
149	.754804	.922386	.883840	.884268	.982435
150	.760119	.938358	.935831	.911730	.995277

TABLE 1--Continued

θ'	λ = 6.0	λ = 6.5	λ = 7.0	λ = 8.0	λ = 9.0
151	.770751	.958323	.956627	.933700	1.008120
152	.776066	.978288	.977423	.944684	1.027383
153	.778724	.998253	1.003419	.972146	1.028025
154	.789355	1.014225	1.024215	.991369	1.028667
155	.797328	1.030197	1.039812	1.005100	1.029952
156	.805301	1.046169	1.076206	1.046293	1.031878
157	.818590	1.062141	1.107400	1.076501	1.091595
158	.829221	1.078113	1.128196	1.098470	1.092237
159	.837195	1.098078	1.143793	1.142409	1.092879
160	.845168	1.126029	1.190585	1.164378	1.094163
161	.853141	1.142001	1.216580	1.175363	1.096089
162	.858457	1.157974	1.247775	1.208317	1.155806
163	.869088	1.185925	1.299765	1.263241	1.157090
164	.877061	1.205890	1.325761	1.301687	1.158375
165	.882377	1.237834	1.351756	1.329149	1.160301
166	.890350	1.261792	1.403747	1.362103	1.220018
167	.903639	1.277764	1.455737	1.378580	1.221302
168	.908954	1.309708	1.481733	1.428011	1.222586
169	.922243	1.325680	1.507728	1.482935	1.224512
170	.930216	1.349638	1.585714	1.537858	1.284229
171	.943505	1.381582	1.611709	1.592782	1.297071
172	.956794	1.405540	1.663700	1.620244	1.322756
173	.970083	1.437484	1.715690	1.658690	1.335598
174	.983371	1.477415	1.767681	1.702629	1.348441
175	.996660	1.517345	1.819672	1.730091	1.361283
176	1.009949	1.557275	1.871662	1.812476	1.393389
177	1.023238	1.597205	1.934051	1.867400	1.412652
178	1.036527	1.637135	2.001639	1.922323	1.425494
179	1.049816	1.677065	2.079625	2.004709	1.457600
180	1.063104	1.716995	2.183606	2.087094	1.476863

TABLE 1--Continued

θ°	λ = 10.0	λ = 11.0	λ = 12.0	λ = 13.0	λ = 14.0
1	54.395548	58.699842	55.541126	67.664018	63.573935
2	51.805284	56.947608	54.060029	66.410981	62.678527
3	46.624756	52.567022	51.838384	65.157943	61.783119
4	41.444227	36.796918	50.357287	61.398831	58.201489
5	36.263699	21.902926	47.395094	56.386682	56.410674
6	25.902642	13.141755	37.027417	43.856308	53.724452
7	15.541585	8.761170	19.254257	30.072897	42.979561
8	7.252739	7.446994	8.886580	20.048598	8.954075
9	4.869696	5.957595	7.405483	11.277336	1.969896
10	3.833591	5.256702	5.331948	8.019439	1.343111
11	3.315538	4.643420	4.739509	5.012149	1.074489
12	2.849290	4.292973	4.147070	3.759112	.984948
13	2.590264	4.030138	3.702741	3.007289	.940177
14	2.383043	3.679691	3.258412	2.506074	.913315
15	2.227627	3.504468	3.110303	2.255467	.886453
16	2.072211	3.373050	2.740028	2.004859	.868545
17	1.968600	3.241633	2.547486	1.879556	.859591
18	1.890892	3.110215	2.369754	1.691600	.850637
19	1.787282	3.022603	2.266077	1.628948	.846160
20	1.709574	2.891186	2.088346	1.503644	.837206
21	1.657769	2.803574	1.955047	1.428462	.832729
22	1.580061	2.628351	1.851370	1.365810	.828251
23	1.528255	2.584545	1.777316	1.278098	.819297
24	1.460909	2.496933	1.644017	1.240507	.814820
25	1.424645	2.409321	1.584773	1.177855	.810343
26	1.393562	2.277904	1.510718	1.152794	.805866
27	1.341756	2.190292	1.451474	1.115203	.801389
28	1.295132	2.146486	1.377419	1.065081	.796912
29	1.258868	2.058875	1.332987	1.027490	.792435
30	1.232965	1.971263	1.273743	1.002429	.787958

TABLE 1--Continued

θ'	λ = 10.0	λ = 11.0	λ = 12.0	λ = 13.0	λ = 14.0
31	1.191521	1.927457	1.229310	.977369	.783481
32	1.139716	1.839845	1.199688	.952308	.779004
33	1.124174	1.769756	1.155255	.927247	.777213
34	1.087910	1.725950	1.125633	.914717	.775422
35	1.046466	1.664622	1.096011	.889656	.773632
36	1.025744	1.594533	1.051578	.864595	.770050
37	1.005022	1.541966	1.036767	.852065	.768259
38	.979119	1.489398	1.007145	.839535	.766468
39	.942856	1.428070	.992334	.827004	.764678
40	.927314	1.406167	.962712	.814474	.762887
41	.891050	1.357981	.947901	.801943	.761096
42	.880689	1.314175	.933090	.789413	.759305
43	.839245	1.287892	.903468	.776883	.757514
44	.828884	1.235325	.896063	.770617	.755723
45	.813342	1.217802	.873847	.764352	.753933
46	.797801	1.173996	.859036	.754328	.752142
47	.777079	1.138952	.844225	.751822	.750351
48	.766718	1.112668	.836819	.739292	.748560
49	.751176	1.068862	.822008	.733026	.746769
50	.735635	1.051340	.814603	.726761	.744979
51	.725273	1.025056	.799792	.720496	.743188
52	.714912	.981251	.784981	.714231	.741397
53	.699371	.963728	.777575	.707966	.740502
54	.689010	.937445	.770170	.705460	.739606
55	.678649	.893639	.755359	.702953	.738711
56	.673468	.884878	.747953	.701700	.737815
57	.663107	.876117	.733142	.695435	.736920
58	.652746	.858594	.725737	.691676	.736024
59	.642385	.841072	.718331	.686664	.735129
60	.637205	.823550	.710926	.682905	.734234

TABLE 1--Continued

θ'	λ = 10.0	λ = 11.0	λ = 12.0	λ = 13.0	λ = 14.0
61	.632024	.806027	.703520	.680399	.733338
62	.626843	.788505	.696115	.677893	.732443
63	.626843	.770983	.688709	.675387	.731547
64	.624253	.762221	.681304	.672881	.730652
65	.621663	.744699	.673899	.670374	.729757
66	.616482	.735938	.666493	.666615	.728861
67	.611302	.718415	.659088	.665362	.727966
68	.606121	.709654	.651682	.662856	.727070
69	.600941	.700893	.644277	.660350	.726623
70	.595760	.683371	.636871	.657844	.726175
71	.590580	.674610	.633909	.655338	.725727
72	.587989	.665848	.629466	.654085	.725280
73	.585399	.657087	.622060	.652832	.724832
74	.582809	.648326	.619098	.651579	.724384
75	.580219	.643946	.614655	.650326	.723936
76	.577628	.639565	.610211	.647820	.723489
77	.577110	.630804	.607249	.645314	.723041
78	.576592	.622043	.604287	.642808	.722593
79	.576074	.617662	.599844	.641555	.722146
80	.575556	.613281	.595400	.639049	.721698
81	.575038	.608901	.593919	.638923	.721250
82	.576592	.604520	.592438	.638798	.720803
83	.577628	.600140	.589476	.638673	.720355
84	.580219	.595759	.586514	.638547	.719907
85	.582809	.591379	.585033	.638422	.719459
86	.585399	.588750	.585033	.638297	.719012
87	.587989	.586998	.585033	.638171	.718564
88	.590580	.585246	.585033	.638046	.718116
89	.593170	.584370	.585033	.637921	.717669
90	.595760	.583493	.585033	.637796	.717221

TABLE 1--Continued

θ'	λ = 10.0	λ = 11.0	λ = 12.0	λ = 13.0	λ = 14.0
91	.598351	.582617	.586514	.637670	.716773
92	.600941	.581741	.587995	.637545	.716326
93	.603531	.580865	.589476	.637420	.718116
94	.606121	.579989	.590957	.637294	.719907
95	.611302	.579113	.592438	.637169	.721698
96	.621663	.578237	.593919	.637044	.723489
97	.624253	.577361	.595400	.636918	.725280
98	.626843	.576485	.596881	.636793	.727070
99	.629434	.575608	.598363	.636668	.728861
100	.632024	.576485	.599844	.636542	.730652
101	.637205	.577361	.601325	.636668	.732443
102	.642385	.578237	.602806	.636793	.734234
103	.647566	.579113	.604287	.636918	.736024
104	.657927	.579989	.605768	.637044	.737815
105	.673468	.580865	.607249	.637294	.739606
106	.676058	.581741	.610211	.637545	.741397
107	.678649	.582617	.613174	.637796	.743188
108	.683829	.583493	.616136	.638046	.744979
109	.689010	.584370	.619098	.638297	.746769
110	.694190	.585246	.622060	.638547	.748560
111	.699371	.586122	.625022	.638798	.750351
112	.678649	.586998	.627985	.639049	.752142
113	.725273	.587874	.630947	.641555	.752231
114	.730454	.588750	.633909	.644061	.752321
115	.735635	.589626	.636871	.646567	.752410
116	.740815	.590502	.642795	.649073	.752500
117	.751176	.592255	.648720	.651579	.752590
118	.766718	.594007	.654644	.654085	.752679
119	.777079	.595759	.660569	.656591	.752858
120	.782259	.597511	.666493	.659097	.761096

TABLE 1--Continued

θ'	λ = 10.0	λ = 11.0	λ = 12.0	λ = 13.0	λ = 14.0
121	.787440	.599264	.670936	.661603	.762887
122	.797801	.601016	.675380	.664109	.764678
123	.813342	.602768	.678342	.665362	.766468
124	.828884	.613281	.681304	.666615	.768259
125	.839245	.615034	.688709	.667868	.770050
126	.849606	.616786	.696115	.669121	.771841
127	.865148	.618538	.703520	.670374	.773632
128	.880689	.620290	.710926	.671628	.776318
129	.891050	.622043	.718331	.672881	.779004
130	.901411	.624671	.725737	.674134	.781690
131	.916953	.628175	.733142	.675387	.785272
132	.973939	.630804	.740548	.676640	.787958
133	.942856	.633432	.746472	.679146	.789749
134	.953217	.636937	.752397	.681652	.791540
135	.968758	.639565	.758321	.684158	.794226
136	.984300	.642193	.764245	.686664	.796912
137	.994661	.645698	.770170	.689170	.798703
138	1.005022	.648326	.777575	.691676	.800494
139	1.020564	.650954	.784981	.694182	.803180
140	1.036105	.654459	.792386	.696688	.805866
141	1.051647	.657087	.799792	.699194	.807657
142	1.072369	.661468	.808678	.701700	.809448
143	1.087910	.665848	.817565	.702953	.812134
144	1.103452	.668477	.826451	.704207	.814820
145	1.124174	.671981	.835338	.705460	.816611
146	1.139716	.674610	.844225	.706713	.818402
147	1.155257	.677238	.851630	.707966	.821088
148	1.175979	.680742	.859036	.709219	.823774
149	1.191521	.683371	.873847	.711725	.826461
150	1.212243	.687751	.888658	.714231	.828251

TABLE 1--Continued

θ°	λ = 10.0	λ = 11.0	λ = 12.0	λ = 13.0	λ = 14.0
151	1.243326	.692132	.903468	.715484	.830042
152	1.258863	.700893	.918279	.716737	.832729
153	1.279590	.705274	.933090	.717990	.826461
154	1.295132	.709654	.947901	.719243	.828251
155	1.310673	.712283	.955307	.720496	.830042
156	1.331395	.715787	.962712	.721749	.841683
157	1.346937	.718415	.970118	.724255	.843473
158	1.367659	.727177	.977523	.726761	.846160
159	1.398742	.735938	.984929	.729267	.847950
160	1.419464	.744699	.992334	.731773	.850637
161	1.450547	.753460	.999740	.734279	.853323
162	1.471270	.758717	1.007145	.736785	.855114
163	1.502353	.765726	1.021956	.739292	.856905
164	1.523075	.770983	1.036767	.741798	.859591
165	1.554158	.774487	1.051578	.744304	.862277
166	1.574880	.779744	1.066389	.746810	.865859
167	1.605963	.871736	1.081200	.749316	.868545
168	1.626685	.788505	1.096011	.751822	.871231
169	1.657769	.792885	1.110822	.754328	.874813
170	1.678491	.797266	1.125633	.756834	.877499
171	1.709574	.801647	1.140444	.759340	.880185
172	1.730296	.806027	1.155255	.761846	.883767
173	1.761379	.810408	1.170066	.764352	.886453
174	1.782101	.814788	1.184877	.766858	.890930
175	1.813184	.819169	1.192282	.769364	.895407
176	1.864990	.823550	1.199688	.771871	.897198
177	1.916795	.827930	1.214499	.774377	.900779
178	1.968600	.832311	1.229310	.776883	.904361
179	2.020406	.841072	1.244121	.779389	.908838
180	2.072211	.849833	1.258932	.781895	.913315

TABLE 1--Continued

θ'	$\lambda = 15.0$	θ'	$\lambda = 15.0$	θ'	$\lambda = 15.0$
1	51.513323	31	.795594	61	.781762
2	50.559372	32	.794640	62	.781666
3	49.605422	33	.793686	63	.781666
4	46.743570	34	.792732	64	.781571
5	45.789620	35	.791778	65	.781380
6	43.881719	36	.790824	66	.781476
7	37.204066	37	.789870	67	.781571
8	2.098690	38	.788917	68	.781666
9	1.526320	39	.787963	69	.781762
10	1.049345	40	.787009	70	.781857
11	.973029	41	.786055	71	.781953
12	.953950	42	.785101	72	.782048
13	.915792	43	.784147	73	.782143
14	.896713	44	.783193	74	.782239
15	.877634	45	.781139	75	.783193
16	.858555	46	.782239	76	.784147
17	.849015	47	.782239	77	.785101
18	.839476	48	.782239	78	.786055
19	.829936	49	.782239	79	.787009
20	.820397	50	.782239	80	.787963
21	.815627	51	.782143	81	.788917
22	.810857	52	.782143	82	.789870
23	.808949	53	.782048	83	.790824
24	.806088	54	.782048	84	.791778
25	.801318	55	.781953	85	.792255
26	.800364	56	.781953	86	.792732
27	.799410	57	.781953	87	.793209
28	.798456	58	.781857	88	.793686
29	.797502	59	.781857	89	.794163
30	.796548	60	.781762	90	.794640

TABLE 1--Continued

Θ'	$\lambda = 15.0$	Θ'	$\lambda = 15.0$	Θ'	$\lambda = 15.0$
91	.795117	121	.830890	151	.870002
92	.795594	122	.831844	152	.871910
93	.796071	123	.832798	153	.874772
94	.796548	124	.833752	154	.877634
95	.797025	125	.834706	155	.879542
96	.797502	126	.835660	156	.881450
97	.798456	127	.836614	157	.883358
98	.799410	128	.837568	158	.885265
99	.800364	129	.838522	159	.887173
100	.801318	130	.839476	160	.889081
101	.802272	131	.840430	161	.890989
102	.803226	132	.841384	162	.893851
103	.804180	133	.842338	163	.896713
104	.805134	134	.843292	164	.899575
105	.806088	135	.844246	165	.903391
106	.807042	136	.845200	166	.906252
107	.807996	137	.846154	167	.909114
108	.808949	138	.847107	168	.912930
109	.809903	139	.848061	169	.915792
110	.810857	140	.849015	170	.918654
111	.812765	141	.850923	171	.922470
112	.814673	142	.852831	172	.925331
113	.816581	143	.854739	173	.928193
114	.818489	144	.856647	174	.932009
115	.820397	145	.858555	175	.934871
116	.822305	146	.860463	176	.937733
117	.824213	147	.862371	177	.941549
118	.826121	148	.864279	178	.944410
119	.828028	149	.866186	179	.949180
120	.829936	150	.868094	180	.953950

TABLE 2

INTEGRATED AXIALLY-SYMMETRIC SCATTERING FUNCTIONS FOR DISCRETE POSITIONS AND WAVE LENGTHS (λ) BASED ON EXPERIMENTAL DATA

Wave Length	Integrated Functions			
λ	$s(\mu_1,\mu_1')$	$s(\mu_1,\mu_2')$	$s(\mu_1,\mu_3')$	$s(\mu_1,\mu_4')$
4.0	5.2976	0.9960	0.6402	0.4889
4.5	4.1760	1.2153	0.7529	0.6175
5.0	3.9193	1.1737	0.9637	0.8655
5.5	4.0026	1.1320	0.7118	0.5738
6.0	4.1034	0.9705	0.7622	0.6770
6.5	3.6815	1.0622	0.7012	0.5473
7.0	4.1637	1.2499	0.6500	0.4631
8.0	3.8309	1.1137	0.7183	0.5347
9.0	4.1665	1.0168	0.7323	0.6333
10.0	3.9144	1.0319	0.7607	0.6202
11.0	4.2027	1.1402	0.8027	0.6301
12.0	3.9778	1.0236	0.7270	0.5181
13.0	4.6582	0.8594	0.6912	0.6467
14.0	4.1096	0.7808	0.7509	0.7289
15.0	3.5009	0.8225	0.8040	0.7930
λ	$s(\mu_1,-\mu_1')$	$s(\mu_1,-\mu_2')$	$s(\mu_1,-\mu_3')$	$s(\mu_1,-\mu_4')$
4.0	1.5991	0.9253	0.6102	0.4911
4.5	1.45609	0.8783	0.7394	0.6224
5.0	1.5861	0.9331	0.6338	0.5019
5.5	1.3401	0.9535	0.6780	0.5696
6.0	1.1445	0.8792	0.7350	0.6518
6.5	1.2817	0.9322	0.6707	0.5476
7.0	1.6296	0.9740	0.6114	0.4734
8.0	1.4981	0.9887	0.6739	0.5192
9.0	1.2306	0.8748	0.7216	0.6474
10.0	1.2121	0.9737	0.7587	0.6356
11.0	1.2113	1.0017	0.7344	0.6032
12.0	1.2441	0.8910	0.7086	0.6114
13.0	1.3185	0.7654	0.6788	0.6426
14.0	0.8442	0.7764	0.7531	0.7338
15.0	0.8640	0.8197	0.8073	0.7989

TABLE 2--Continued

Wave Length	Integrated Functions			
λ	$s(\mu_2,\mu_1')$	$s(\mu_2,\mu_2')$	$s(\mu_2,\mu_3')$	$s(\mu_2,\mu_4')$
4.0	0.9960	5.2567	0.8392	0.5373
4.5	1.2153	4.0966	0.9099	0.6512
5.0	1.1737	3.8962	0.8705	0.5812
5.5	1.1320	3.9727	0.8997	0.6358
6.0	0.9705	4.0924	0.8670	0.7564
6.5	1.0622	3.6415	0.8507	0.6025
7.0	1.2499	4.1155	0.8860	0.5434
8.0	1.1137	3.7775	0.9121	0.6365
9.0	1.0168	4.1325	0.8465	0.6336
10.0	1.0319	3.8474	0.8219	0.6316
11.0	1.1402	4.2182	1.0317	0.7460
12.0	1.0236	3.9592	0.8386	0.6673
13.0	0.8594	4.6640	0.7617	0.6690
14.0	0.7808	4.1003	0.7526	0.7283
15.0	0.8225	3.4925	0.8000	0.7866
λ	$s(\mu_2,-\mu_1')$	$s(\mu_2,-\mu_2')$	$s(\mu_2,-\mu_3')$	$s(\mu_2,-\mu_4')$
4.0	0.9253	0.7818	0.6392	0.5362
4.5	0.8783	0.9751	0.7861	0.6754
5.0	0.9331	0.7933	0.6296	0.5334
5.5	0.9535	0.8248	0.6765	0.5907
6.0	0.8792	0.8071	0.7127	0.6322
6.5	0.9322	0.8338	0.6820	0.5903
7.0	0.9740	0.8372	0.6265	0.5137
8.0	0.9887	0.8873	0.6672	0.5363
9.0	0.8748	0.8327	0.7490	0.7034
10.0	0.9737	0.9388	0.7496	0.7164
11.0	1.0017	0.8182	0.6493	0.5947
12.0	0.8910	0.8068	0.7131	0.6378
13.0	0.7654	0.7067	0.6716	0.6456
14.0	0.7764	0.7751	0.7614	0.7465
15.0	0.8197	0.8237	0.8175	0.8142

TABLE 2--Continued

Wave Length	Integrated Functions			
λ	$s(\mu_3,\mu_1')$	$s(\mu_3,\mu_2')$	$s(\mu_3,\mu_3')$	$s(\mu_3,\mu_4')$
4.0	0.6402	0.8392	5.9187	0.9078
4.5	0.7529	0.9099	4.3549	0.9624
5.0	0.9637	0.8705	4.5400	0.9803
5.5	0.7118	0.8997	4.4935	1.0027
6.0	0.7622	0.8670	5.3565	0.9446
6.5	0.7012	0.8507	5.0757	0.9426
7.0	0.6500	0.8860	4.6728	0.9883
8.0	0.7183	0.9121	4.2906	1.0724
9.0	0.7323	0.8465	4.6410	0.8483
10.0	0.7607	0.8219	4.43182	0.8504
11.0	0.8027	1.0317	4.5525	1.2318
12.0	0.7270	0.8386	3.8558	0.9116
13.0	0.6912	0.7617	6.1097	0.7505
14.0	0.7509	0.7526	6.2781	0.7534
15.0	0.8040	0.8000	3.4428	0.7866
λ	$s(\mu_3,-\mu_1')$	$s(\mu_3,-\mu_2')$	$s(\mu_3,-\mu_3')$	$s(\mu_3,-\mu_4')$
4.0	0.6102	0.6392	0.7389	0.6984
4.5	0.7394	0.7861	0.9637	0.8655
5.0	0.6338	0.6296	0.7098	0.6704
5.5	0.6780	0.6765	0.7552	0.7070
6.0	0.7350	0.7127	0.7120	0.6732
6.5	0.6707	0.6820	0.7770	0.7389
7.0	0.6114	0.6265	0.7704	0.6787
8.0	0.6739	0.6672	0.7778	0.6829
9.0	0.7216	0.7490	0.8369	0.8357
10.0	0.7587	0.7496	0.9511	0.9360
11.0	0.7344	0.6493	0.6443	0.6327
12.0	0.7086	0.7131	0.7545	0.7449
13.0	0.6788	0.6716	0.6764	0.6764
14.0	0.7531	0.7614	0.7780	0.7846
15.0	0.8073	0.8175	0.8378	0.8405

TABLE 2--Continued

Wave Length	Integrated Functions			
λ	$s(\mu_4,\mu_1')$	$s(\mu_4,\mu_2')$	$s(\mu_4,\mu_3')$	$s(\mu_4,\mu_4')$
4.0	0.4889	0.5373	0.9078	10.0369
4.5	0.6175	0.6512	0.9624	6.3336
5.0	0.8655	0.5812	0.9803	7.9527
5.5	0.5738	0.6358	1.0027	7.8346
6.0	0.6770	0.7564	0.9446	8.7145
6.5	0.5473	0.6025	0.9426	8.0955
7.0	0.4631	0.5434	0.9883	8.1149
8.0	0.5347	0.6365	1.0724	7.4964
9.0	0.6333	0.6336	0.8483	8.0003
10.0	0.6202	0.6316	0.8504	7.2729
11.0	0.6301	0.7460	1.2318	8.0950
12.0	0.6181	0.6673	0.9116	8.0056
13.0	0.6467	0.6690	0.7505	9.6892
14.0	0.7289	0.7283	0.7534	9.5403
15.0	0.7930	0.7866	0.7886	7.9642
λ	$s(\mu_4,-\mu_1')$	$s(\mu_4,-\mu_2')$	$s(\mu_4,-\mu_3')$	$s(\mu_4,-\mu_4')$
4.0	0.4911	0.5362	0.6984	1.0331
4.5	0.6224	0.6754	0.8655	1.3455
5.0	0.5019	0.5334	0.6704	0.9518
5.5	0.5696	0.5907	0.7070	0.9722
6.0	0.6518	0.6322	0.6732	0.8029
6.5	0.5476	0.5903	0.7389	1.0484
7.0	0.4734	0.5137	0.6787	1.1035
8.0	0.5192	0.5363	0.6829	1.0821
9.0	0.6474	0.7034	0.8357	1.0582
10.0	0.6356	0.7164	0.9360	1.3223
11.0	0.6032	0.5947	0.6327	0.7145
12.0	0.6114	0.6378	0.7449	0.9358
13.0	0.6426	0.6496	0.6764	0.7218
14.0	0.7338	0.7456	0.7846	0.8369
15.0	0.7989	0.8142	0.8405	0.8795

TABLE 3

$$\tfrac{1}{2}\left[\sum_{n=1}^{4} a_j \, s(\mu_i, \pm\mu_j)\right]$$

FOR DISCRETE POSITIONS OF INCIDENT RAY AND WAVE LENGTHS (λ)--BASED ON EXPERIMENTAL DATA

Wave Length λ	Direction of Incident Ray			
	μ_1	μ_2	μ_3	μ_4
4.0	1.2021	1.4859	1.5749	1.4848
4.5	1.1822	1.4008	1.4324	1.2899
5.0	1.1229	1.2893	1.3575	1.3139
5.5	1.1306	1.3272	1.3823	1.3440
6.0	1.1117	1.3380	1.5178	1.4334
6.5	1.0757	1.2567	1.4696	1.3590
7.0	1.1546	1.3394	1.3887	1.3284
8.0	1.1248	1,3028	1.3575	1.3151
9.0	1.1335	1.3543	1.4261	1.3917
10.0	1.1297	1.3282	1.4213	1.3677
11.0	1.1779	1.3980	1.4171	1.3959
12.0	1.1073	1.3100	1.2735	1.3674
13.0	1.12017	1.3653	1.5833	1.4651
14.0	1.05712	1.3053	1.6618	1.5207
15.0	1.0485	1.2494	1.2432	1.4338

APPENDIX B

Θ_{ij} (BASED ON $\Delta\varphi = 10°$) FOR DISCRETE POSITIONS OF INCIDENT RAY AND WAVE LENGTH

TABLE 4

Θ_{ij} (BASED ON $\Delta\varphi = 10°$) FOR DISCRETE POSITIONS OF INCIDENT RAY AND WAVE LENGTH

Values of Θ in Degrees									
$\Theta_{1,1}$	$\Theta_{1,-1}$	$\Theta_{1,2}$	$\Theta_{1,-2}$	$\Theta_{1,3}$	$\Theta_{1,-3}$	$\Theta_{1,4}$	$\Theta_{1,-4}$	$\Theta_{2,2}$	$\Theta_{2,-2}$
0	9	15	23	38	46	64	72	0	39
10	19	18	26	39	47	65	73	10	40
20	29	25	30	42	50	66	74	19	43
30	39	33	38	46	53	67	75	28	48
40	49	42	46	52	59	70	78	38	55
50	59	51	54	60	65	73	80	47	62
60	69	60	64	65	71	76	83	57	70
70	77	70	73	73	78	79	86	66	79
80	82	80	82	80	85	83	90	75	88
90	90	89	91	88	92	86	94	84	96
98	100	98	100	95	100	90	97	92	105
103	110	107	110	102	107	94	101	101	114
111	120	116	120	109	115	97	104	110	123
121	130	126	129	115	120	100	107	118	133
131	140	134	138	121	128	102	110	125	142
141	150	142	147	127	134	105	113	132	152
151	160	150	155	130	138	106	114	137	161
161	170	154	162	133	141	107	115	140	170
171	180	157	165	134	142	108	116	141	180

TABLE 4--Continued

Values of θ in Degrees									
$\theta_{2,3}$	$\theta_{2,-3}$	$\theta_{2,4}$	$\theta_{2,-4}$	$\theta_{3,3}$	$\theta_{3,-3}$	$\theta_{3,4}$	$\theta_{3,-4}$	$\theta_{4,4}$	$\theta_{4,-4}$
23	55	49	88	0	84	26	110	0	137
24	62	49	88	7	85	27	111	3	137
29	64	51	90	15	86	29	112	7	138
34	68	53	90	22	89	31	113	11	139
41	72	55	93	30	91	34	114	15	140
48	77	58	95	37	96	37	117	18	141
57	83	61	98	44	100	40	119	21	143
63	89	65	101	50	105	44	122	24	145
70	96	68	104	57	111	47	125	27	147
77	103	72	108	63	117	51	129	30	150
84	110	76	112	69	123	55	133	33	153
91	117	79	115	75	130	58	136	35	156
97	123	82	119	80	136	61	140	37	159
103	132	85	122	84	143	63	143	39	162
108	139	87	125	89	150	66	146	40	165
112	146	90	127	91	158	67	149	41	169
116	151	90	129	94	165	68	151	42	173
118	156	92	131	95	173	69	153	43	177
125	157	92	131	96	180	70	154	43	180

APPENDIX C

NUMERICALLY INTEGRATED AXIALLY-SYMMETRIC SCATTERING FUNCTION FOR DISCRETE POSITIONS AND SIZE PARAMETER (α)

APPENDIX C

TABLE 5

NUMERICALLY INTEGRATED AXIALLY-SYMMETRIC SCATTERING FUNCTION FOR DISCRETE POSITIONS AND SIZE PARAMETER (α)--BASED ON THEORETICAL DATA SPHERICAL PARTICLES, REFRACTIVE INDEX 1.6

Size Parameter	Integrated Functions			
α	$s(\mu_1,\mu_1')$	$s(\mu_1,\mu_2')$	$s(\mu_1,\mu_3')$	$s(\mu_1,\mu_4')$
2	1.43671	1.34821	0.77463	0.58122
3	1.99736	1.69822	0.76401	0.25075
α	$s(\mu_1,-\mu_1')$	$s(\mu_1,-\mu_2')$	$s(\mu_1,-\mu_3')$	$s(\mu_1,-\mu_4')$
2	1.22867	1.20665	0.77973	0.42696
3	1.54406	1.33614	0.50062	0.21109
α	$s(\mu_2,\mu_1')$	$s(\mu_2,\mu_2')$	$s(\mu_2,\mu_3')$	$s(\mu_2,\mu_4')$
2	1.34821	1.49750	1.25648	1.04734
3	1.69822	2.07478	1.51562	0.49900
α	$s(\mu_2,-\mu_1')$	$s(\mu_2,-\mu_2')$	$s(\mu_2,-\mu_3')$	$s(\mu_2,-\mu_4')$
2	1.20665	0.89952	0.50756	0.24208
3	1.33614	0.70709	0.28506	0.16147
α	$s(\mu_3,\mu_1')$	$s(\mu_3,\mu_2')$	$s(\mu_3,\mu_3')$	$s(\mu_3,\mu_4')$
2	0.97463	1.25648	1.94134	2.17055
3	0.76401	1.51562	2.54656	2.10988

TABLE 5--Continued

Size Parameter	Integrated Functions			
α	$s(\mu_3, -\mu_1')$	$s(\mu_3, -\mu_2')$	$s(\mu_3, -\mu_3')$	$s(\mu_3, -\mu_4')$
2	0.77973	0.50756	0.25442	0.15083
3	0.50062	0.28506	0.20591	0.18599
α	$s(\mu_4, \mu_1')$	$s(\mu_4, \mu_2')$	$s(\mu_4, \mu_3')$	$s(\mu_4, \mu_4')$
2	0.58122	1.04734	2.17035	3.64634
3	0.25075	0.49900	2.10988	5.35301
α	$s(\mu_4, -\mu_1')$	$s(\mu_4, -\mu_2')$	$s(\mu_4, -\mu_3')$	$s(\mu_4, -\mu_4')$
2	0.42696	0.24208	0.15083	0.16210
3	0.21109	0.16147	0.18599	0.24173

APPENDIX D

TABLE 6

$$\tfrac{1}{2}\left[\sum_{n=1}^{4} a_j \, s(\mu_i, \pm\mu_j)\right]$$

FOR DISCRETE POSITIONS OF INCIDENT RAY AND PARTICLE SIZE PARAMETER (α)--BASED ON THEORETICAL DATA SPHERICAL PARTICLES, REFRACTIVE INDEX = 1.6

Size Parameter	Direction of Incident Ray			
α	μ_1	μ_2	μ_3	μ_4
2	1.022	1.013	1.000	1.008
3	1.049	1.077	1.052	1.008

APPENDIX E

ANGULAR DISTRIBUTION OF SCATTERING FUNCTION CURVES

BASED ON THEORETICAL DATA - MIE CURVES

REFRACTIVE INDEX 1.6

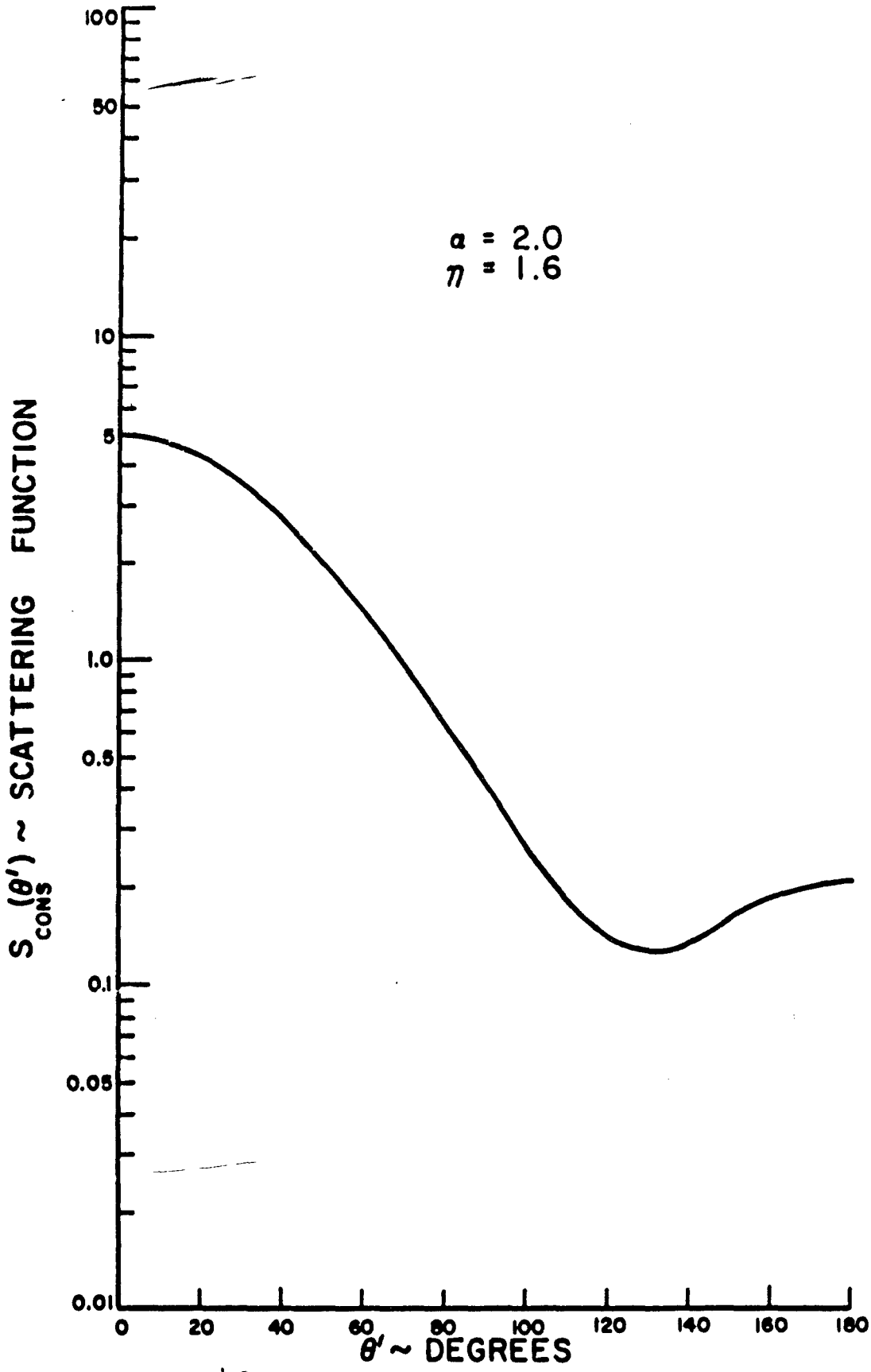

Figure 40. Angular Distribution of Scattering Function--Theoretical Data

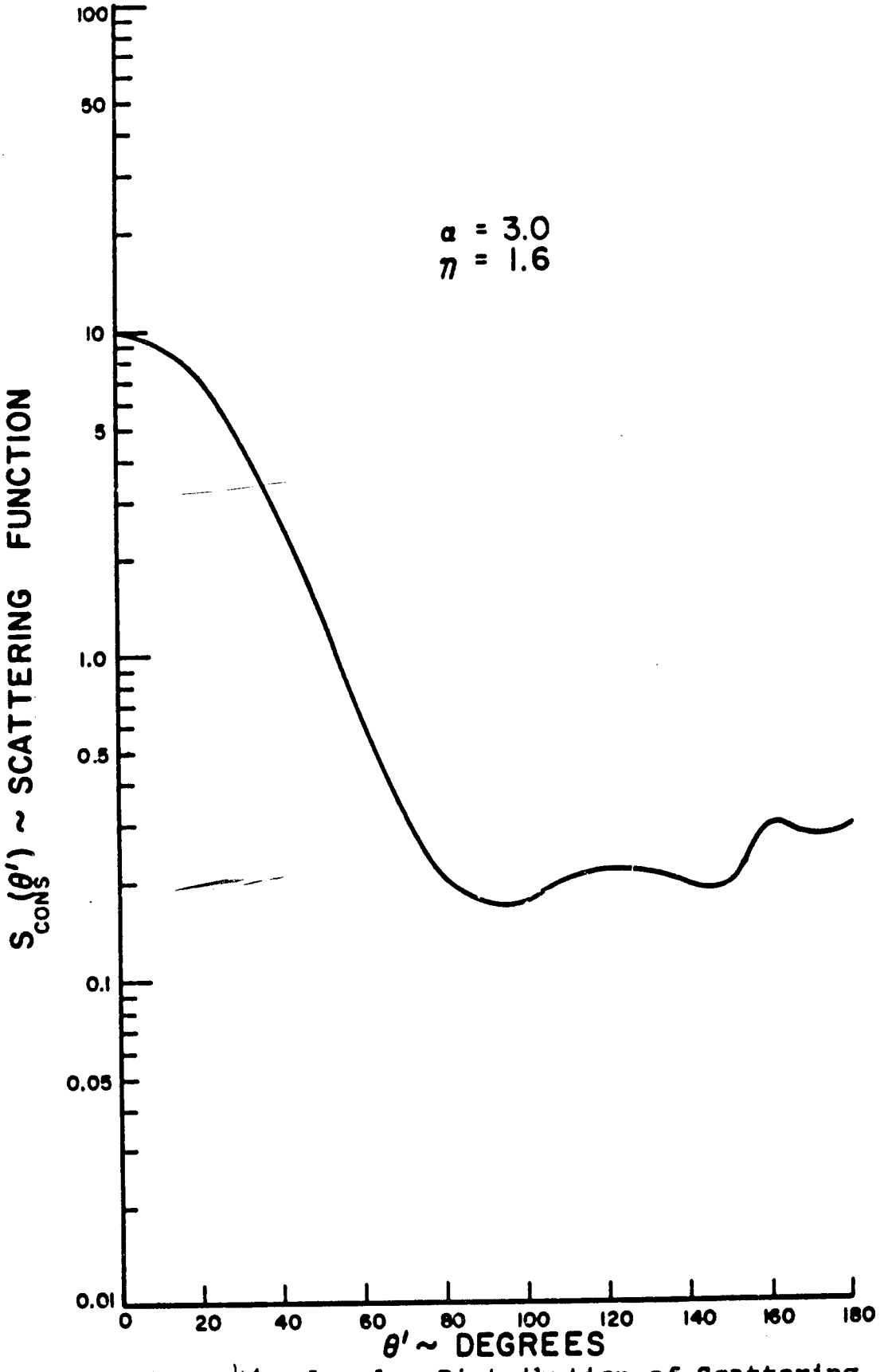

Figure 41. Angular Distribution of Scattering Function--Theoretical Data

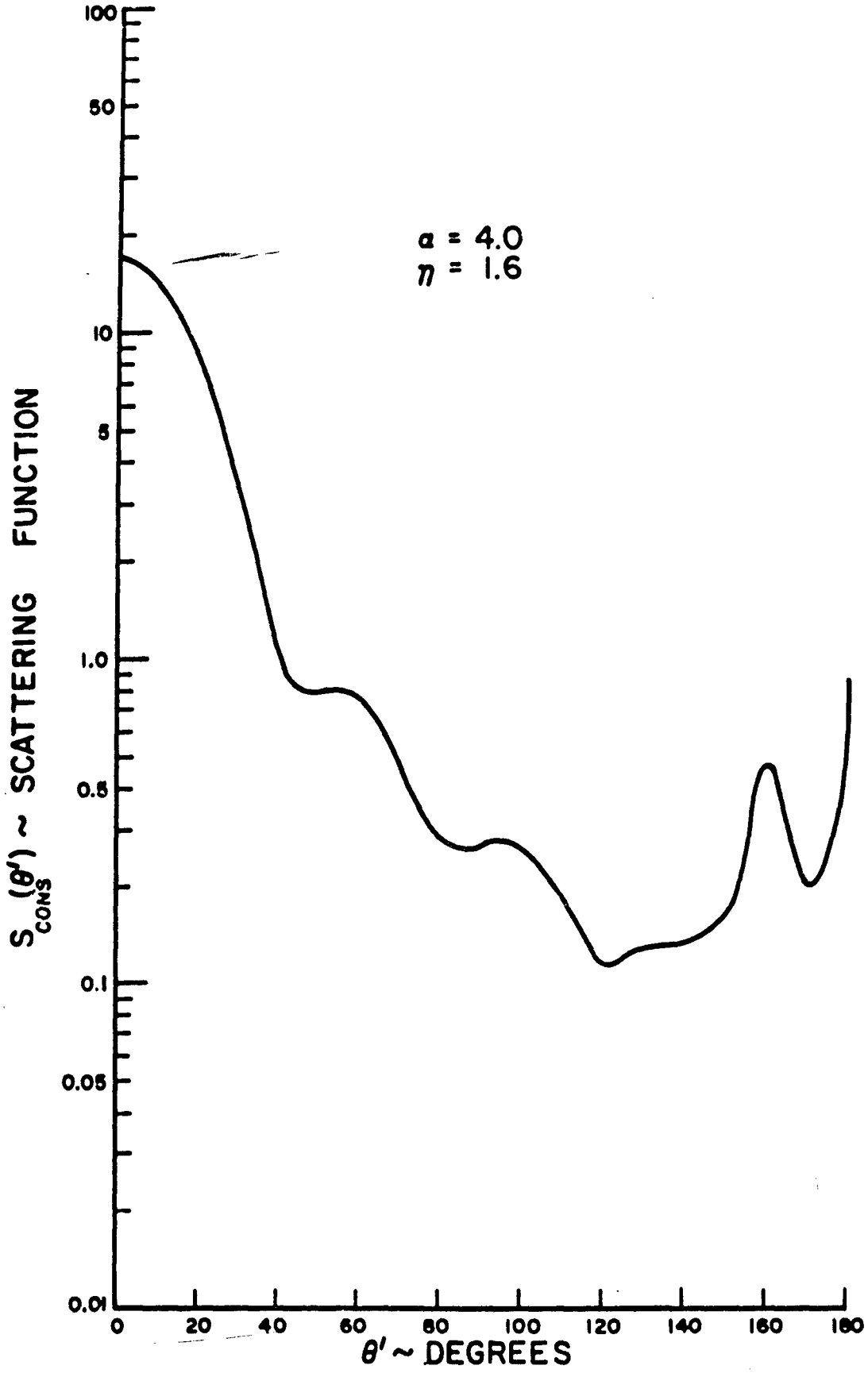

Figure 42. Angular Distribution of Scattering Function--Theoretical Data

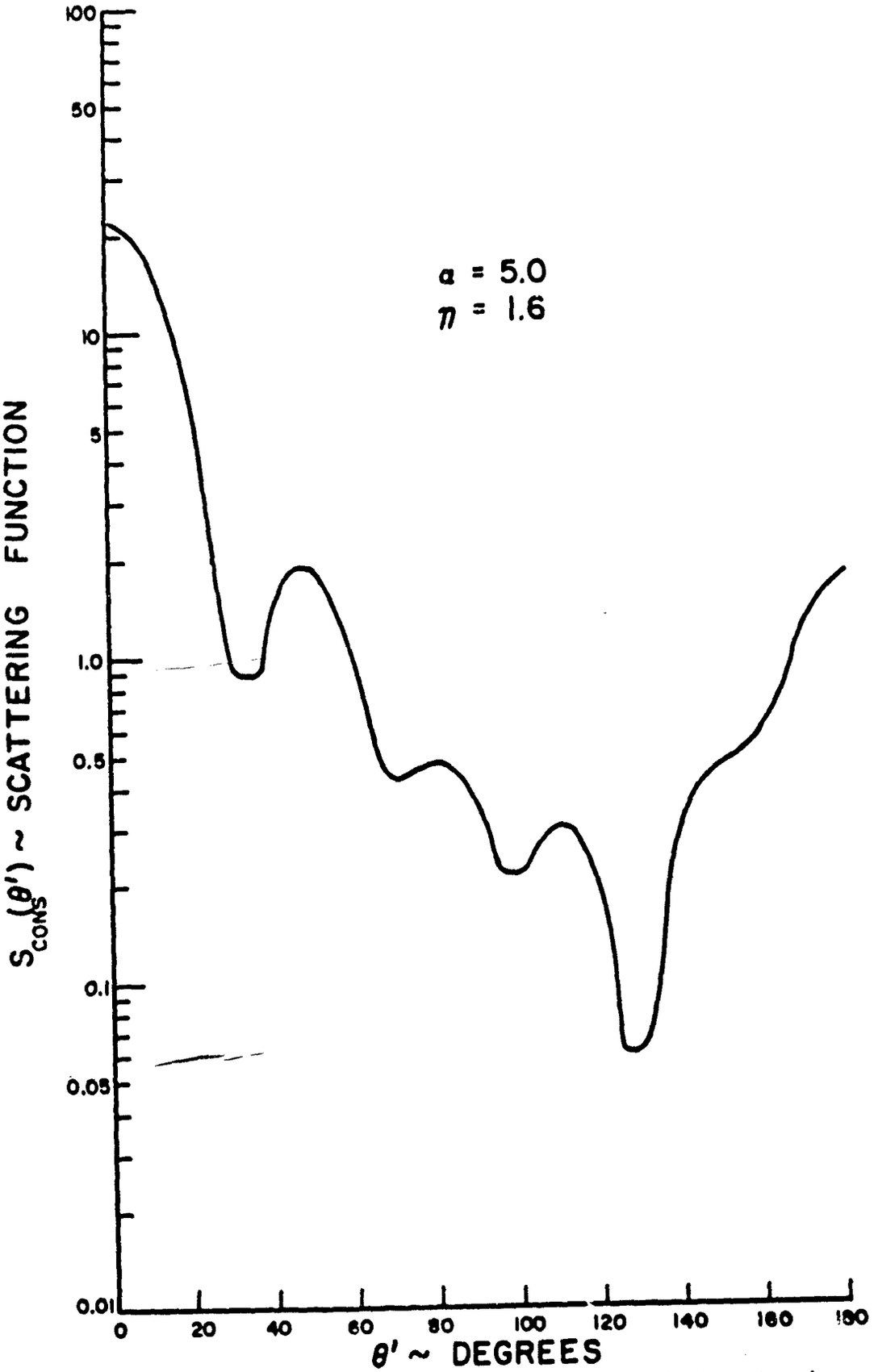

Figure 43. Angular Distribution of Scattering Function--Theoretical Data

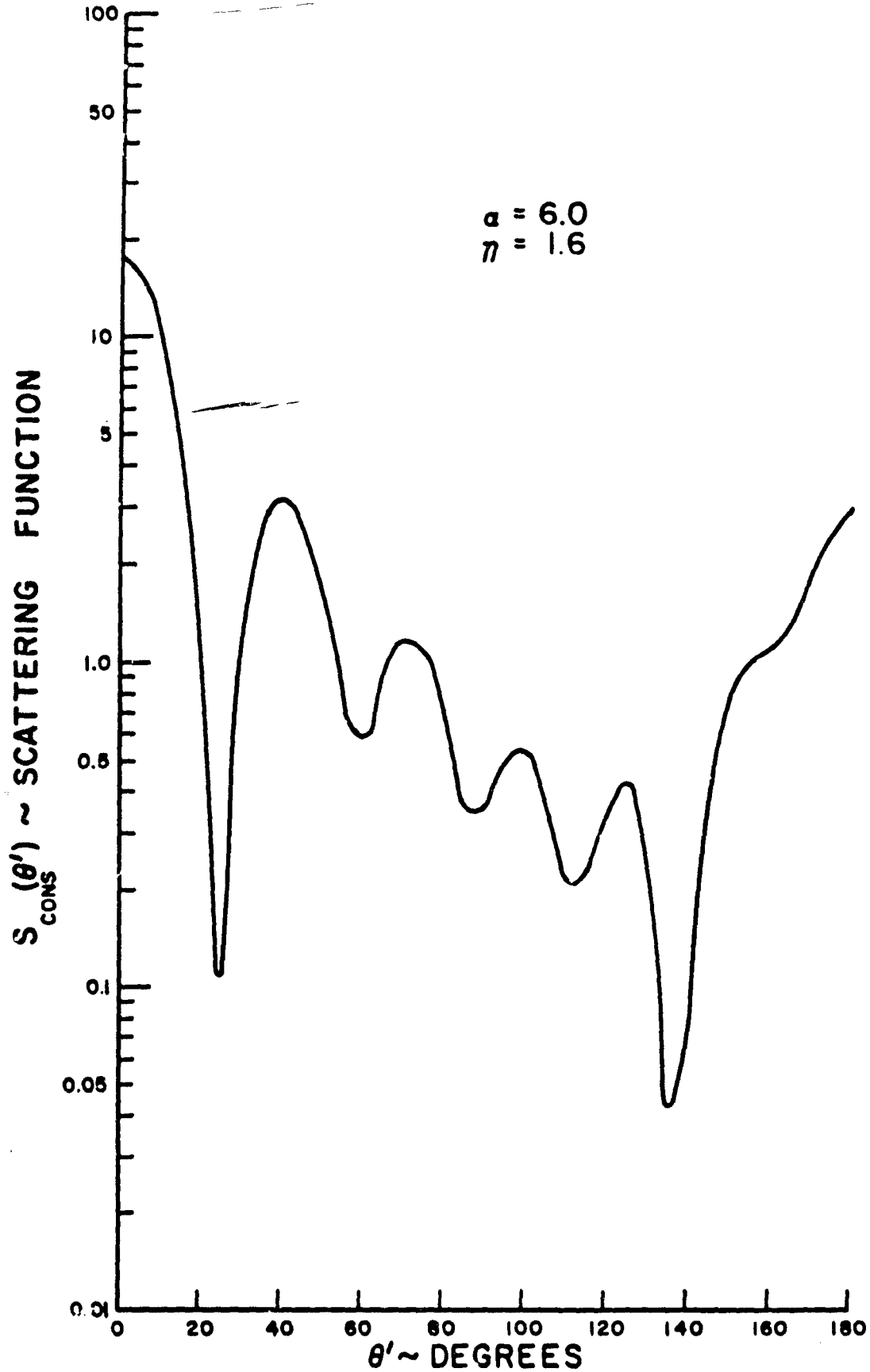

Figure 44. Angular Distribution of Scattering Function--Theoretical Data

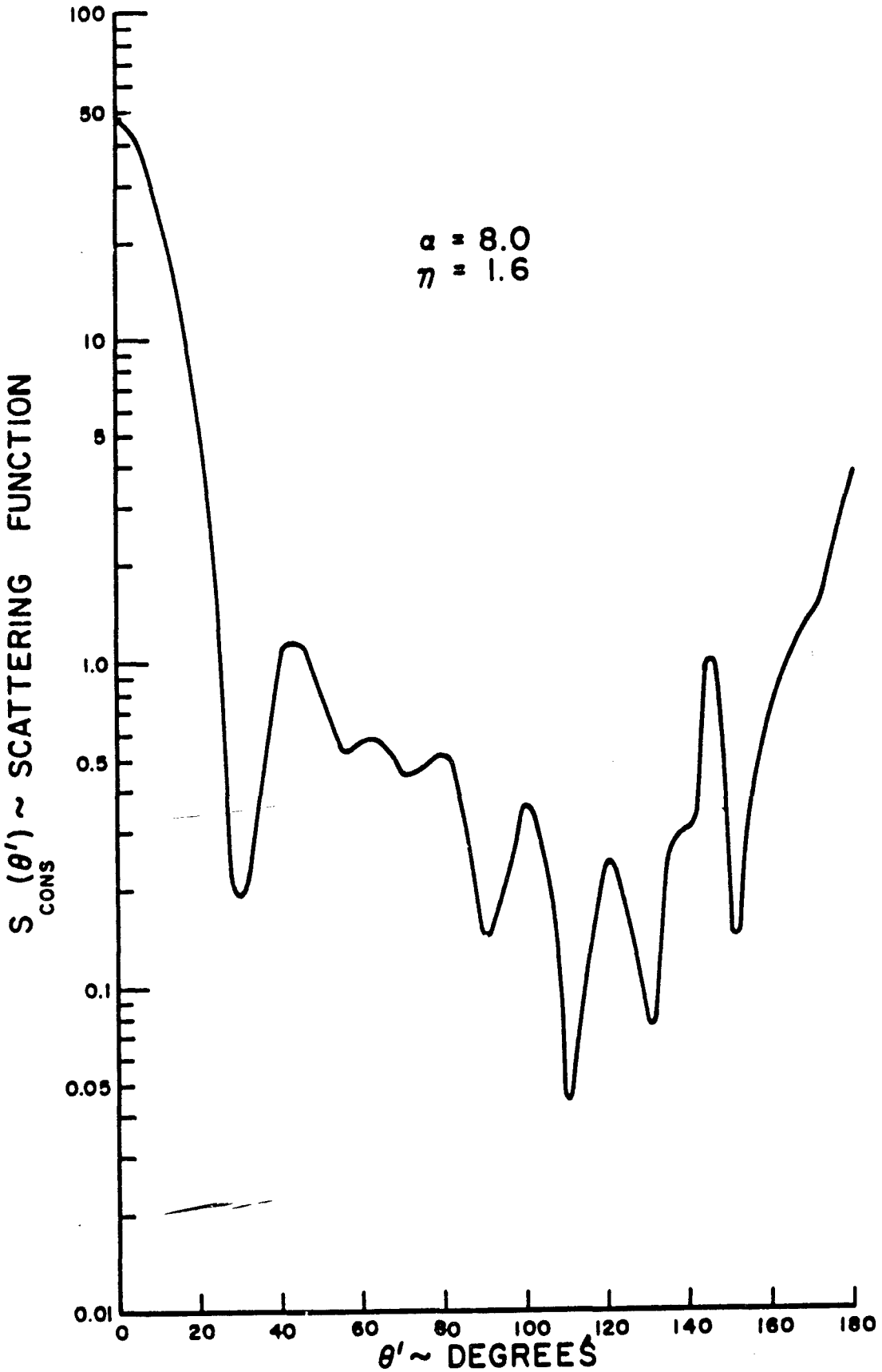

Figure 45. Angular Distribution of Scattering Function--Theoretical Data

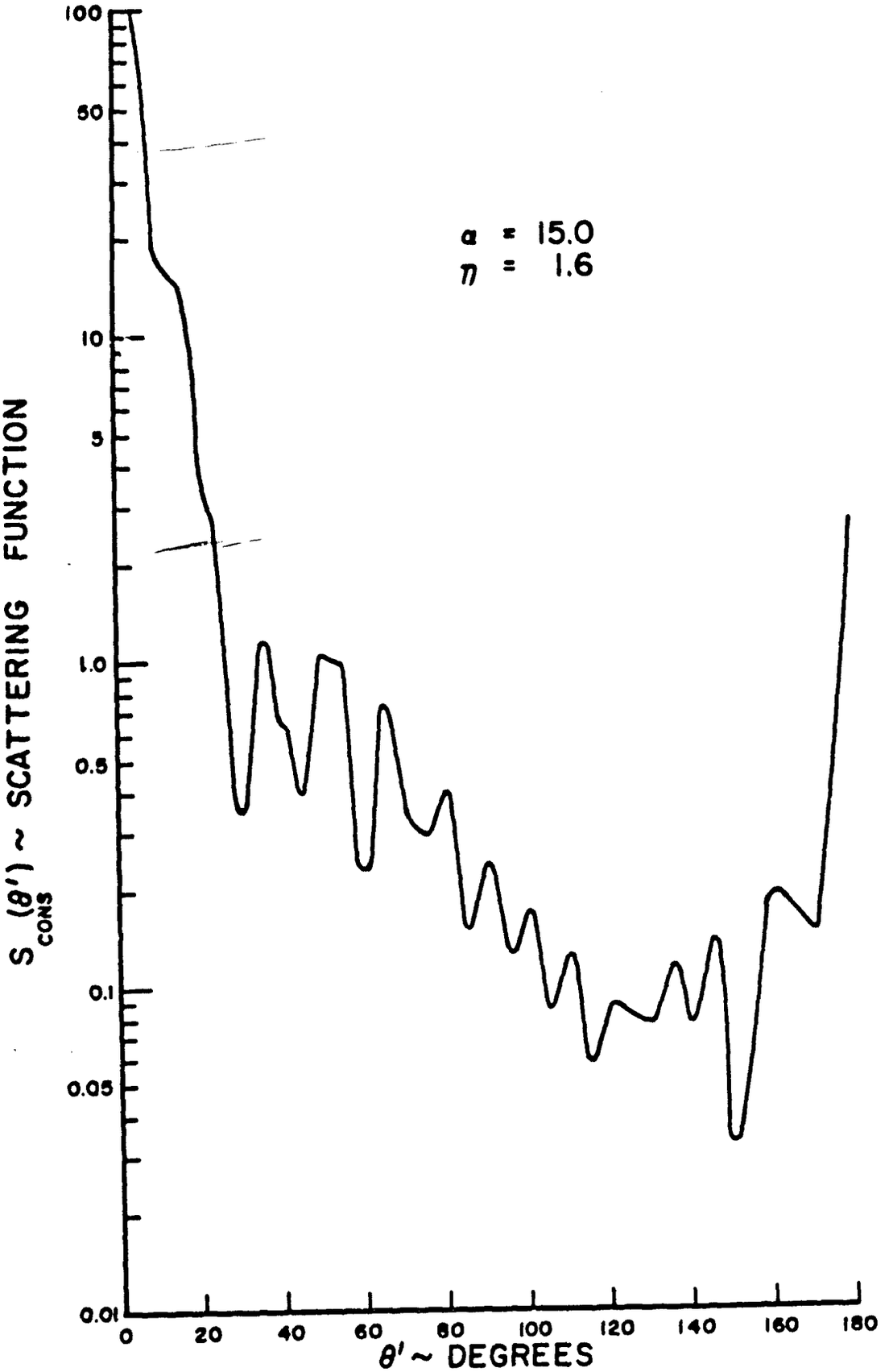

Figure 46. Angular Distribution of Scattering Function--Theoretical Data

APPENDIX F

SAMPLE DATA

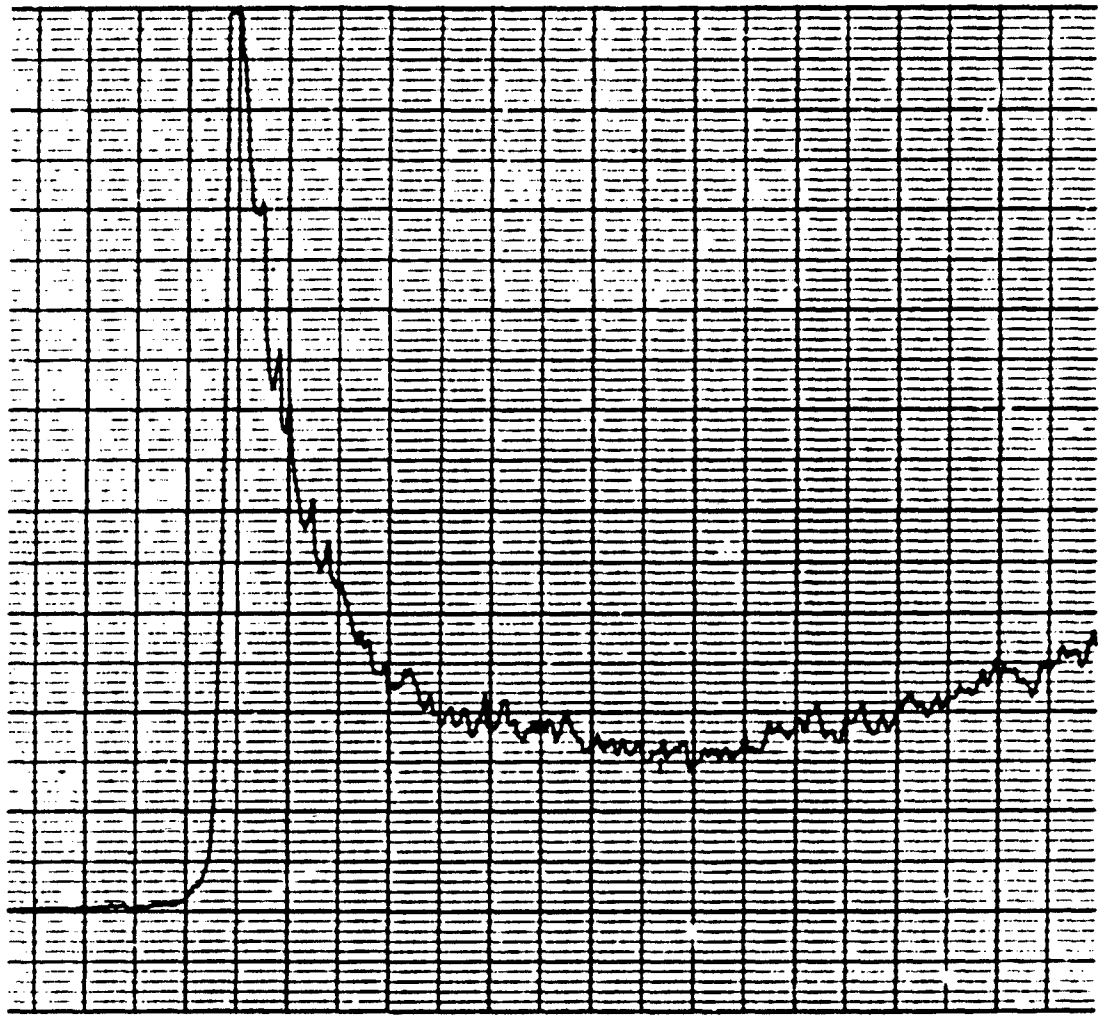

Figure 47. Experimental Data. Angular Distribution of Intensity--2.0

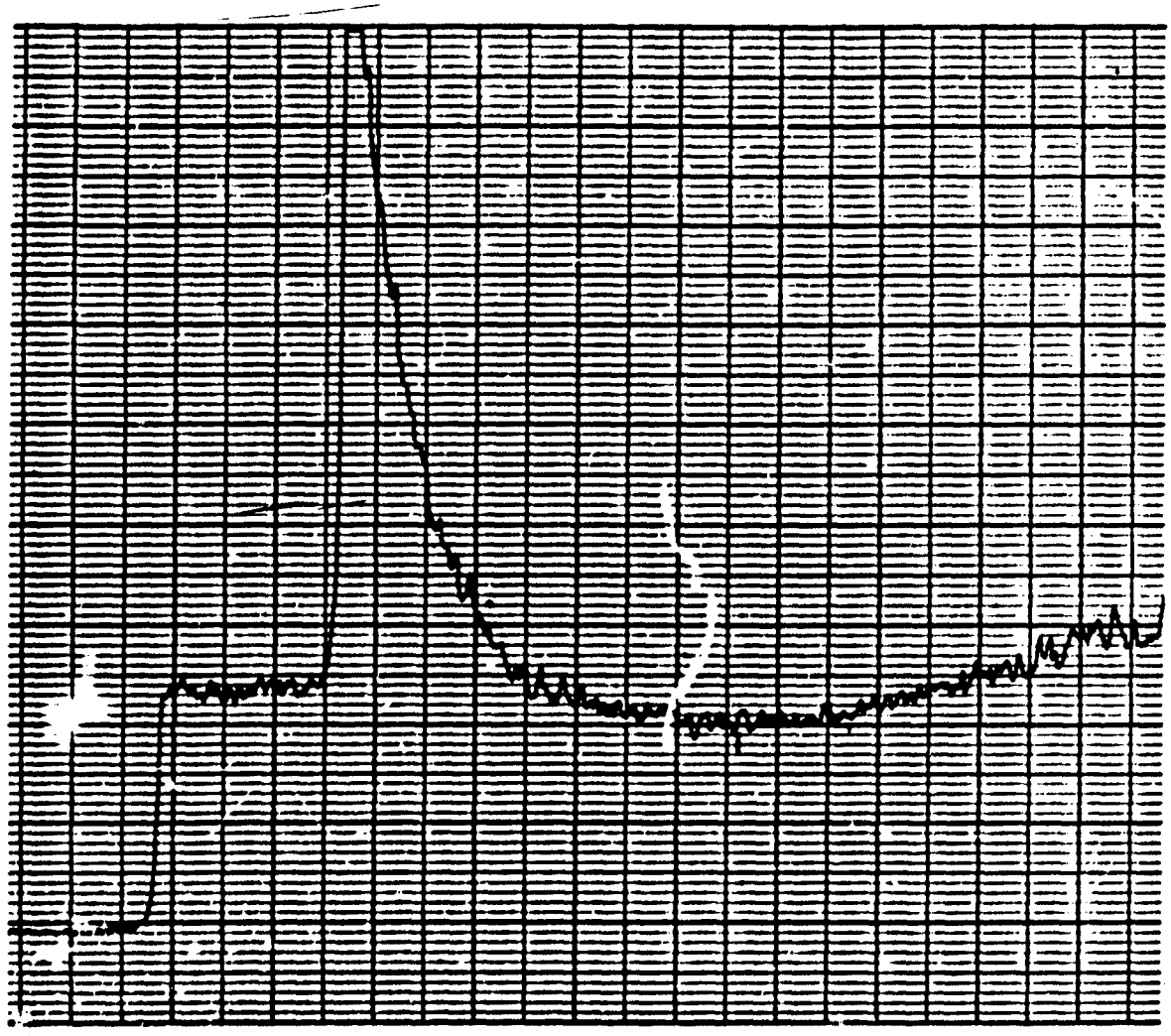

Figure 48. Experimental Data. Angular Distribution of Intensity--2.5

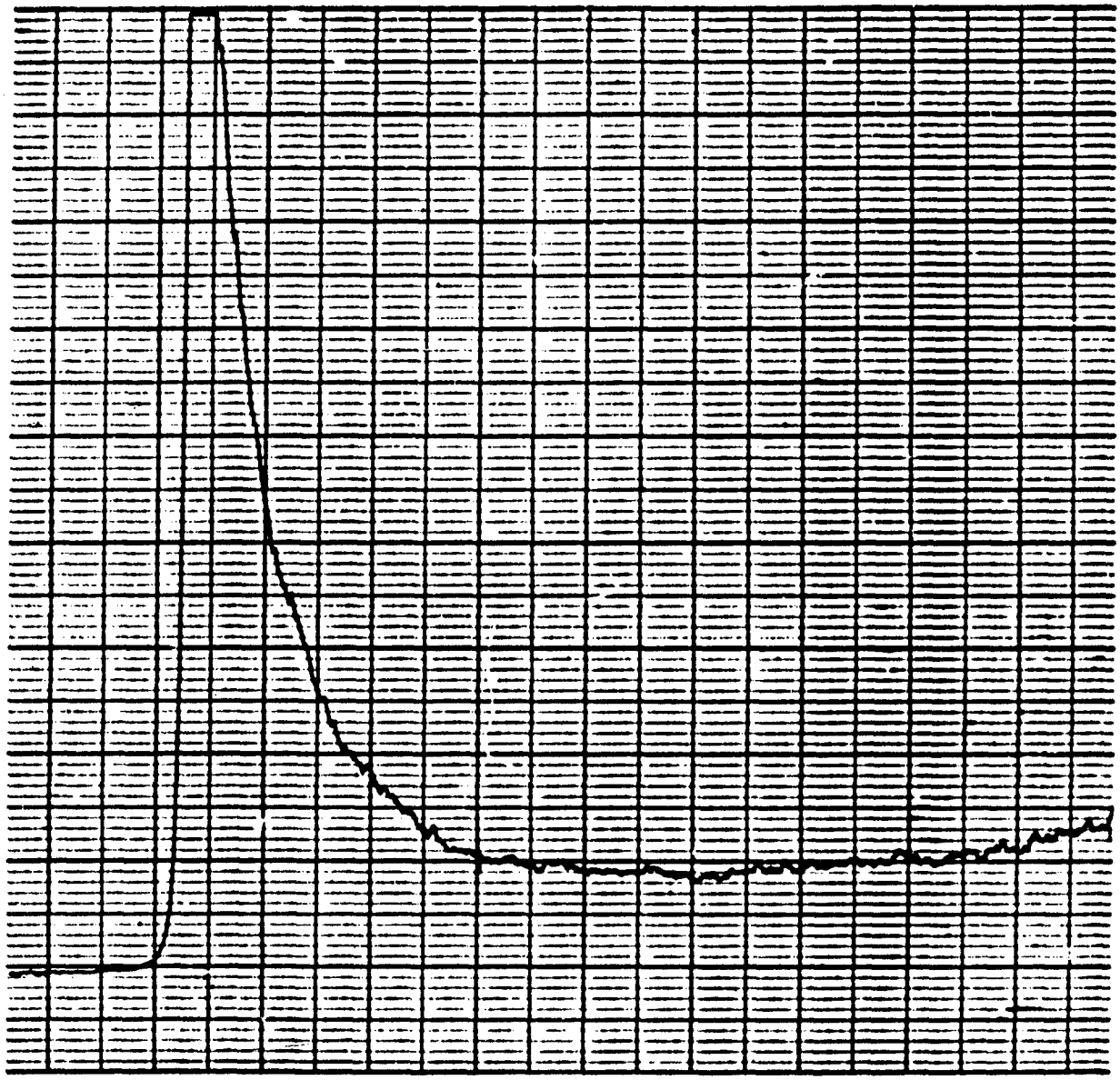

Figure 49. Experimental Data. Angular Distribution of Intensity--3.0

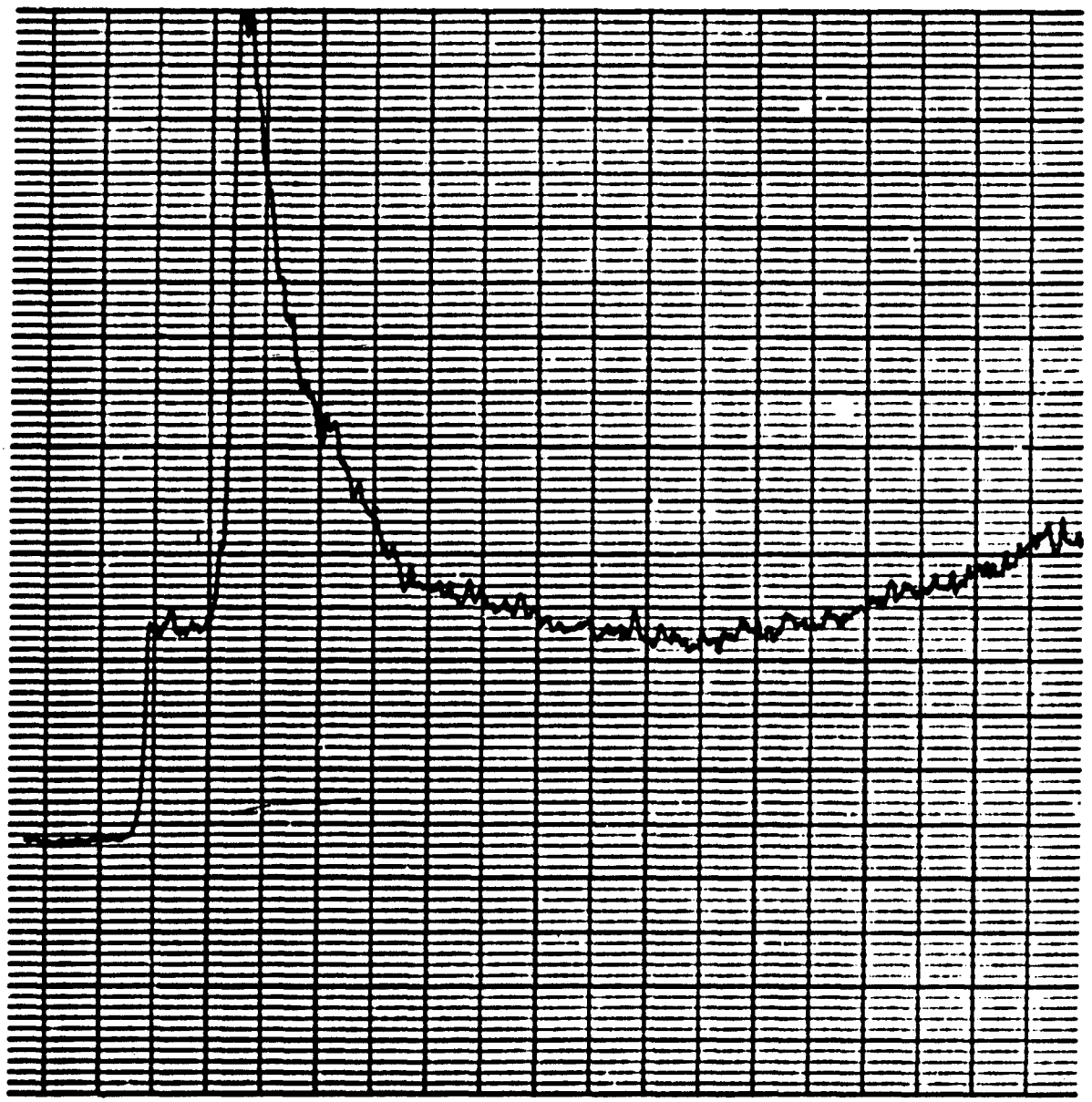

Figure 50. Experimental Data. Angular Distribution of Intensity--3.5

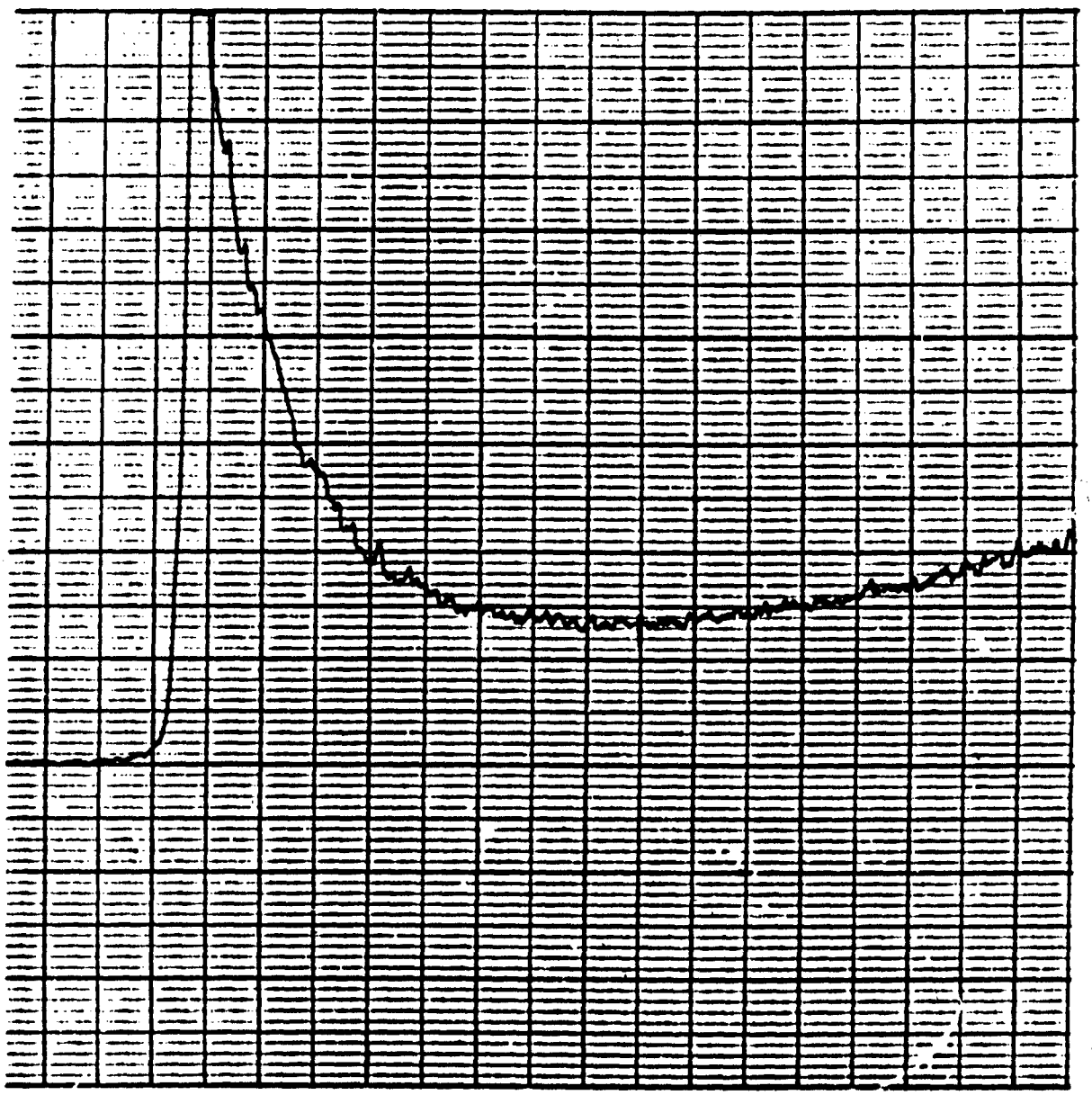

Figure 51. Experimental Data. Angular Distribution of Intensity--4.0

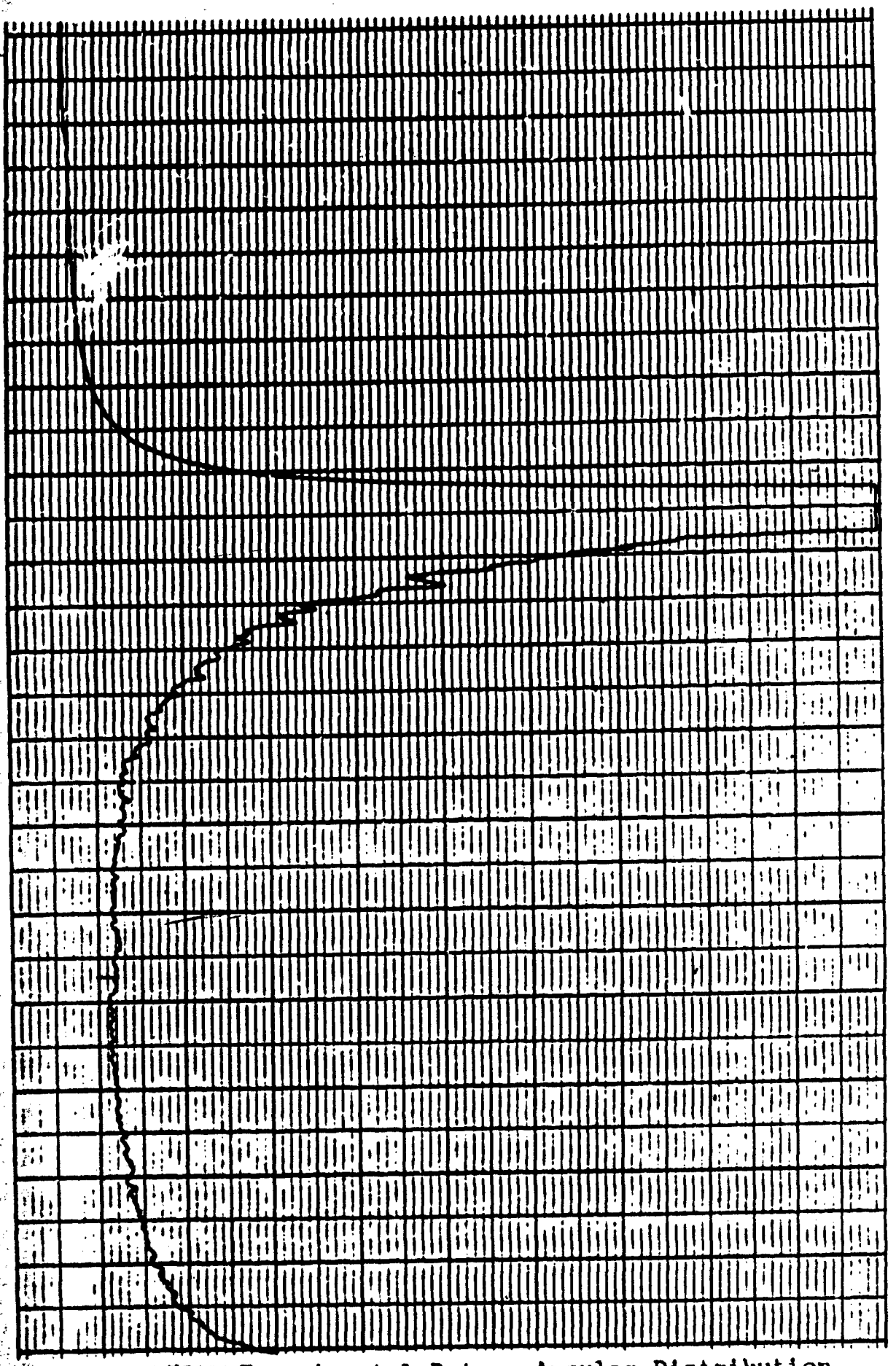

Figure 52. Experimental Data. Angular Distribution of Intensity--4.5

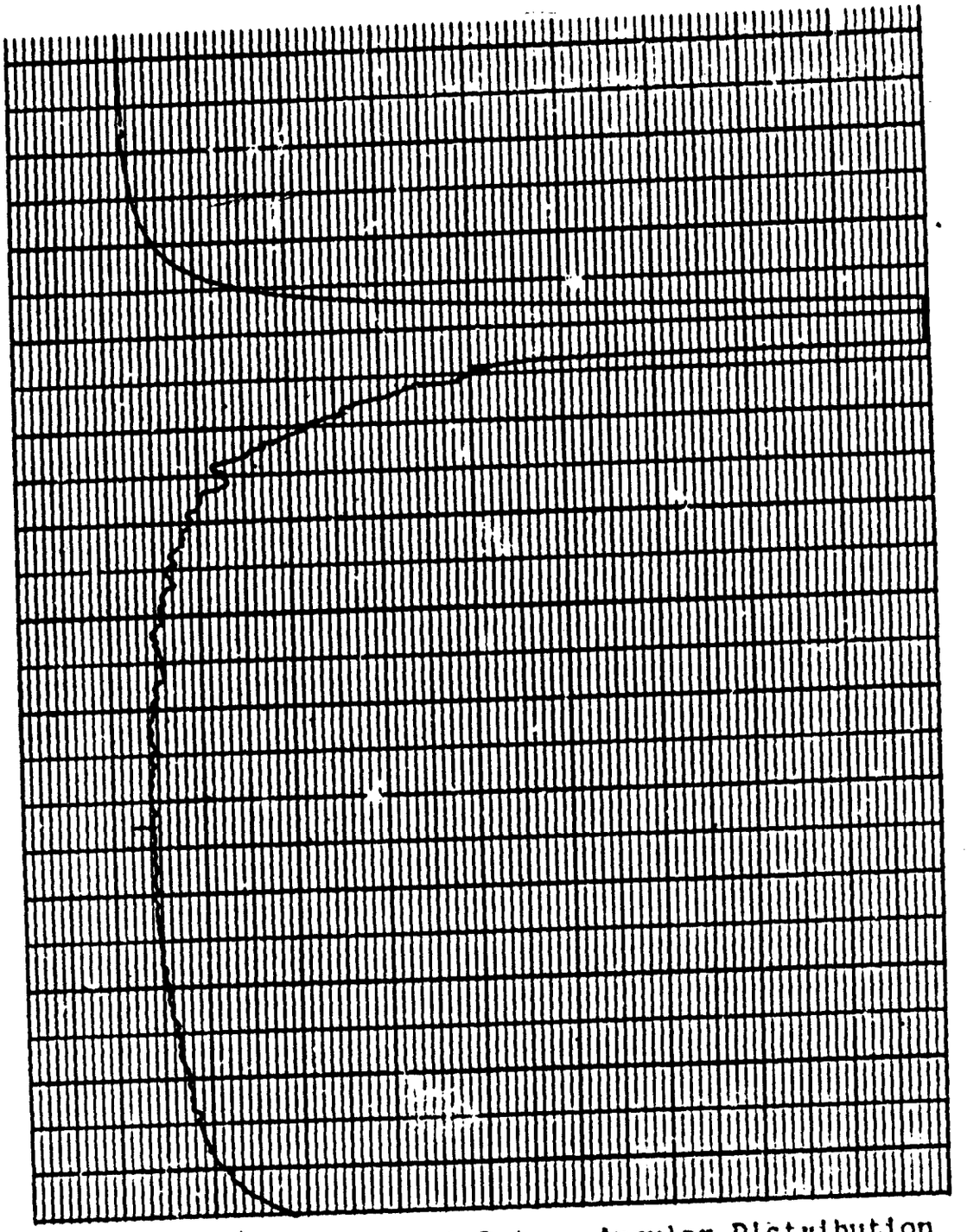

Figure 53. Experimental Data. Angular Distribution of Intensity--5.0

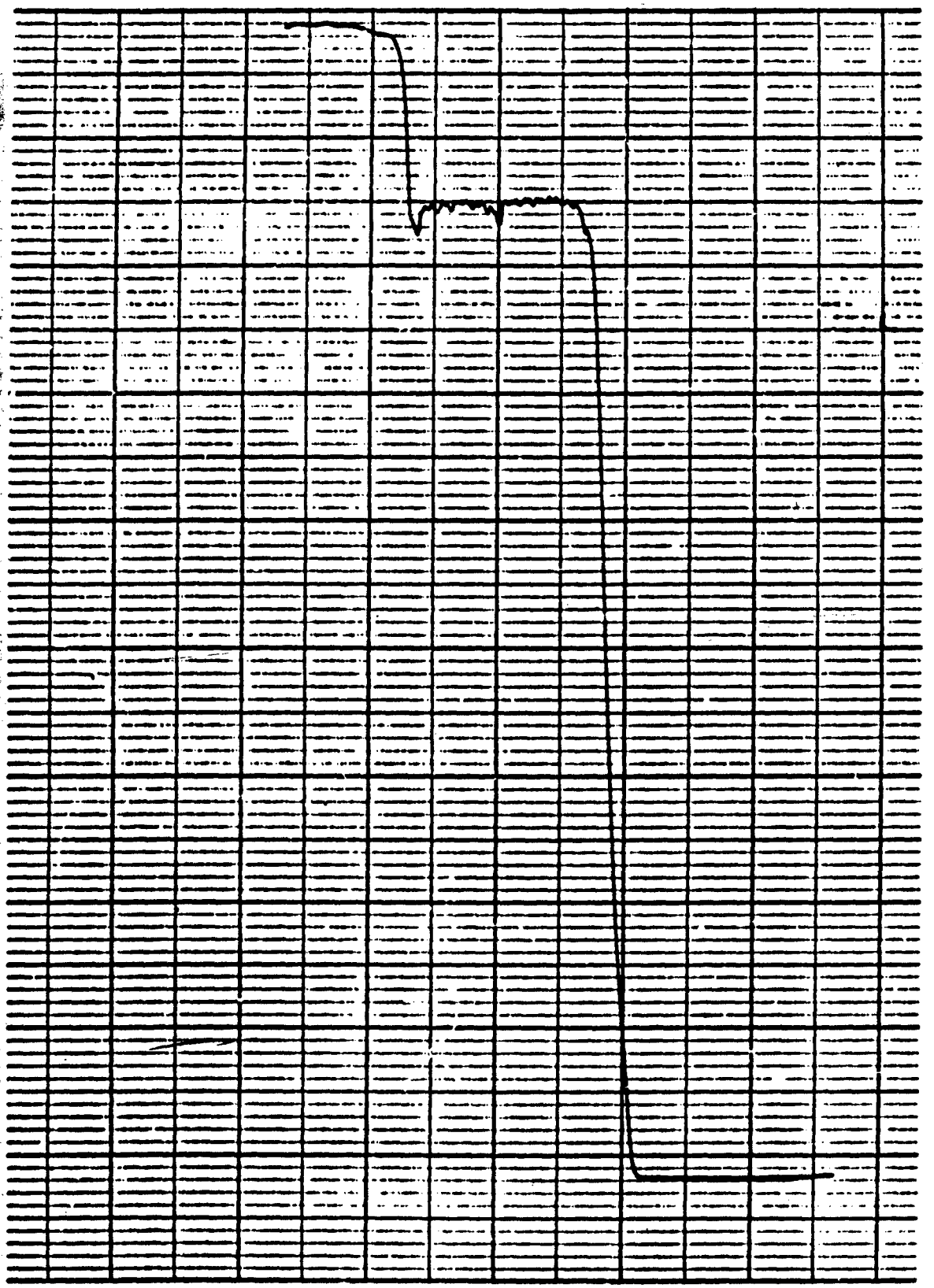

Figure 54. Experimental Data. Extinction--3.0

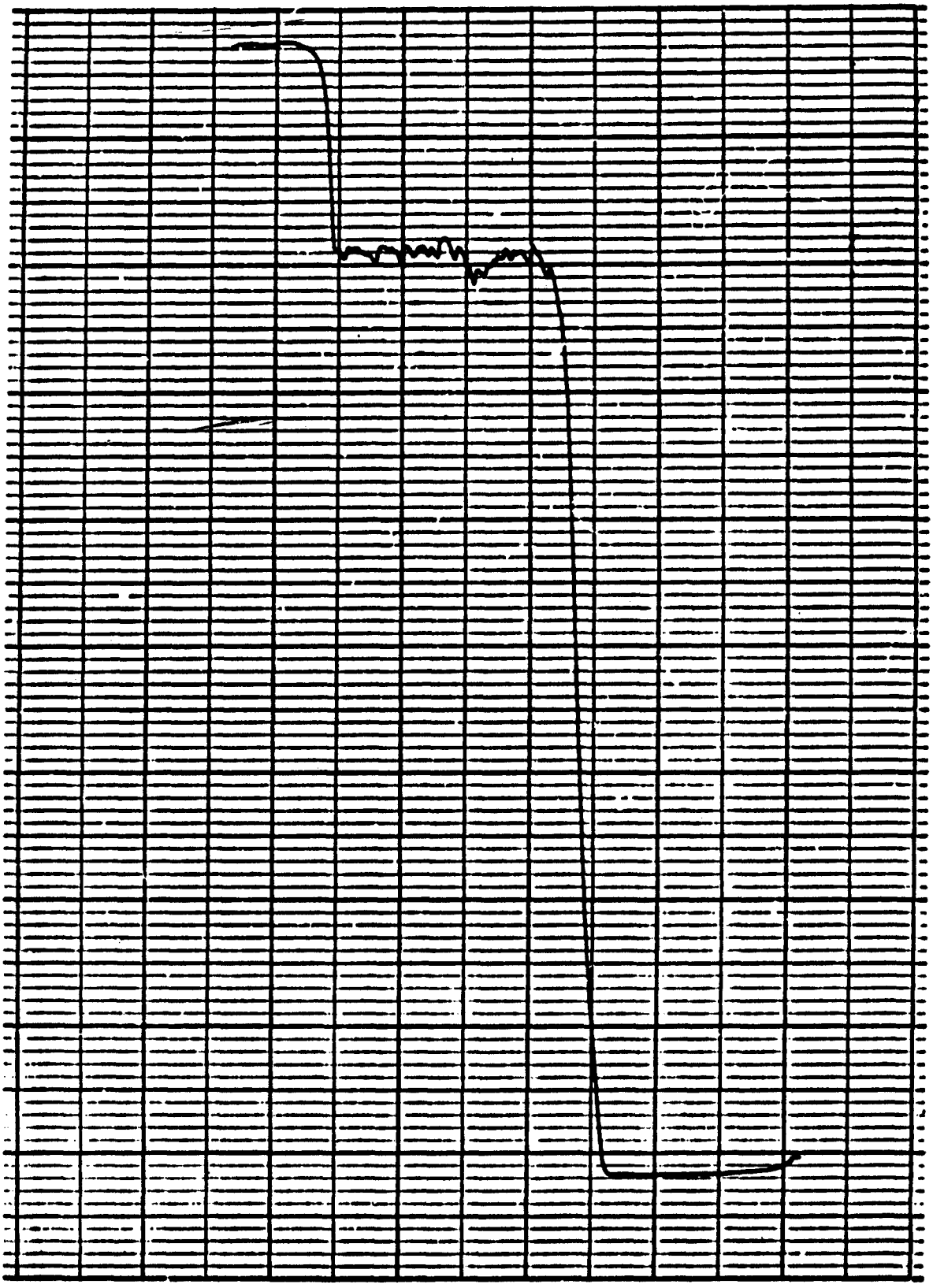

Figure 55. Experimental Data. Extinction--3.5

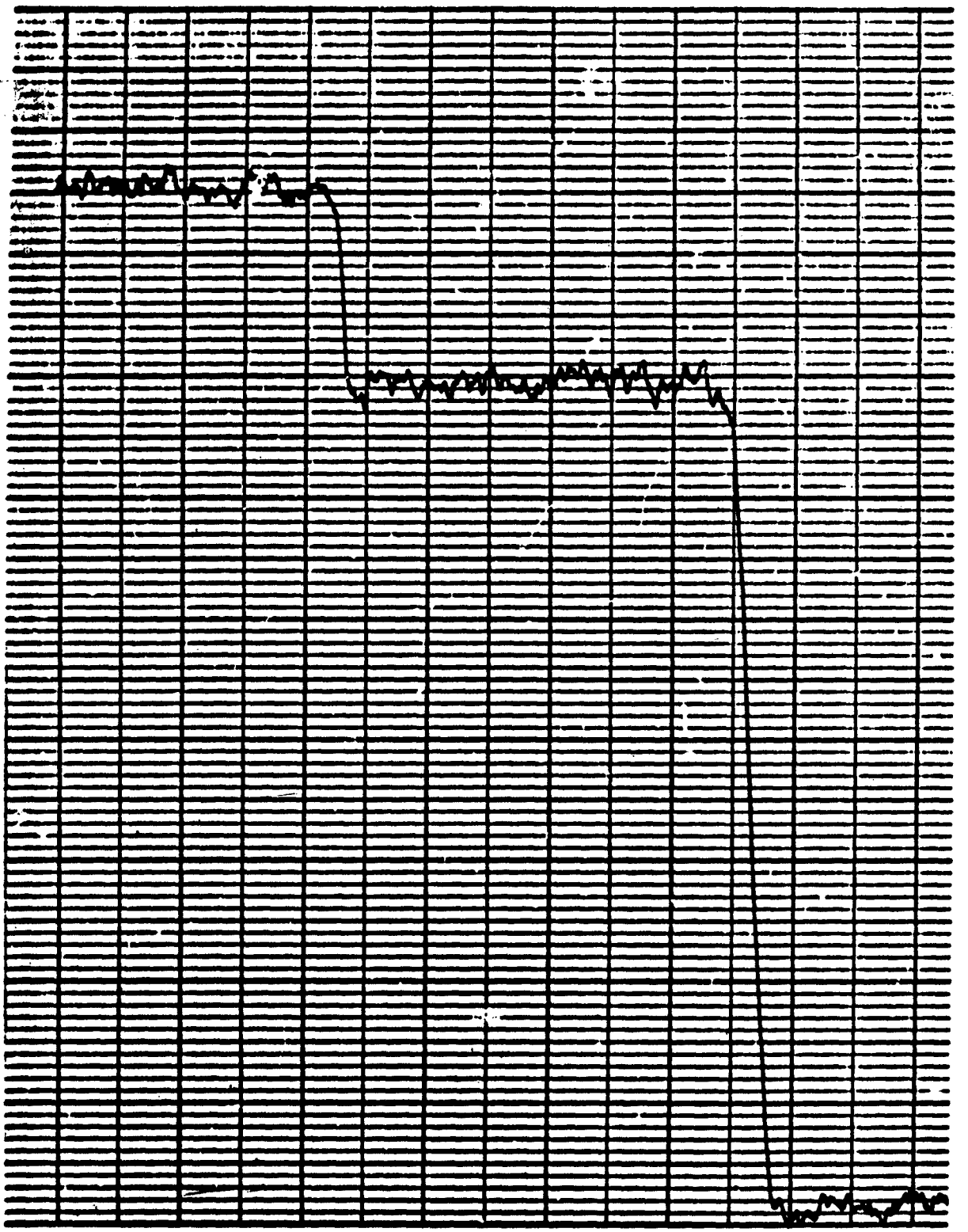

Figure 56. Experimental Data. Extinction--12.0

APPENDIX G

NOTES ON LITERATURE ON LIGHT SCATTERING

As mentioned in the body of this dissertation, the survey of the literature is by no means complete, and it has not been assumed to be. The literature reported in the bibliography represents some of the papers that were considered important in relation to this investigation. Most of them were studied to enlighten the investigator on the techniques of light scattering measurements. This appendix, covering additional notes on available literature, has been added for the benefit of those readers who might be interested in further study of the theoretical applications of this technique or the practical adaptations of its methods for use in particular fields of research.

Johnson and LaMer (73)[1] presented a very good discussion of the Mie theory. Particle radius can be determined by measuring the angular position of the "red orders" of the higher-order Tyndall spectra for mono-dispersed sols. The experimental apparatus consisted essentially of four elements: (1) an intense collimated beam of light; (2) a transparent cell to hold the sol; (3) a telescope in which to observe the scattered light; and (4) a protractor in which to measure the angle between the incident beam and the telescope. Angular positions were considered accurate to within one degree. In addition, previous work of LaMer and co-workers was discussed, including the description of the method in which alpha minimum was used to analyze and verify the Mie theory.

A LaMer and Barnes paper (90) included a note on symbols in which the authors suggested the standardization of symbols since they felt that the literature contained widely varying symbolism which was confusing. They suggested that clearer, unambiguous descriptions of scattering be standardized, and they offered definitions to be considered for adoption.

DeVore and Pfund (29) experimented with dielectric powders of zinc sulfide and titanium dioxide. Using the changing position of the Mie minimum with variation of refractive index and an extrapolation procedure, they were able to measure the refractive index of various powders. In addition, they reported on an interesting way to predict the Mie minimum for substances of known refractive indices. "The wave length of the 'Mie minimum' changes as the refractive index of the medium surrounding the particle is changed." And "The spectral-transmission curve of a film of dielectric powder having uniform particle size shows a very pronounced minimum corresponding to the Mie scattering maximum." The method is restricted, however, to the following: (a) the sample must have very uniform particle size; and (b) the particle size must be such that the Mie minimum will fall in a measurable region of the spectrum.

---

[1] Numbers in parentheses refer to items in the bibliography.

Sinclair (132) discussed the factor of 2 for extinction cross sections of large particles, originating with the work of Rayleigh. He briefly related the historical progress of Mie and Rayleigh, and noted previous experimental work. The Mie equations are theoretically valid for any value of size parameter (alpha), but they are difficult to calculate for larger values and become impractical to calculate for alpha greater than 10 or 12, due to the slow convergence of the series in the equations. He discussed briefly the work in which Debye presented an approximate formula for calculations for large values of alpha. For large values of alpha the extinction cross section is $K = 2\pi r^2$. From geometrical optics it can be seen that for large spheres the scattering cross section is equal to two times the geometric cross sections. He then concluded that (1) either the Mie theory was wrong for large alpha (although correct for smaller alpha), or (2) the theory is correct but is difficult to verify experimentally for large spheres. It now appears that the Mie theory is correct and the theoretical cross section for large spheres is $2\pi r^2$ when both diffracted and intercepted light is considered. In most practical measurements, only the intercepted light can be detected since the diffracted light is indistinguishable from the incident beam.

Henry (66) considered the transmission of powder films in the infra-red region. A globar source was used and the powder was prepared on a disc for transmission measurements. In general, he found that the dry powder films consisting of small particles adhering to transparent plates have spectral transmission curves considerably different from those of the same materials in bulk form. The infrared spectra from 1 to 14 microns were investigated.

Hardy and Young (51) discussed the use of Beer's law for mixtures. "The dependence of light absorption on length of path in a homogeneous medium was correctly stated by Bouguer in 1729." In 1852 Beer discovered that varying the concentration of an absorbing substance has the same effect as varying the length of path. Both Bouguer and Beer's law have been observed to fail if the light is not sufficiently monochromatic. The authors attempt to explain that Beer's law does not fail when a substance fails to obey the law, but it is the improper use of the law that is the cause of the failure. For a mixture of substances Beer's law must be applied to each component of the mixture. The paper discusses multi-component systems.

Zimm (166) presented theoretical expressions for the intensity of light scattering as a function of angle in concentration. Included is a discussion of apparatus used to measure light scattering from polystyrene solutions. White light has been used in conjunction with a filter to obtain a particular wave length.

Sinclair and LaMer (134) made one of the very important contributions to the field of light scattering as a measure of particle sizes in aerosols. The paper contains a very good background of the Mie and Rayleigh equations and discusses the "factor of 2 error" which has appeared in some equations found in the literature. (This discussion appeared in earlier papers.) For the experimental

measurements monochromatic light was used whose wave length of .524 plus or minus .01 micron was obtained through the use of a filter. Measurements of angular distributions of 3 to 175 degrees were made at frequent intervals. The resulting measurements were integrated over the entire sphere and compared with the Mie theory. The variation in particle size was used to establish the particle size parameter, alpha, variation. The scattering cross section was obtained by comparison with the brightness of a diffuse reflector of known reflectivity. Use was made of the fact that for single scattering the intensity is a function of concentration. This is true, of course, only if the concentration is sufficiently low that secondary scattering is negligible. If single scattering exists, the intensity scattered in a particular direction and from a given volume will vary with the particle number concentration, as well as with the particle radius raised to some power, as given in the equation $I = nkr^p$. Variation of the exponent p with r has been evaluated. The authors discussed a method to obtain size distribution in a fog of non-uniform droplet size by allowing it to settle in a convection-free fog chamber and observing the decrease in scattering intensity with time. The paper also discussed Gucker's measurements, using what is believed to be the most sensitive aerosol detector reported, $100(10)^{-3}$ micrograms or 10^{-9} grams per liter. A method is discussed for producing fogs of uniform droplet sizes which do not vary more than 10 percent from the average found by microscopic measurement. The droplets are below 0.2 micron. Plots calculated with the aid of mathematical tables are included for the angular distribution functions i_1 and i_2 which are complicated functions of particle size parameter, refractive index, and scattering angle theta. Polar diagrams for m = 1.55 and alpha = 1.5 and 3.6 are presented to show a typical diagram. Unfortunately, no curves or scattered diagrams are presented for the fogs of non-uniform droplet size, which would enable a comparison of their work with that of other investigators. Included in the appendix is a discussion of absorption and complex refractive index,

> "Absorption may arise from two causes: (1) in conducting media for which the conductivity, sigma, is finite, and (2) in dielectrics when the incident wave length is not far from that of an emission line. The first type of absorption is the only one considered in the derivation of the Mie theory. The second type of absorption results from the interaction of bound electrons and the incident electro-magnetic wave."

Kerker and LaMer (82) used the polarization ratio method to analyze scattering light for equal size distribution of sulfur hydrosols. Filtered white light of 4360 angstroms and 5460 angstroms was used. The polarization ratio method can be considered, using measurements of the ratio of the intensities of the horizontal to vertical components of the scattered light, provided that alpha is less than 2. For values of alpha larger than 2 the ratio is no longer monotonic but undergoes a highly irregular fluctuation as a function of alpha. If the ratio is plotted as a function of angle of observation for a specific value of alpha, the resulting curve exhibits the

maxima and minima. The angular position and number of these maxima and minima vary in a regular manner with increasing alpha. When alpha is greater than 1.5, these maxima and minima move toward the forward direction as alpha increases.

Dandliker (25) obtained the particle size of polystyrene latex from angular positions of minimum intensity. The method is quite similar to that of LaMer and Sinclair in their study of aerosols and to the investigations of Johnson and LaMer in the determination of particle sizes of sulfur hydrosols. The apparatus used was the modified Debye apparatus. Angular distribution of intensities was measured at angles between 20 and 144 degrees. A mercury arc source was used with monochromatic light of wave length 4358 angstroms. The positions of minimum intensity in an angular dependence curve are functions of both refractive index and particle size parameter; hence, the location of these positions, that is, theta minimum, can be used to determine the size of a sphere. This is a method similar to that used by LaMer and Sinclair and by Johnson and LaMer when they studied the particle size of sulfur hydrosols. Dandliker has extended these studies and the measurements are carried out in the presence of true absorption. Results of his investigation were compared with the sphere-diameter measurement using an electron microscope, and results were considered within experimental error.

A paper by Carr and Zimm (13) considers light scattering from liquids, using three methods: (1) transmission, (2) integrated scattering, and (3) scattering at 90 degrees. The errors of their design have been discussed: (a) refractive index of cell, correction is required, (b) volume of cell as "seen" by photometer, correction is required, and (c) the sensitivity of the photo cell variation. The electronic system was nearly the same as that used by Zimm (167), although it was modified slightly. Corning filters were used to obtain wave lengths 4358 and 5461 angstroms. Scattering of liquids such as benzene, carbon tetrachloride, dibenzyl, and sucrose octaacetate was measured. Turbidity measurements were included.

Hart and Montroll (53) presented a theoretical evaluation of the solutions of the electro-magnetic theory (closed-form approximation of Rayleigh and Mie theories). The approximate theory yields total scattering cross sections in good agreement with exact methods for refractive indices 1 to 1.5. The Rayleigh-Gans theory is summarized for spheres of uniform density and of Gaussian density. No absorption is considered.

In a paper by Cleveland and Raymond (22) the introduction offers a particularly good review of the theoretical and experimental work in light scattering. The authors were the first to make measurements of integrated scattering by metallic spheres; however, results were obtained on layers of particles rather than on an aerosol. A Perkin-Elmer spectrometer, Model 12A, was used. The extinction, rather than angular scattering, was measured. The slit width was varied to maintain full deflection on chart; consequently, angle reception also varied. Carbonyl iron was used in their experiment with a particle

size of 2.7 microns on the average and with a range of 0.5 to 5 microns. The specimen consisted of a layer of particles or a film of particles of rather close proximity (3.4-micron diameter maximum). The investigation covered a wave length range of 0.45 to 15 microns, utilizing a sodium chloride prism. The measured size of spheres was not considered to be accurate. The curves plotted were scattering area coefficient, k, versus particle size parameter, alpha; however, alpha was based on multi-dispersed systems. Since the size of the particles was not accurately determined, the particle size parameter was based on an average size of particle. It was reported that the error in k was probably due to the uncertainty in the obtained transmission values and the measured area coverage factors. The area coverage factor was used in the determination of the particle size parameter, alpha. It was suggested that the error in alpha, estimated to be within 3 to 5 percent, was due to the uncertainty in sphere size.

Gumprecht and Sliepcevich (48) define and discuss the terms: apparent and actual scattering coefficients. The actual scattering coefficient is based on the total amount of light scattered by a particle in all directions, whereas the apparent scattering coefficient k_a is based on the amount of light scattered by a particle in all directions except within a cone of half-angle theta in the forward direction. Scattering coefficient k is defined as the ratio between the scattering cross-section and the geometric cross-section of the spherical particle. For large values of alpha k_t approaches the value of 2 rather than 1. This phenomena, which might appear impossible for a large spherical particle, is explained on the basis of Babinet's principle of diffraction by opaque circular discs. Since the apparent scattering coefficient has a value of 1 and approaches a value of 2, depending upon the value of the half angle theta of the cone of reception, a distinction is made between k_a and k_t, with the ratio k_a to k_t being defined as R. The defined term R is computed from diffraction theory and compared with the Mie theory. The advantages of the lens-pinhole detector are discussed. Also discussed is experimental work on the transmission of light through dispersions of glass spheres suspended in water to test the validity of computed values of R. According to this report, the lens-pinhole optical system excludes practically all stray light from the photo tube. The exact value for the half-angle theta can be calculated readily from a direct measurement of the diameter of the pinhole and the focal length of the lens. The value of theta is a constant and is independent of the location of the illuminated particle in the path of the beam or in the fringes of the beam. For the above three reasons, the lens-pinhole optical system is preferred.

In another paper Gumprecht and Sliepcevich (49) discussed their particle size measurements on poly-dispersed systems. Their previous analytical and experimental investigations of light transmission equations were combined with Stoke's law of settling. The ratio of actual to total scattering coefficients, R, defined in earlier work, was used in the transmission equation. Light transmission measurements were made on a dispersion containing particles above the

colloidal size range. The intensity of the transmitted light will, of course, gradually increase as the particles settle out under the influence of gravity. The size range of particles settling during any interval of time can be computed from Stoke's law. Consequently, a combination of Stoke's law and the transmission equations permitted light transmission measurements on a dispersion undergoing tranquil settling with time, making possible direct measurement of the relationship between intensity and time and calculation of the number of particles as a function of diameter of the largest particle to obtain the so-called size-frequency distribution curve.

Kerker and Hampton (81) used unfiltered light in an attempt to improve results obtained in the measurement of particle sizes by monochromatic light and measuring polarization ratio. Results from the unfiltered light method are comparable to those from monochromatic light, and the authors conclude that it is unnecessary to filter light when using polarization methods.

Maron and Lou (101) utilized light scattering measurements for the determination of molecular weights. In this work Ludox (a finely-dispersed colloid of silica in water) was used with results being reported as very good.

Aughey and Baum (1) designed a device to measure the angular distribution of intensity very near the zero direction (forward scattering). Their angular dependence light scattering device, using a mercury arc as a source, was constructed by Dupont de Nemours. The intensity was varied with filters and through use of a slit control. Angular variation was from 140 degrees to .05 degrees. This was the only device described in the literature that could measure the angular distribution of intensity to such a small angle or so close to the forward direction. The author's experiment, using white light and filters, was restricted in wave length. This was the first paper encountered which mentioned continuous scanning. The incident beam used was not parallel, and this varied from most experiments reported in the literature. A photo-multiplier was used. The optical system is exceptionally good.

Tabibian, Heller, Epel (150) offer an introduction and review which is particularly good for background material.

Sekera (13) has presented a theoretical paper on light scattering which discusses the experimental techniques of light scattering as applied to atmospheric studies. The integro-differential equation of radiative transfer is discussed for atmospheric radiation. The normalized scattering function is expressed in the equation. Rayleigh type of scattering is assumed and the expression for the scattering function is that expressed by Chandrasekhar. A photoelectric polarimeter was constructed for measurements.

Heller and Pangonis (62) considered turbidity measurements on a theoretical basis. Mie, Rayleigh-Gans, Debye, and Einstein equations are compared briefly in the introduction.

Heller and Tabibian (64) summarize errors in colloidal cells used in turbidity measurements.

Heller and Pugh (63) report on an experiment on particles of .67 micron in diameter and a refractive index of 1.2. This was an experimental investigation on the effect of light scattering upon the refractive index of a colloid or of colloidal particles. An uncertainty of .003 in the refractive index will give 5 percent error in particle size measurements, calculated from turbidity measurements. Therefore, the refractive index should be known to four decimal places.

Tabibian and Heller (149) made scattering measurements at 90 degrees on very small spheres, that is .046 to .824 micron in diameter. Plots were included which show the concentration dependence of light scattering at 90 degrees for several substances. Variation of light scattering at 90 degrees with particle diameter is also included. Curve shows maxima and minima comparable to the theoretical Mie equations for turbidity measurements (that is, extinction measurements). Considerable discussion has been devoted to those curves which exhibit a decrease in the 90 degree intensity ratio with increasing concentration and to a point of inflection which occurs in some of the curves of 90 degree intensity versus concentration. Some of this is explained by the lateral radiation of multiple scattering. The point has been made that measurements of angular distribution should be taken with various solid angles and that the solid angle for the 90 degree measurement should be sufficiently small to consider scattering from a single particle. This procedure for the variation in solid angle should be followed unless the solid angle that is used is small enough that the ratio of the intensity of 90 degrees to the incident intensity is independent of solid angle. The solid angle used was reported to be $4.1(10)^{-4}$ steradian.

Penndorf (116) discusses an approximation method for solution of Mie equations for refractive indices less than 2, but for any value of particle size parameter, alpha. The paper is based on the scattering theory for spheres of refractive indices near 1. Phase and amplitude of scattering coefficient at the extrema are computed. The results are plotted in three-dimensional form, which permits graphical interpretation. The investigation was a theoretical presentation as opposed to experimental. The author concludes that his method is much less time-consuming than using an exact solution to the Mie equations and that a complete description of the functional relationship between the scattering coefficient k and the size of the sphere exists.

Heller, Nakagaki and Wallach (61) present a theoretical analysis or a comparison of the Rayleigh-Gans and the Mie theories. Investigation is for non-absorbing spheres.

Bateman, Wenack, and Eshler (4) determined the particle size and concentration from spectral photometric transmission. Experimental measurements for characterization of biological hydrosols in the

micron range with respect to size, concentration, and refractive index are reported. Measurements were made in the visible and long ultraviolet range. The spectro-photometer design made careful note of the specifications set by Heller and Tabibian in their "error study".

Bonnelycke and Dandliker (8) used a colloidal of silica, Ludox, for their scattering measurements, since it supposedly does not absorb at wave lengths of interest, that is, using a mercury arc and wave lengths of 4358 and 5461 angstroms. The transmission versus 90-degree readings were compared for particles 10 to 15 micro-microns in diameter with a weight of 10^6.

A paper by Heller and Nakagaki, No. VII in a series, (61) refers to dissymmetry, which relates to the fact that the scattered light in the forward direction is greater than the scattered light in the backward direction. The theoretical calculation of dissymmetry is 90 + delta gamma and 90 - delta gamma. Delta gamma is the angle between the scattered intensity and incident ray and is equal to 45 degrees, giving dissymmetry at 45 and 135 degrees. The delta gamma equal to 90 degrees was presented in papers V and VI. The spheres considered had a refractive index of 1.2. The Mie theory was considered, using the particle size parameter 0.2(0.2)15.2. The diameter is equal to 0.2 microns for the green mercury line, that is, at the 15.2 value of the particle size parameter. This paper, as all of Heller's work, is a very detailed theoretical examination of the results of the Mie equation, and it can be considered one of the most extensive works in the area.

Greenberg (43) used the scalar wave equation which is applicable to quantum-mechanics and acoustical problems as a basis for calculations. Non-spherical scatterers are compared with sperical scatterers.

Pritchard and Elliott (124) discuss the polar nephelometer and the transmissometer. These two instruments were used to measure light scattering and transmission of the atmospheres. The scattering function was referred to as the scattering index. They found that if white light and a broad band receiver were used large errors in scattering and attenuation measurements resulted. The article contains a description of the nephelometer, which can be called a device for measuring the scattering of atmosphere. It utilizes a photomultiplier detector. Scattering in the atmosphere was considered, and irregular shaped particles were encountered. The resulting curves were smooth functions. The only irregularity appearing in their curves was attributed to unstable conditions on a particular experiment in fog.

Kerker and Matijevic (84) experimentally analyzed light scattering of mono-dispersed polystyrene latexes at 45, 90, and 135 degrees, in another investigation to verify the Mie theory. The experimentally determined polarization ratio was compared with the Mie theory. Discrepancies noted between theory and experiment were attributed to secondary scattering. Measurements were made on systems

containing latex particles of sizes 1380, 2640, 5110, and 5570 angstroms. A photometer was used for measuring the scattered intensity.

Brackett and Charney designed an apparatus for measuring the spectral dependence of light scattering from large particles. However, a very narrow angular range, 26.5 to 86 degrees, was used.

Keith and Derrick (77) studied the measurement of particle size distributions and concentrations of cigarette smoke. The significance of this paper to the current investigation is contained in the centrifugal aerosol collector designed to collect particles in the range .05 to 10 microns in diameter. The investigation sought to find the distribution of particle sizes in cigarette smokes.

Langer and Lieberman (92) discuss the difficulties in obtaining mono-dispersed aerosols. The atomization of mono-dispersed latex lattice does not necessarily produce mono-dispersed aerosol.

Coumou (24) developed an apparatus with which he measured the Rayleigh factor for benzene and some other pure liquids. Light scattering by liquids or solutions is determined by comparison with a standard liquid, for which the scattering power has been previously determined. In general, the standard is benzene. The absolute scattering of light by liquid can be characterized by the Rayleigh factor and the equation for this is presented.

Frei and Gunthard (39) consider the distortion of signals from a photometer due to slit widths, scanning speeds, and type of filter used. Influence parameters are defined and discussed.

Quoting from a paper by Greenberg, Pedersen, and Pedersen (44), in general it can be said that

> "Particles with spherical symmetry present no difficulties. Similarly, several types of axially symmetric scatterers can be treated by analytical and numerical methods for the situation in which the radiation is directed along the axis of symmetry, except for certain special cases there exists no suitable solutions for non-spherical particles. It is for this reason that we have developed an experimental method, which uses micro-wave techniques for obtaining both photo cross sections and angular scattering distributions from arbitrarily-shaped particles."

> "By proper scaling, the results are applicable to the scattering of light or of any wave length of electro-magnetic radiation, so long as the mechanism of scattering can be considered a classical application of electro-magnetic theory."

Angular distribution measurements were made for angles between 10 degrees and 170 degrees, at 5-degree increments rather than continuous scanning. The total cross section was investigated. Single spheres

with refractive index 1.603 (luicite) were used and results were plotted on the theoretical Mie curve. In addition, spheroids and cylinders were used to make measurements, some of which were made with 3 centimeters wave length (1.25 inches). The size of particle was 3 centimeters, that is, the same order of magnitude as the wave length. The angular scattering distributions of spheres are fairly well in agreement with theory. The Mie and Van de Hulst solutions are applicable. They were interested in solutions to inter-stellar dust problems. Particles with real refractive indices were used.

Pangonis, Heller, and Economou (114), in another of a series of papers published by Heller and co-workers on light scattering, considered various refractive indices 1.05 (.05)(1.3), and particle size parameter, alpha, .2(.2)25.6. The ratio of intensity at 90 degrees to the incident intensity was plotted versus alpha for the various refractive indices. Secondary fluctuations were noted for the larger values of refractive index. The ratio of intensity was higher at smaller values of particle size parameter and was also higher for larger values of refractive index. The data included in this report, together with that in previous reports, supplies the data required for emulsion studies for particles between 0 and 3.3 microns in diameter and for mercury-vacuum wave length (5460.73 angstroms).

Gibbon, Nichols, Laughridge, and Rudkin (40) used a nephelometer to measure transmission and scattering properties at night on the Nevada desert atmosphere. Particles were assumed to be in a range 0.1 to 0.6 micron in diameter, and source receivers were located at a distance of 0.51 to 13.17 miles. The scattered intensity at a particular angle, as compared to the scattered intensity at 10 degrees, was plotted as a function of the scattering angle. The data was then extrapolated to 0 from 10 degrees. White light was used with wave lengths 0.4, 0.45, 0.5, and 0.55 micron. No mention was made of the method used in extrapolation. The ratio of the scattered intensity at 0 degrees as compared to that at 90 degrees was 50 or more. The angular distribution was measured in 10-degree intervals over a range from 10 to 170 degrees. It is of particular interest to the investigation presented here that the curves are smooth functions, as would be expected with particles of irregular size.

Deirmendjian, Clasen, and Viezee (27) made detailed computations of Mie scattering at Rand Corporation, considering complex indices of refraction. Most of the results were presented in graphic form for spheres of various optical properties. Scattering and absorption characteristics were calculated. The summary and comments in this paper are particularly noteworthy. It is pointed out that small changes in the absorption index have large influences on the intensity and polarization of scattered flux. "Both theory and experimental measurements show that the scattering properties of a polydispersed media tend to be smooth functions of the scattering angle." Theoretical investigations have shown that flux scattered at angles between 0 and 40 degrees exceed the back-scattered flux at angles between 140 to 180 degrees by 2 to 40 orders of magnitude. The authors noted that the ratio mentioned above does not depend on the

absorption properties in a simple manner. In addition, they pointed out that secondary maxima and minima are absent in the case of absorbing particles.

Gucker and Egan (45) measured angular variation by developing an elaborate system and exercising great care in suspending single particles of dioctyl phthlate 0.7 to 1.5 microns in radius between electro-static plates 19 millimeters apart and 75 millimeters in diameter. A very ingenious method was used to suspend a single particle for measurement, the size of which was calculated from Stoke's law. After measuring the rate of fall while viewing the particle through a microscope, the results were compared to the Mie theory based on calculations with 10-degree intervals. Curves were normalized to obtain a fit between the experimental and theoretical results. The first maxima, with theta approximately equal to 42 degrees, served as a standard. The distribution of angular intensity over a range of 40 to 140 degrees was considered, and white light with a filter was used to obtain a wave length of 436 milli-microns with a band width of 7 milli-microns. The following explanation was offered for the deviation of the experimental results from the theoretical results: In theory the light was collected by infinitesimal aperture, while the experimental results were obtained through the use of a lens system which integrated the radially varying intensity over a 5.3 degree range. Also, in theory, monochromatic light is considered, whereas in the experimental work a wave length band of 7 milli-microns was necessary. This seems to be the only paper available in the literature covering an investigation in which measurements on a single particle were made to validate the Mie theory.

Dezelic and Kratohvil (30) reevaluated previous work on latexes. The particle size measured was lower than that obtained from the electron microscopy, but no reason was given for this.

Gibbons, Laughridge, Nichols, and Krause (40), in a test similar to one completed in 1959 but using measurements made under cloudy skies, used both white and near infra-red sources. In a comparison of the results with those of the previous investigations, the results with partial cloud coverage were similar to clear sky, but the full cloud coverage had more influence. All the curves presented were smooth functions.

Keller (78) presents an excellent discussion on the geometrical theory of diffraction, with an exceptionally good introduction. It is a paper that should be read in conjunction with books on electromagnetic wave theory; for example, the work of Stratton.

Butler (12) examined the effects of light scattering on absorption spectra and presents analytical expressions which predict spectral characteristics of light scattering media. In general, little work has been done to describe the transmission and absorption properties of materials; however, Butler has investigated the absorption of light on such materials as calcium carbonate and aluminum oxide powders as well as polystyrene latexes.

Heller, Bhatnegar, and Nakagaki (58), in another of the series of papers by Heller and co-workers, note that one of the characteristic features of light scattering by non-absorbing spheres whose diameter is small compared to wave length (Rayleigh scattering) is that the specific turbidity at infinite dilution can be expressed as the Rayleigh factor, which is k_r^{-4}. A method of "wave length exponent" which is comparable to Debye's dissymmetry method for determining size of particles which are negligibly small compared to wave length is discussed. These have in common the important advantage that the concentration of the scattering material does not need to be known, although single scattering must be prevalent. A theory of wave length exponent is given and theoretical calculations are presented.

Penndorf (117) presents a very good discussion of the Mie theory with explanations of various definitions of scattering coefficients, intensity and scattering functions, etc. It points out the fact that generalizations and conclusions of the Mie theory require quite extensive computations.

A publication by Kratohvil, Dezelic, and Kerker (86) is a survey of papers, both experimental and theoretical, which have used the Rayleigh ratio of benzene as a standard for calibration. It points out the discrepancies between authors which are not attributable to experimental error.

For those interested in light scattering publications of a theoretical nature, the following papers should be consulted in addition to those already mentioned: Heller (55, 56, 58), Nakagaki (110, 111), Schiff (128, 129), and Wyatt (163).

APPENDIX H

NOMENCLATURE

English Symbols

a_j = Quadrature weight factor

c = Velocity of light, $(ft)(hr)^{-1}$

d = Particle diameter, (ft)

h = Planck's constant, $(Btu)(hr)^{-1}$

I = Monochromatic intensity of radiation, $(Btu)(ft)^{-2}(steradian)^{-1}$

K^e = Extinction cross section

k = Boltzman's constant, $(Btu)(R)^{-1}$

s = Scattering function

s = Distance along a ray, (ft)

x = Normal coordinate distance, (ft)

Greek Symbols

α = Particle size parameter

β = Monochromatic mass extinction coefficient, $(ft)^2(lb_m)^{-1}$

ϑ = Polar angle, radians

Θ = Angle between incident and leaving ray, radians

$\varkappa$ = Monochromatic mass absorption coefficient, $(ft)^2(lb_m)^{-1}$

λ = Radiation wave length, (ft)

μ = Cosine θ

ν = Frequency of Radiation, $(hr)^{-1}$

π = 3.1416

ρ = Mass density, $(lb_m)(ft)^{-3}$

σ = Monochromatic mass scattering coefficient, $(ft)^2(lb_m)^{-1}$

τ = Optical depth

φ = Azimuthal angle, radians

ω = Solid angle, stearadian

Subscripts

i = Iteration index

j = Iteration index